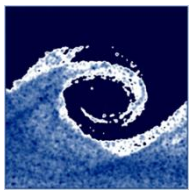

CONSTRUCTION AND TESTING OF A SMALL TEST SECTION WIND TUNNEL

By

Péter KURDI
/JDN8CN/

Submitted to the
Department of Fluid Mechanics of the
Budapest University of Technology and Economics
In partial fulfilment of the requirements for the degree of
Master of Science in Mechanical Engineering Modelling

On the 7th of December, 2012

MSc Thesis

Final Project
/BMEGEÁTMWD2/

Supervisor:
Márton BALCZÓ, assistant research fellow

Evaluation Team Members, advisors:
Balázs ISTÓK, research engineer
Viktor SZENTE, assistant lecturer

Department of Fluid Mechanics
Faculty of Mechanical Engineering
Budapest University of Technology and Economics

ASSIGNMENT

MSc FINAL PROJECT (BMEGEÁTMWD2)

Title:	**Construction and testing of a small test section wind tunnel**
Author's name (code):	**Péter KURDI (JDN8CN)**
Curriculum :	MSc in Mechanical Engineering Modelling / Fluid Mechanics
Supervisor's name, title: Affiliation, address:	Márton BALCZÓ, assistant research fellow Department of Fluid Mechanics / BME H-1111 Budapest, Bertalan L. 4-6.
Advisor's name, title: Affiliation, address:	András GULYÁS, departmental fellow Department of Fluid Mechanics / BME H-1111 Budapest, Bertalan L. 4-6.
Handed out / Deadline:	**3rd of September 2012. / 07th of December 2012.**
Curriculum subjects (code):	1. Computational Fluid Dynamics (BMEGEÁTMW02) 2. Flow Measurements (BMEGEÁTMW03) 3. Building Aerodynamics (BMEGEÁTMW08) 4. Aerodynamics and its Application for Vehicles (BMEGEÁTMW09)
Title of the Major Project (BMEGEÁTMWD1):	Construction and testing of a small test section wind tunnel
Description / refinement of the Major Project (BMEGEÁTMWD1):	The Department of Fluid Mechanics is in need of small test section wind tunnels for educational purposes. Such a tunnel has been designed in the previous semester with v_{max} = 23 m/s, 0.35m x 0.35m test section. Current major project will cover the installation and testing of the tunnel, including the review of the construction and if needed, its redesign based on measurement results. 1/ Literature review on wind tunnel design and construction. 2/ Installation of the wind tunnel from the components already manufactured. 3/ Testing of the wind tunnel: basic parameters and flow homog eneity measurements using Pitot-static tube or hotwire anemometry. 4/ If necessary, redesign of the tunnel should be performed, after which repeated measurements should prove the effectiveness of the changes.
Description of the Final Project (BMEGEÁTMWD2):	1/ Design and test of a split diffuser and comparison of flow homogeneity results to a diffuser with screens 2/ Investigation of the experienced flow velocity fluctuations of the Helios fans with measurement. Explanation of phenomena. 3/ Propose methods to suppress the flow velocity fluctuations in the wind tunnel and perform flow quality measurements to prove their effectiveness.

Budapest University of Technology and Economics
Faculty of Mechanical Engineering
Department of Fluid Mechanics

Hungary, 1111 Budapest, Bertalan L. u. 4-6.
Telefon: (36-1) 463-4072 Fax: (36-1) 463-3464
http://www.ara.bme.hu

Budapest, 3rd of September 2012.

(L.S.)	…….. supervisor	……. Dr. János VAD, associate professor Head of Department

Approved by:
Budapest, 3rd of September 2012.

(L.S.)

…….
Prof. Tibor CZIGÁNY
Dean of Faculty

Received by:
Budapest, 3rd of September 2012.

The undersigned declares that all prerequisite subjects of the Final Project have been fully accomplished. Otherwise, the present assignment for the Final Project is to be considered invalid.

…….
student

Supervisor's declaration of acceptance:	The submitted Thesis fulfils all requirements of the Department of Fluid Mechanics, Budapest University of Technology and Economics. The Thesis is accepted for review process and public defence.
Supervisor's proposal for final grade of the thesis:	The proposed final grade* of the MSc Thesis: …….... * Please, select one: excellent (5), good (4), medium (3), acceptable (2), fail (1)
Date:	Budapest, 7th of December, 2012.
Name / Signature:	…… supervisor

Reviewer's proposal for final grade of the thesis:	The proposed final grade* of the MSc Thesis: …….... * Please, select one: excellent (5), good (4), medium (3), acceptable (2), fail (1)
Date:	
Name / Signature:	…… reviewer

DECLARATION

Full Name (as in ID):	Péter KURDI
Neptun Code:	JDN8CN
University:	Budapest University of Technology and Economics
Faculty:	Faculty of Mechanical Engineering
Department:	Department of Fluid Mechanics
Major/Minor:	MSc in Mechanical Engineering Modelling Fluid Mechanics major / Solid Mechanics minor
Project Report Title:	Construction and testing of a small test section wind tunnel
Academic year of submission:	2012/13 - I.

I, the undersigned, hereby declare that the Thesis submitted for assessment and defence, exclusively contains the results of my own work assisted by my supervisor. Further to it, it is also stated that all other results taken from the technical literature or other sources are clearly identified and referred to according to copyright (footnotes/references are chapter and verse, and placed appropriately).
I accept that the scientific results presented in my Thesis can be utilised by the Department of the supervisor for further research or teaching purposes.

Budapest, 7th of December, 2012

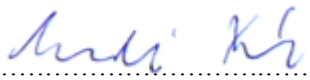

……

(Signature)

FOR YOUR INFORMATION

The submitted Thesis in written and in electronic format can be found in the Library of the Department of Fluid Mechanics at the Budapest University of Technology and Economics. Address: H-1111 Budapest, Bertalan L. 4-6. „Ae" building of the BME.

ABSTRACT

Within the confines of the Thesis, a small test-section wind tunnel was built, tested and optimized for educational purposes. Firstly the theoretical results of the design are demonstrated, and then the construction, the operation, the most important physical properties, the design parameters and the technical specification of the different components follows. Thereafter, the design, manufacture and installation process of an additional guide vane series is presented. Then comes the assembly of the whole wind tunnel from its basic elements. After that, several modifications are implemented to improve flow homogeneity. Different measurements are carried out to check flow quality changes and find the optimal configuration. Finally, the first missions of the assembled, tested and optimized wind tunnel are demonstrated as well as the further development possibilities.

KIVONAT

Ezen diplomamunka keretein belül egy kis mérőterű szélcsatorna lett megépítve, tesztelve és optimalizálva, oktatási célokra. Először is áttekintem a szélcsatorna tervezésének elméleti eredményeit, majd bemutatom a különböző részegységek felépítését, működését, legfontosabb tulajdonságait és irányadó tervezési, illetve kiválasztási szempontjait. Ezután bemutatom a ventilátor utóterelő lapátozás tervezési, gyártási és beszerelési lépéseit. Ezt követi a teljes szélcsatorna megépítése annak alkotó elemeiből. Az összeszerelés után többféle módosítás is megvalósításra került, a kilépő áramlás egyenletességét javítandó. Különböző méréseket végeztem a változtatások ellenőrzése, és az optimális kialakítás megtalálása céljából. Végül az összeszerelt, letesztelt és optimalizált szélcsatorna első gyakorlati alkalmazását mutatom be, valamint a fejlesztési lehetőségekről lesz szó.

TABLE OF CONTENTS

1. INTRODUCTION

1.1. General description

Wind tunnels are built to ensure prescribed flow conditions in a given test volume, so they are designed for a specific purpose and speed range. Therefore, there are many different types of wind tunnels and several different classification viewpoints. In this section various types of wind tunnels and some unique features will be presented.

1.1.1. Modelling problems

Figure 1 - Flow visualization around a real vehicle [1] and around a city model [2]

Fluid mechanics, and thereby wind tunnel tests play essential rule in many application fields, but basically there are two frequent problems, which need to be modelled.

a) Flow past solid objects
   Theoretically, the flow velocity (modelling the relative motion) should be constant in the whole test volume and the turbulence intensity is zero. The cross-section ratio between the solid body and the test section must be taken into account. The effect of the moving ground should also be modelled, with a moving belt system for instance [14].
   Typical application: flow around cars, buses, or airplanes [Figure 1, left].
b) Atmospheric boundary layer
   The flow velocity should be zero close to the lower flat boundary of the test volume and increases upwards according to the velocity distribution in the atmosphere. The vertical distribution of the turbulence intensity and the size of the vortices are prescribed too. These characteristics are mainly influenced by the roughness of the ground surface [14].
   Typical application: flow around wind turbines, buildings, bridges, roads or entire cities [Figure 1, right].

1.1.2. Speed range

Wind tunnels are often denoted by the speed in the test section relative to the speed of sound. The ratio of the air speed to the speed of sound is called the Mach number [3].

a) Low speed ($Ma \leq 0.3$)
b) Subsonic ($0.3 \leq Ma \leq 0.8$)
c) Transonic ($0.8 \leq Ma \leq 1.2$)
d) Supersonic ($1.2 \leq Ma \leq 5$)
e) Hypersonic ($Ma \geq 5$)

The distinction by Mach number is caused by the relative importance of compressibility effects. On one hand, for subsonic flows the effects of compressibility can be neglected, on the other hand for hypersonic flows, also additional considerations for the chemical state of the gas must be made. Compressibility affects the design of the test section of a wind tunnel: for subsonic tunnels the test section has the smallest cross-sectional area of the tunnel, but for supersonic tunnels the nozzle has the smallest area and the test section area is chosen to achieve a desired Mach number [3].

1.1.3. Arrangement

Wind tunnels are also designated by the geometry of the tunnel. A wind tunnel that is open on both ends and draws air from the room into the test section is called an open return tunnel. A wind tunnel that is closed and re-circulates the air through the test section is called a closed return tunnel. There are three arrangement aspects as follows [14].

a) Flow of air
    - Open circuit
    - Closed circuit
b) Pressure in the test-section compared to the ambient
    - Pressurized
    - Evacuated
    - Ambient pressure
c) Relation of test-section and environment
    - Open test-section
        - Easy access
        - Minor or no wind tunnel corrections are required
        - Shear layer entrainment and increased turbulence at the edges
        - Higher pressure than the ambient and increases downstream
        - Velocity deviation from axial direction at the confuser outlet
    - Closed test-section
        - Downstream decreasing pressure and thickening boundary layer
        - Increasing velocity beside the investigated body
        - Flat sidewalls, but curved streamlines (slotted walls are better)
        - Major wind tunnel corrections (because of the previous problems)
        - Lower area blockage ratio (compared to open test-section type)

1.2. Main properties

This wind tunnel was designed at the Department of Fluid Mechanics for educational purposes. The guiding design criteria were the followings:

- Design for a given radial fan (Helios BKD 560/4/80/50)
- Pressurized-type (the ventilator blows the air towards the test section)
- Open circuit (no connection between the suction side and the pressure side)
- Open test-section (but also capable for receiving closed test-section)
- Small test-section area (350x350 mm^2)
- Low speed (23 m/s)
- Low turbulence intensity (under 1%)
- Easily transportable and modifiable (movable scaffolding)

1.3. Theoretical construction

1.3.1. Sketch

The final result of the theoretical design is represented below [Figure 2], which was given thanks to the formerly performed diploma work [12]. This construction fulfils all prescribed criteria in theory.

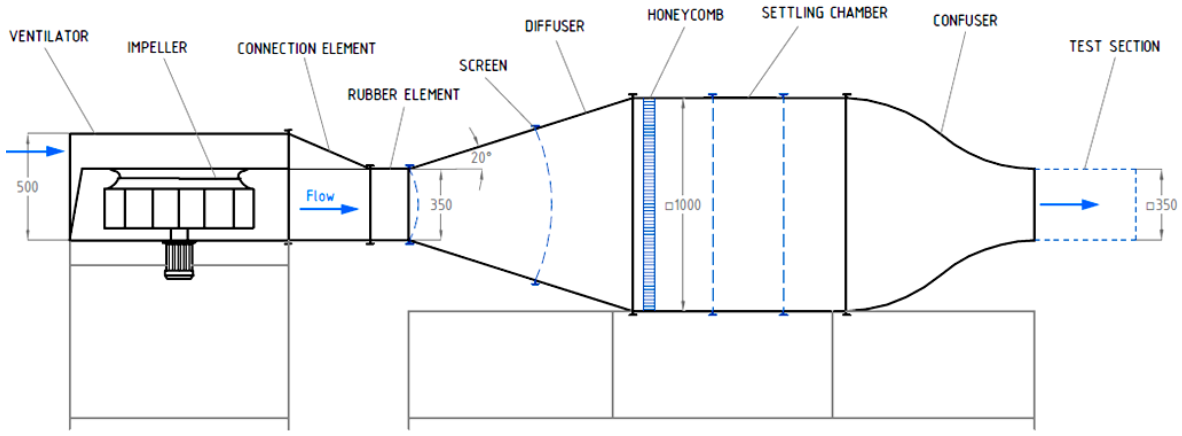

Figure 2 - Theoretical construction

The radial ventilator sucks the air from the surroundings and directs the flow to the diffuser. The diffuser decreases the air velocity, which is necessary to get the flow through the honeycomb and the settling chamber without major pressure losses. These sections with the confuser filter out disturbances and make the airflow more and more uniform, thus providing the conditions of accurate measurements. Lastly, the confuser speeds up the flow to obtain high enough velocity in the test section.

1.3.2. Cross-sections

The outlet cross-section sizes of the different elements are listed in Table 1. All cross-sections are rectangular, dimensions are in millimetres.

Ventilator	800 x 500
Connection element	690 x 350
Rubber element	690 x 350
Diffuser	1000 x 1000
Settling chamber	1000 x 1000
Confuser	350 x 350

Table 1 - Cross-section sizes

1.4. Parts and properties

Now a detailed description of the wind tunnel parts follows. The construction, the physical properties, the operation, the design parameters and the technical specification of the components will be introduced.

1.4.1. Ventilator

Two unused Helios BKD radial fans are owned by the Department, so the wind tunnel was designed around these elements. The technical data and construction of the fans can be seen below in Table 2.

Type	Helios BKD 560/4/80/50
Application	Smoke extraction
Speed of revolution	1420 RPM
Volume flow rate	12770 m^3/h
Power input	4.8 kW
Sound pressure level	65 Db(A)
Impeller diameter	560 mm
Weight	142 kg

Table 2 - Ventilator data [4]

Impeller properties:

- Direct-drive
- Radial impeller
- Backward curved blades
- Galvanized steel material
- Dynamic-balanced

For research and also for educational applications the ability of changing the measuring velocity (so the volume flow rate) precisely is very important. The most precise and efficient method to perform this task is to attach a frequency converter to the ventilator. Therefore, *YASKAWA AC Drive V1000* type frequency converters were ordered for both fans.

1.4.2. Connection element

The connection element provides the connection between the fan outlet and the diffuser inlet. It bridges the cross-section difference and smoothes the airflow. This element will be more important later on.

1.4.3. Rubber element

It is a very simple constant cross-sectional part, which reduces the vibration caused by the fan and makes the assembly easier due to its elasticity as well.

1.4.4. Diffuser

The diffuser means an expansion for the airflow due to downstream widening cross-section. Flow through a diffuser depends on the geometry defined by the area ratio, diffuser angle, wall contour and cross-section shapes. Other parameters like the initial conditions, boundary layer control method and the presence of separation could also affect the flow, thus making it very difficult to predict. Almost all acquired knowledge about diffusers is empirical.

Two basically different types exist: exit diffusers and wide-angle diffusers [6]. For this wind tunnel, a wide-angle diffuser was designed between the fan and the settling chamber [12]. The reason is that length reduction to a given area ratio was more important than effecting the pressure recovery. Therefore, the cross-section area increases so rapidly that separation can be avoided only by boundary layer control. Meshes usually have to be applied inside the diffuser to increase the velocity near the wall, thus prevent separation. Meshes are useful to place just before the supposed separations. It is more advantageous to apply more meshes with low pressure drop instead of one with high pressure drop.

The design was carried out using the experimental results and guiding methods documented by Mehta and Bradshaw [6]. The basic parameters were the followings:

- Area ratio
- Diffuser angle
- Number, pressure loss and arrangement of meshes

The main properties [6] and the specific parameters [Table 3] of the final configuration can be read below.

- *Mesh*: Theoretically three meshes are enough to avoid separation. Two of them have to be installed at the ends of the diffuser, and one more at the middle of the diffuser, between the others. The mesh material needs to be steel to resist higher wind loads without serious deformation.
- *Wall shape:* Curved surface could be better in fluid mechanic point of view, but because of the lack of detailed theoretical background and high manufacturing costs, it should be avoided. Therefore, linear wall shape was designed.
- *Cross-section:* The diffuser transforms a rectangular cross-section into square. Therefore, two different diffuser angles exist.

Area ratio	4
Diffuser angle	40°
Number of meshes	3
Diffuser efficiency	39%
Diffuser length	933 mm

Table 3 - Diffuser parameters

The diffuser also was manufactured by an external company, but the meshes were installed at the Department.

1.4.5. Screens

Screens (or meshes) make the flow more homogeneous as they eliminate the abnormal velocity components. They also increase the flow velocity near the walls, thus reduce the threat of separation. Such a mesh is represented by Figure 3.

Figure 3 - Steel mesh roll

The most important properties are the wire diameter with the hole size (so the open area ratio) and the weave method. Meshes direct the flow in the same direction, but also cause a pressure loss. The two main designing parameters are the deflection coefficient and the pressure drop coefficient, which can be determined from different empirical correlations [6].

Meshes can be manufactured of steel or polymer as well. However, steel meshes are more advantageous in terms of fluid mechanics, because of the higher loadability and the greater velocity growth near the walls [7]. Therefore wind tunnel screens are normally made of steel wires interwoven to form square or rectangular meshes. They can be applied in diffusers to avoid separation and in settling chambers to smooth the airflow.

Remark: Mesh is a flexible sheet, and if it is glued on a rigid steel frame, than usually called as a screen. Screens means large area meshes with higher stiffness in fact, thus applied typically in the settling chamber section.

For the different sections of the wind tunnel, different screens were ordered. Smoother and smoother meshes are required downstream to get as uniform velocity profile as possible. The dimensions of the ordered meshes are shown in Table 4.

	Small screen	Coarse screen	Medium screen	Fine screen
Cross-section	□ 560 mm	□ 1060 mm	□ 1060 mm	□ 1060 mm
Hole size	□ 2 mm	□ 2 mm	□ 1.25 mm	□ 0.9 mm
Wire size	Ø 0.6 mm	Ø 0.6 mm	Ø 0.32 mm	Ø 0.2 mm

Table 4 - Dimensions of ordered screens

1.4.6. Honeycomb

The honeycomb [Figure 4] also makes the flow more uniform, while reduces the turbulence. It works effective at relatively small velocity angles (usually lower than 10°) and in case of purely or nearly laminar flows.

More precisely, it removes swirl and lateral velocity fluctuations if it operates optimally. Especially, the lateral turbulence components are inhibited by the honeycomb cells and almost complete disposal can be achieved in a length of about 5-10 cell diameters. However, the cell edges themselves generate small scale turbulence. This effect is stronger for laminar flow, because of the basic instability of the laminar near wakes.

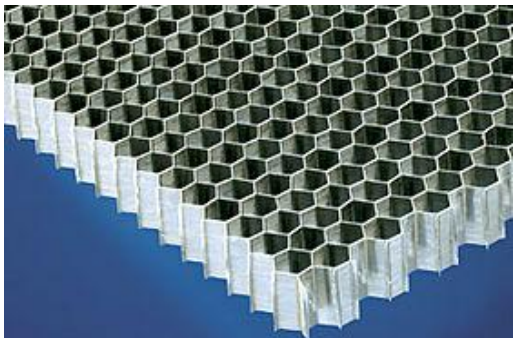

Figure 4 - Honeycomb structure

Designing for the optimum, the cell diameter should be smaller than the smallest lateral wavelength of the velocity variation. Furthermore, the cell length should be about 6-8 times its diameter. The cross-sectional shape of the cells is usually hexagonal, but sometimes square or triangular due to construction. Honeycombs can be manufactured of metal or impregnated paper. Paper is good for small tunnels, but for professional applications aluminium is the adequate material. Aluminium honeycombs have more precise dimensions, resist higher wind loads and have better other mechanical properties. The technical parameters of the ordered part can be seen below in Table 5.

Type	CEL® honeycomb
Material	Aluminium alloy
Cross-section	□1005 mm
Cell size	Ø6 mm
Cell length	50 mm

Table 5 - Honeycomb properties

1.4.7. Settling chamber

The general arrangement consists of a honeycomb followed by well-spaced screens. The number of screens depends on the turbulence level, pressure loss and space requirements. If sudden brake or swirl is expected in the flow from the wide-angle diffuser, it is advisable to install one screen upstream of the honeycomb. Thus the flow angles are reduced. The honeycomb should be installed some way downstream of the diffuser-exit, so that the flow has a chance to become even more uniform.

The spacing between the screens is at least in the order of large energy eddies and provides fully recovered static pressure before the next element. However, much higher distance leads to unnecessary boundary layer growth. The optimal spacing was found to be about 20% of the settling chamber diameter due to independent experiences [6].

The design was carried out in accordance with the former statements. The settling camber was divided into several sections. The first scaffolding contains the honeycomb and the following sections involve two screens to avoid separation and get as uniform airflow as possible. The elements – the honeycomb, frames and screens – were ordered and manufactured by external companies.

1.4.8. Confuser

Confuser means a contraction, so increases the mean velocity. This allows the honeycomb and screens to be placed in a low speed region, thus reducing pressure losses. Further, it reduces both mean and fluctuating velocity variations to a smaller fraction of average velocity. The most important single parameter which describes these effects is the contraction ratio *c*. The higher the contraction ratio is, the greater outlet velocity can be achieved. However, this leads to higher construction and running costs besides possible noise and separation problems near the end. Therefore, contraction ratio is usually between 6 and 9 for smaller wind tunnels.

The main design criteria are the production of a uniform and steady outlet flow, avoidance of the separation, minimum exit boundary layer thickness and minimum contraction length. It is always possible to avoid separation by making the contraction long enough, but this results an increase of tunnel length, cost and exit boundary layer thickness. Noncircular cross-sections are problematic, because the flow tends to migrate laterally near the walls, especially at the corners of polygonal sections. Although recent investigations show that this can be avoided in well-designed square contradictions. Another important thing is that a certain gap is recommended between the last screen and the confuser inlet in order to get smoother velocity profile.

The confuser was designed based on the numerical solution of Stokes's stream function and on some experimental results as well [12]. The design method was developed and documented by Watmuff in 1986 [8], then developed further by Bell and Mehta in 1988 [9]. The wall shape was calculated by matching two polynomial curves and their derivatives at the inflexion point.

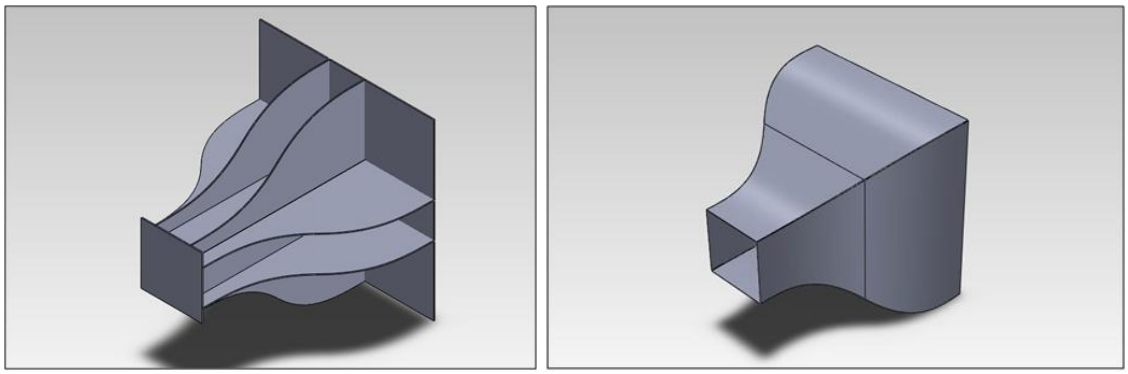

Figure 5 - Manufacture technique of the diffuser [12]

The manufacturing technique was not so obvious, because of the special shape and high accuracy requirements of the geometry. Finally, a very smart solution was developed [Figure 5] with the help of the Department of Polymer Engineering. A positive tool was designed at first. It was manufactured by cutting to size plywood plates with water-jet technique, and then very thin single aluminium sheets were fixed on it. The polymer material was laminated on the surface in multiple layers. After drying out, the tool was removed and the diffuser was finished.

Type	Self-developed
Inlet dimension	□1000 mm
Outlet dimension	□350 mm
Contraction length	1000 mm
Contraction ratio	8.16
Outlet velocity	22.7 m/s

Table 6 - Diffuser dimensions

The final specifications of the confuser are listed in Table 6. The designed outlet velocity is approximately 23 m/s due to the basic criteria. The contradiction ratio is pretty high, but falls within the recommended interval.

1.4.9. Test section

The test section is directly behind the outlet of the confuser. The airflow is actually a free jet, but a closed test section with independent scaffolding is planned to construct and install later. The cross-section size [Table 1] and the outlet velocity were mentioned before. The expected turbulence intensity, which is lower than 1% should be provided in this section.

1.4.10. Scaffolding

To avoid vibration propagation caused by the fan, two independent scaffoldings were designed; one for the ventilator and another for all other parts of the wind tunnel. Due to ergonomic and transport requirements, unique scaffoldings were designed and ordered. The construction builds up of special aluminium profiles, developed by the *Bosch* company. Figure 6 shows the assembling principle.

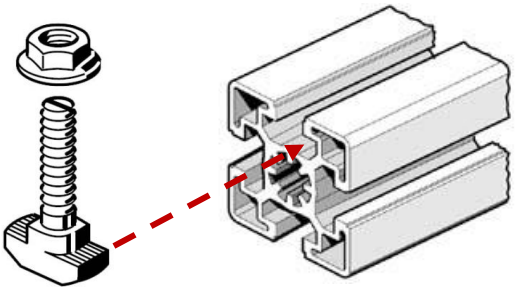

Figure 6 - Bosch profile

The largest advantage of this profile is the easier assembling process and the possibility of further modifications. Therefore different elements can be fixed on the scaffolding with hammerhead screws quite easily and quickly.

Figure 7 - Lockable wheel and adjustable feet

The scaffoldings also have lockable wheels for moving or fixing, and adjustable heavy-duty feet for leveling the construction [Figure 7].

2. GUIDE VANES DESIGN

2.1. Problem

The velocity distribution at the fan outlet along the center line was known from an LDA measurement, which was performed earlier [12]. The measurement results can be seen below [Diagram 1].

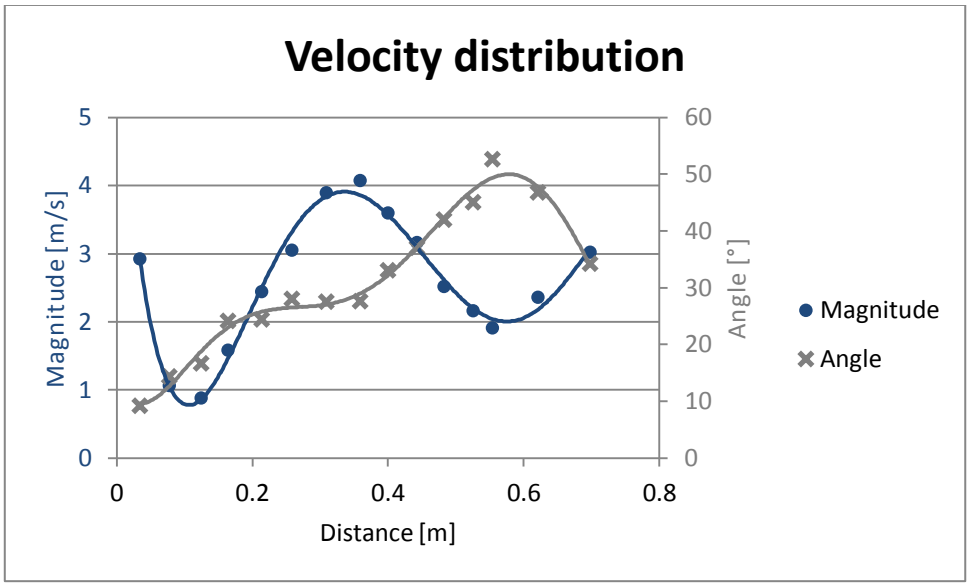

Diagram 1 - LDA measurement results

As the diagram shows, the distribution is very irregular also from velocity magnitude and direction point of view. Other problem was the very strong fluctuation over time, since the average turbulence intensity was over 110% which is absolutely unacceptable for a wind tunnel! My task was to design a series of guide vanes into the Connection element in order to get smoother velocity profile.

2.2. Design

First of all, a polynomial curve was fitted on the measurement points. Then the inlet cross-section of the Connection element was divided equally. Due to the dimensions, it was found that five vanes are enough to change the flow direction effectively. Thereafter – applying the continuity equation – I tried to divide the outlet cross-section with differently positioned vanes to get nearly equal average velocities in each section. Finally, the geometry was constructed taking into account the inlet velocity directions. As the sketch shows below, curved vanes were designed [Figure 8]. However, a minimum radius was established in order to avoid strong separation. Thus two different curves form the third vane.

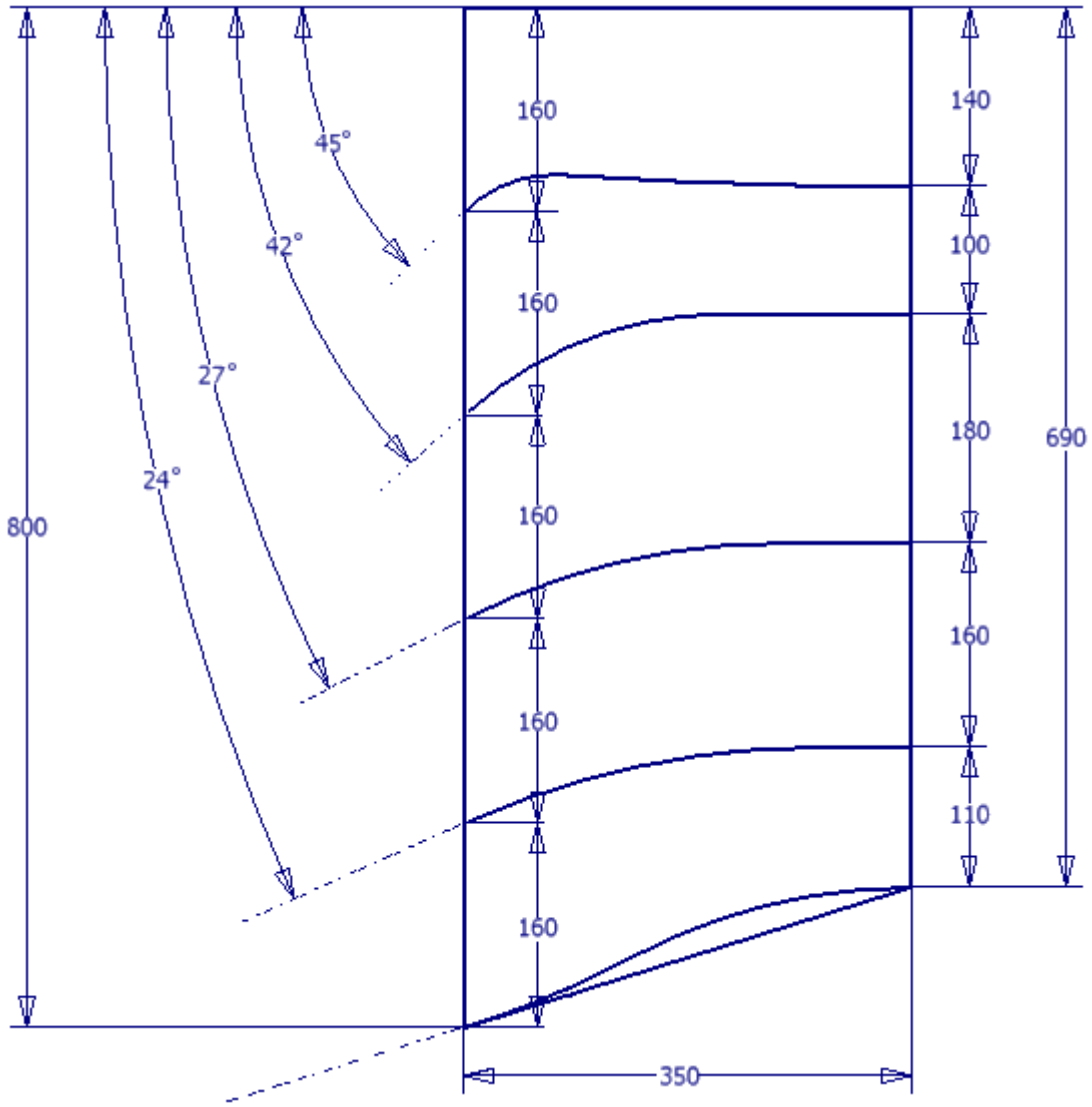

Figure 8 - Geometry of the vanes

2.3. Optimization

The previously described designing method is just a rough approximation of course, but provides a good basic for further investigations. Now the optimization of the vane series arrangement follows using CFD techniques. Originally, this thesis did not contain any simulation tasks, but it was useful due to the need of several redesign and modification steps. Nevertheless CFD simulation was applied as a „quick tool" instead of a top-level technique. The simulations were performed in *ANSYS Workbench*.

The 2D geometry was created in *Autodesk Inventor* and then exported into *ANSYS*. A more than 1 meter long section was attached after the vanes in order to get fully developed flow and avoid reversed flow or CFD-errors. The boundary conditions were quite simple and obvious. The given velocity profile was defined at the inlet and outflow at the outlet as Figure 9 shows.

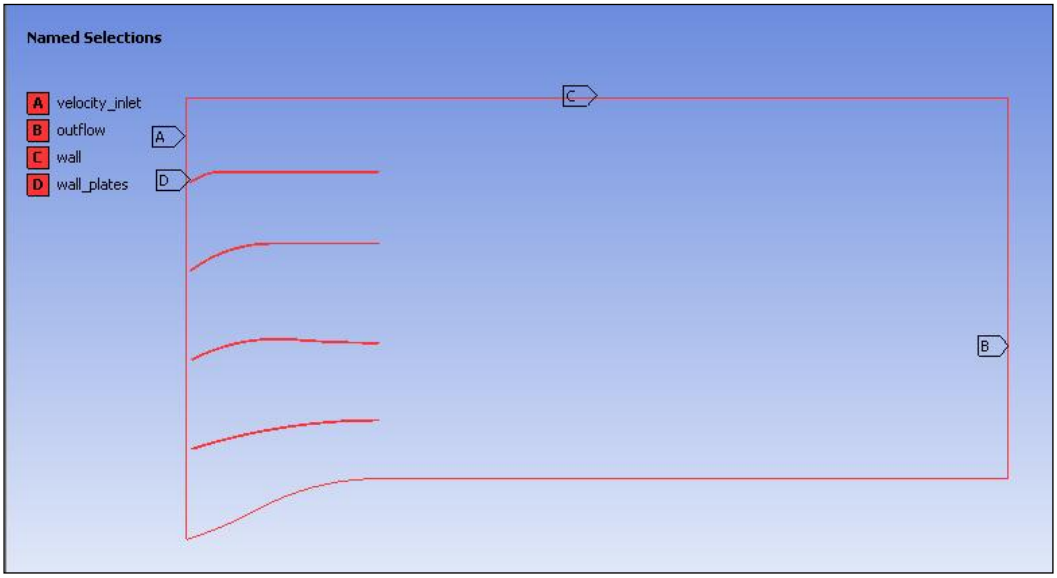

Figure 9 - Boundary conditions

The numerical mesh was generated using the automatic *Workbench Mesher* algorithm, but with some prescribed refinements near the walls and around the vane edges. The following parameters characterize the mesh quality:

- Quad elements
- 11.000 cells
- Maximum cell skewness = 9.60050e-001
- Maximum aspect ratio = 1.46357e+001

These values are not very good in general, but in case of such simple simulations they provide sufficient accuracy as my former experiences proved. And the aim of the simulations were not to pushing the envelope of the CFD preciseness, rather get fast and comparable results. The CFD-model setup was defined to reach as simple and fast simulation as possible. The next settings were applied:

- Pressure-based, Steady, 2D space solver
- Viscous, Realizable k-Epsilon model with Enhanced Wall Treatment
- Constant air properties
- Simple scheme, Second Order Upwind
- Convergence criterion of Residuals up to 10^{-6}

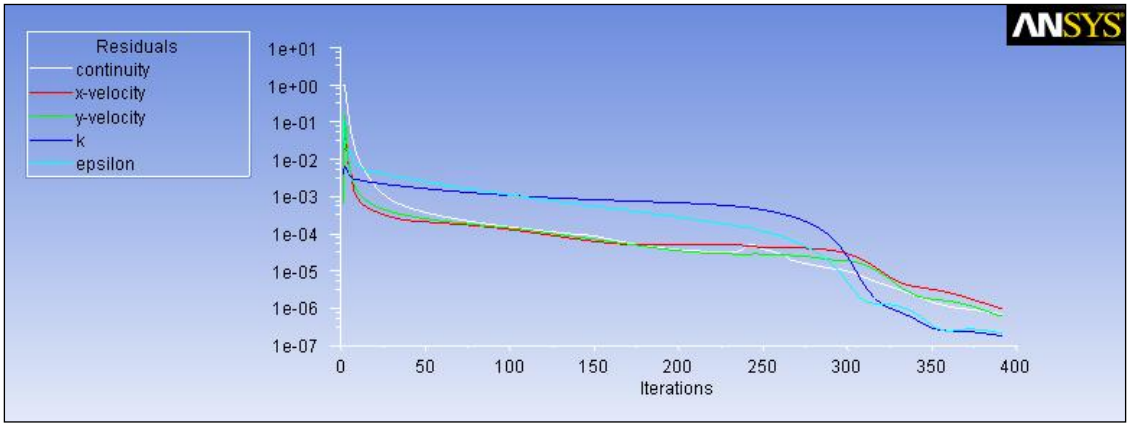

Diagram 2 - Simulation iterations

Since only 400 iterations were needed, the simulation run very quickly [Diagram 2]. After finished, the velocity distributions were queried **directly behind the vanes** (at 350 mm from the inlet) and also **in the additional section** (at 1000 mm from the inlet). Thereafter, the distance between the outlet edges of the vanes were modified to smooth out the flow and the simulation was performed over again. This was a long iterative process, about ten or eleven different configurations were under investigation. But a great development was achieved as Diagram 3 shows.

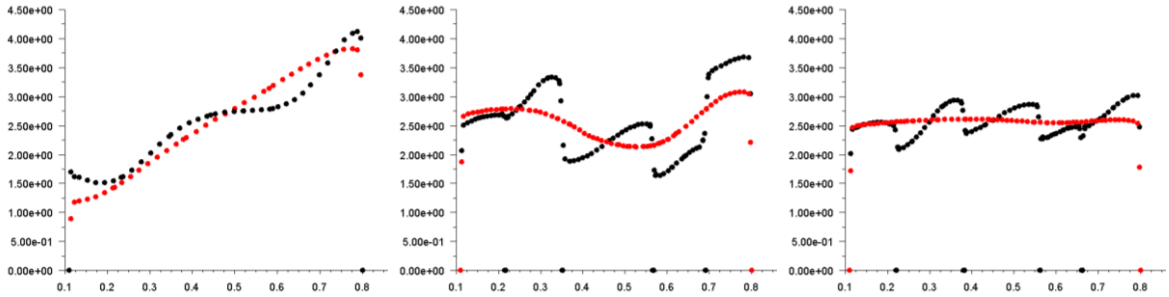

Diagram 3 - Velocity profiles 1) Without vanes 2) First version with vanes 3) Final version with vanes

2.4. Realization

The entire manufacture process of the vane series was carried out in the workshop of the Department. From the simulation the optimal dimensions and arrangement were known for the vanes. First of all, drawings, sketches and flat pattern calculations had to be made. After that, looking for raw materials followed such as aluminium sheets, plywoods or screws. My tasks also involved continuous communication, supervising the manufacture and taking part as needed.

Without knowing the measured effectiveness of the vane series, it was important to make the part removable. The vanes were screwed on two plywood plates, so they form a single part which can be easily assembled or removed from the Connection element. The final result can be seen on the next photos [Figure 10].

Figure 10 - Manufacture of vane series

The first step of the assembly was to install the ventilator on its scaffolding. Not an easy task, because it weights more than 140 kilograms. A green hand pallet and some volunteers were provided by the Department. The fan had to be lifted up over the scaffolding, then rotated upside down and moved to the final position. It was a great physical challenge, which is documented by the following photos [Figure 11].

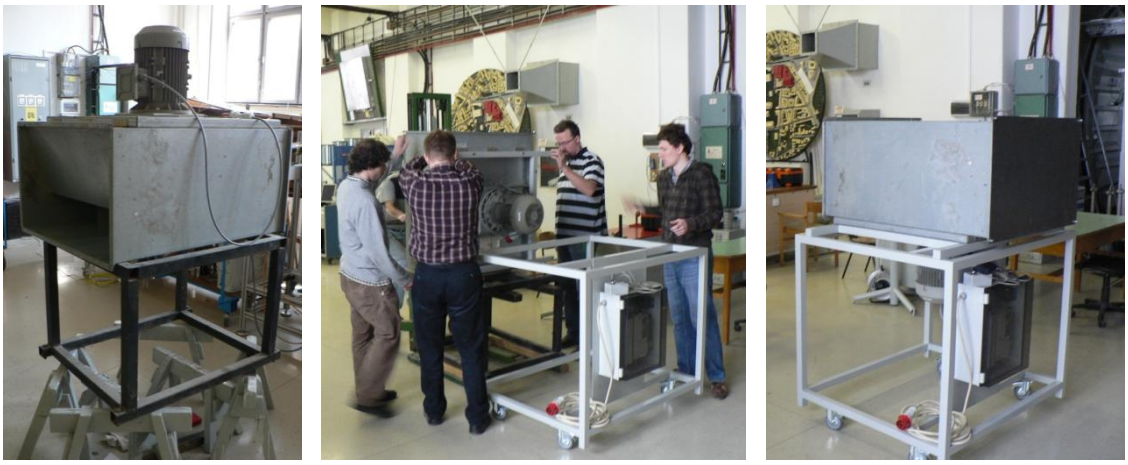

Figure 11 - Installing the ventilator

Finally, the sealing was stuck up on the contact surface and the Connection element was screwed to the ventilator with the guide vanes inside [Figure 12].

Figure 12 - Ventilator and connection element with guide vanes

2.5. Measurement

The velocity-distribution was measured along the horizontal midline of the cross-section using two totally different techniques. The first one was based on pressure measurement (using a so-called Prandtl-tube), while the second one was based on heating power measurement (using a thermal anemometer).

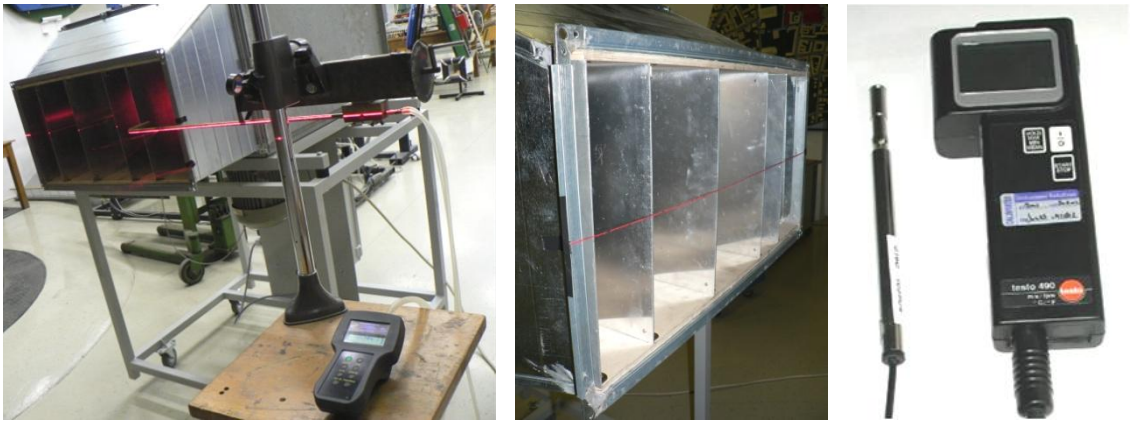

Figure 13 - Guide vane series measurement techniques

Figure 13 illustrates the measurements. The Prandtl-tube was mounted into a moveable clamp which was fixed to a stand. The pressure difference was measured using a digital manometer, which was attached with silicone tubes. The midline was appointed by a laser plane. In the second case, a marked rope showed the midline and also the measurement points for the thermal anemometer.

The measurements were carried out point by point with the same, 30 millimeters division. The frequency converter was set to 20 Hz, which means about 40% power for the fan. Thus the airflow velocity was high enough to neglect measurement errors, but not too high in order to avoid the disturbance of other people or measurements in the laboratory. The results are showed below [Diagram 4].

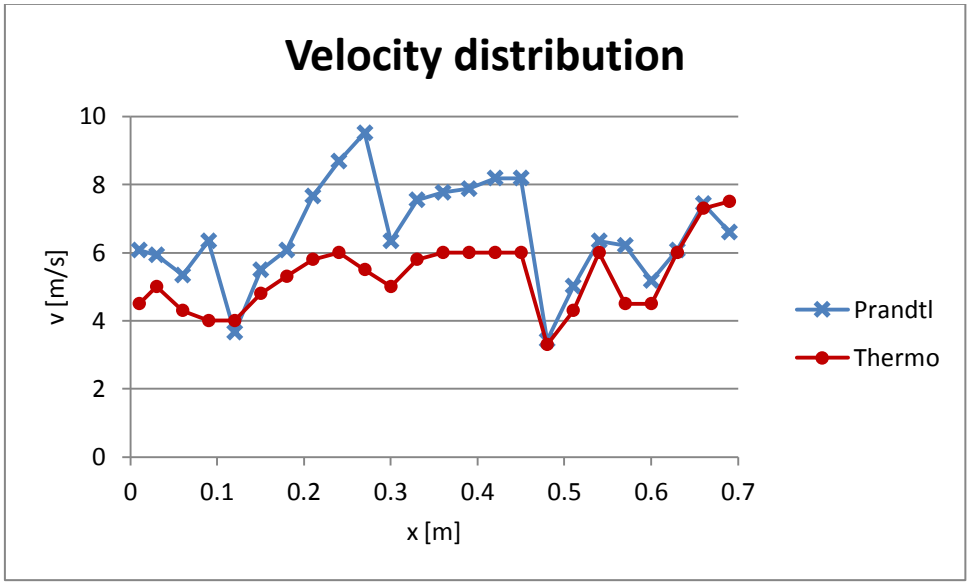

Diagram 4 - Velocity profiles after the vanes @20Hz

The first measurement technique was very slow and uncertain. The digital manometer was not adequate device, because of the high pressure fluctuations. Unlike the other, measuring with a thermal anemometer was more convenient, more precise and quicker as well. Therefore only the second measurement results were taken into account for further investigations and comparisons. Diagram 5 is the point of the measurements. It gives a great overview of the vane effectiveness and the simulation accuracy. The given velocity profiles were recalculated to the same volume flow rate, so that get comparable curves.

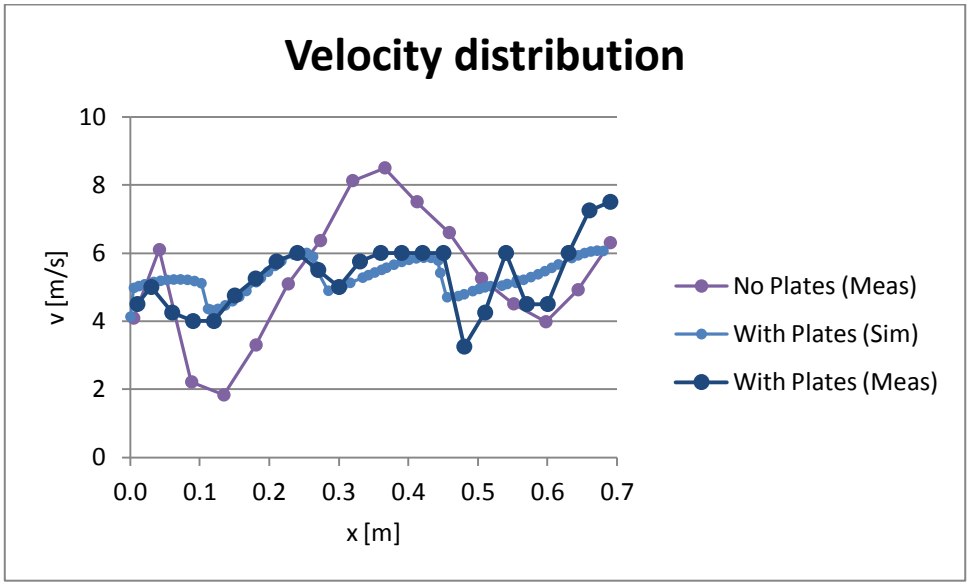

Diagram 5 - Effect of vane series

As it was expectable, the measured and the simulated velocity profile differ from each other. However, in the middle section they are pretty close. Unfortunately, in the outer sections the situation is quite different. The reason is probably the separation, because after the fan the velocity profile was given at lower speed. Therefore the vane series was designed for lower volume flow rate. However, at higher speeds stronger fluctuations can be caused by the impeller, which also can lead to such differences. Taken all round, the designed vane series improved the flow homogeneity, so it was decided to keep it.

3. ASSEMBLY PROCESS

3.1. Preparation

At this point, the ventilator was fixed to its scaffolding and the connection element with the vane series inside was attached to the ventilator. However, all other parts were not out position.

First of all, the middle mesh was installed into the diffuser. It was a special task, because the mesh had to be fixed on the outer surface of the diffuser to avoid flow disturbance on the inner surface. After that, the confuser was corrected. The inner surface was not smooth and precise enough, so it was plastered and sanded again at the necessary areas. The appearance of the corrected confuser was not very nice, but inevitable to get smooth velocity distribution. The following pictures show these processes [Figure 14].

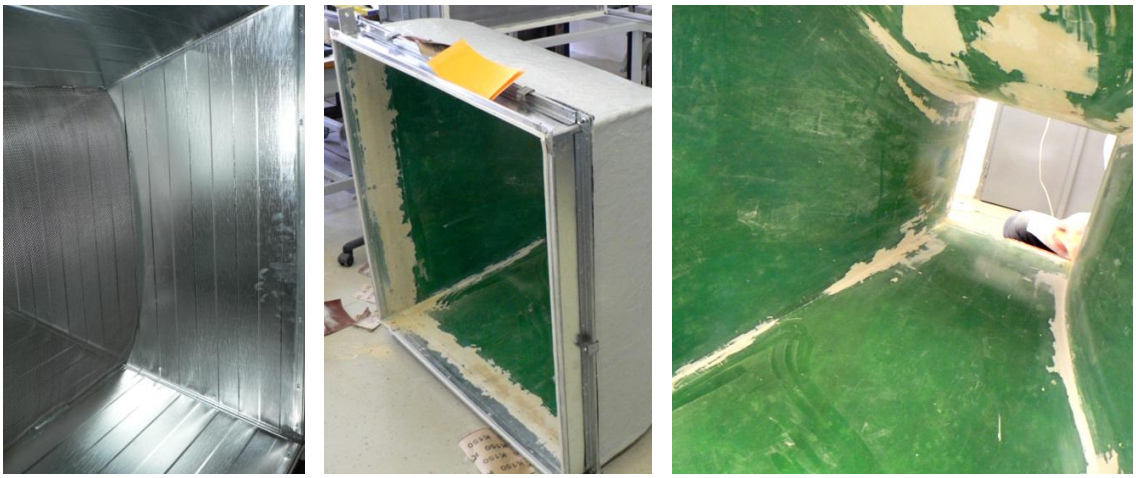

Figure 14 - Final touches on the diffuser and the confuser

3.2. Technique

A sealing technique was needed to be found at the contact of the elements, but there were many requirements to satisfy as follows.

- Durable (works at least for 5-6 years without any maintenance)
- Closes hermetically (even at high pressure loads)
- Low space requirements (narrow, slim design)
- Easy to fix on and remove from the surface
- Low acquisition time
- Moderate price

Therefore several methods and products were under investigation to find the best solution. Finally, a common stick-on silicone band was chosen, which was developed for fenestrations and similar applications. It fulfils all prescribed criteria. The elements were fixed together with screws and double-washers at the corners, plus with screw-clamps along the edges.

3.3. Assembly

The applied sealing and fixing method provided a tight contact between the elements, which is otherwise easily removable if necessary. The next few photos demonstrate the implementation of the technique [Figure 15].

Figure 15 - Sealing and fixing

The different parts were assembled on the base scaffolding. The Bosch-profile provided easy moving and fixing possibilities for each element. However, it did not solve the main problem of the assembling process: namely the leveling. The precise position of the parts was crucial from assembling and also from flow homogeneity point of view. A little uncertainty may cause gaps or breaks on the inner surface, which could mean disturbance and so turbulence source in the airflow. Moreover the accurate vertical and horizontal positions are essential for fluid mechanics measurements. Therefore it was very important to ensure as precise assembling and leveling as possible.

The ventilator scaffolding and the base scaffolding both have adjustable feet by design. So firstly the diffuser (with the rubber element) was installed on the base scaffolding. Then the connection element (which was attached to the ventilator earlier) was set to the same level with the diffuser by twisting the feet of the ventilator scaffolding. Thereafter, the bores were matched and the screws were inserted. Finally, the whole construction was set to horizontal using a bubble level instrument. Photos of Figure 16 illustrate the main steps.

Figure 16 - Leveling technique

After leveling, the remaining parts; so the honeycomb, the settling chamber with the screens and the confuser were attached on the base scaffolding. The result was a working wind tunnel, which can be seen below in Figure 17.

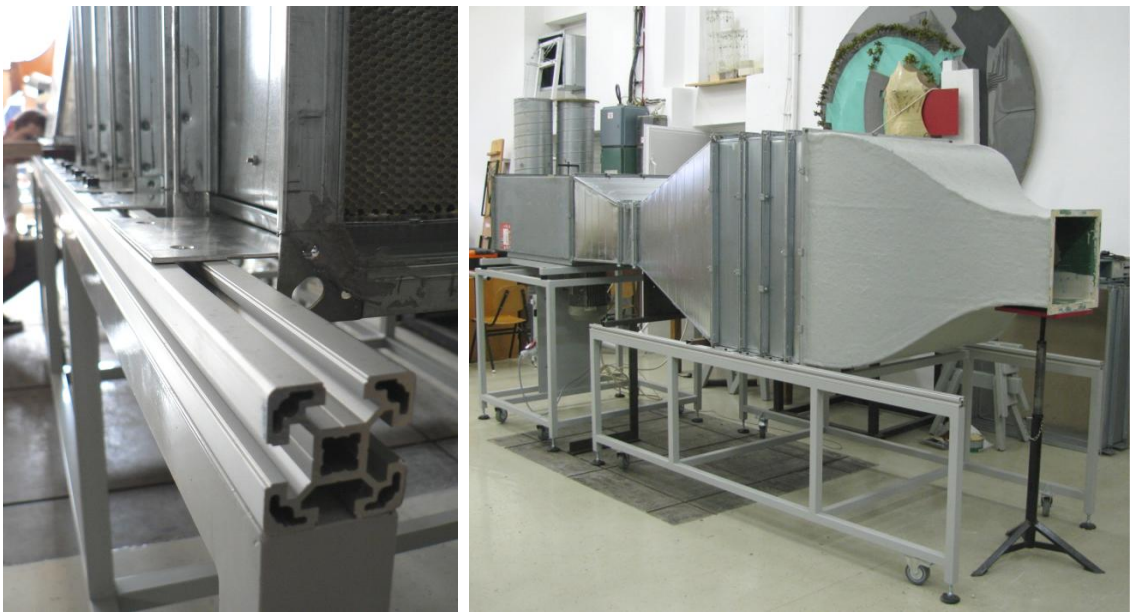

Figure 17 - Assembly

The assembly was documented quite shortly. However, it has to be mentioned that this process required the most of time in the project. During assembling the wind tunnel components and measurement devices, several problems were appeared and high delivery times or delays caused unpredictable difficulties. Weakly brainstorming and high level of organization was needed to comply with these challenges.

4. INTERMEDIATE MEASUREMENTS

During the assembling process velocity distribution measurements were carried out in certain cross-sections to get a greater overview on the efficiency of different elements and flow homogenity development. Thermal anemometer was used, because it provides quick and reliable measurements without calibration. The horizontal and vertical centrelines were measured along at the diffuser outlet, after the honeycomb section and after the screens. The following diagrams represent the measured velocity distributions.

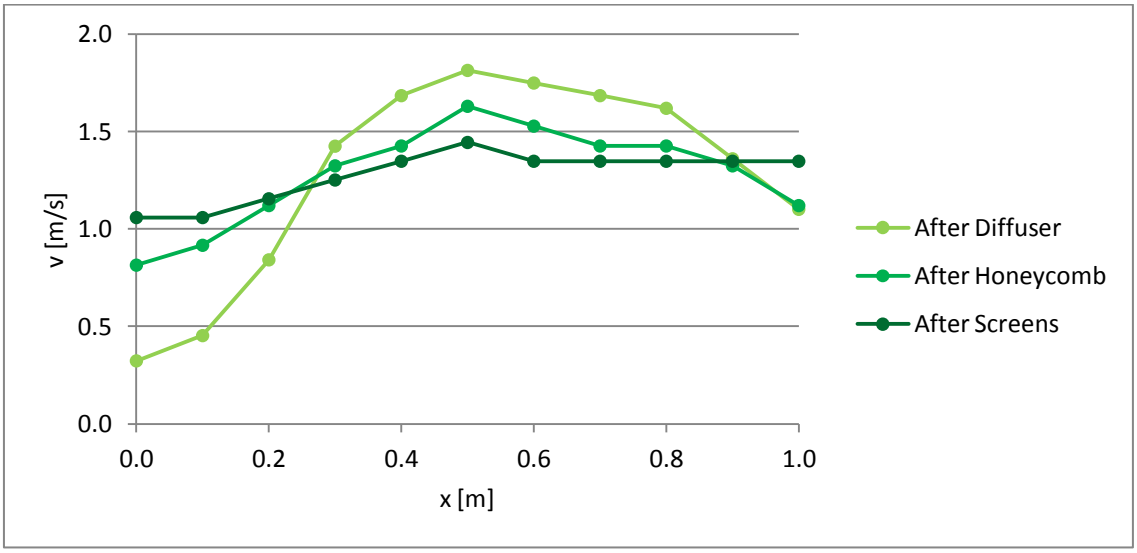

Diagram 6 - Horizontal velocity distributions

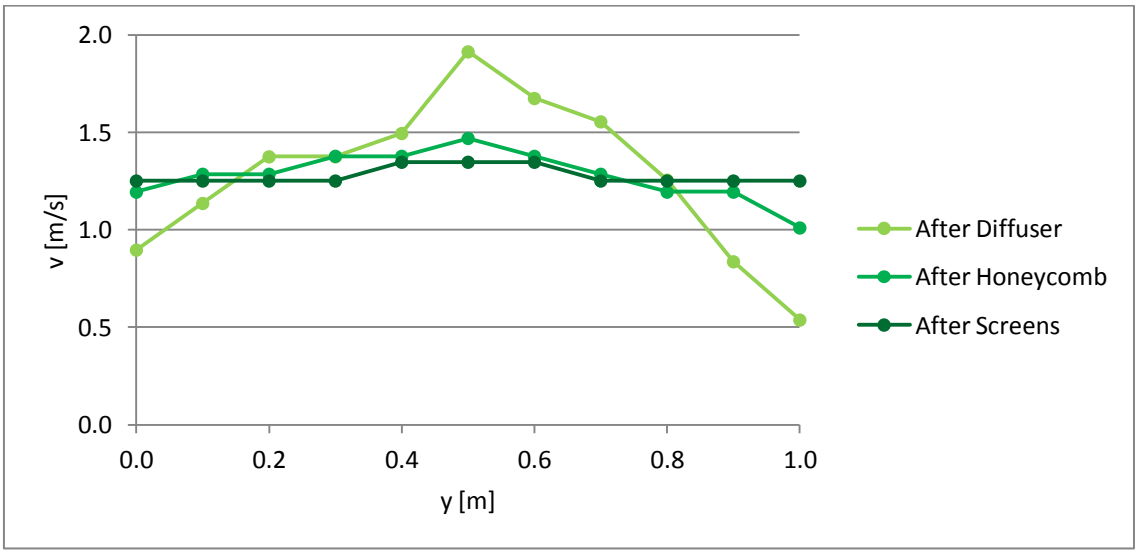

Diagram 7 - Vertical velocity distributions

Considering both diagrams, the velocity profiles after the diffuser are very non-uniform. At the left side [Diagram 6] and at the upper section [Diagram 7] the velocities are much lower than the average. The reason is probably the strong flow separation effect, which could be a consequence of the wide-angle design. However, the honeycomb and the screens make the velocity distribution smoother and smoother, thus the outlet profiles after the screens are quite acceptable.

5. RASTER MEASUREMENT I.

5.1. Arrangement

After assembling the wind tunnel, a hot wire anemometer measurement was performed directly behind the confuser to get an accurate velocity profile. A complete traverse system on special scaffolding was installed near the outlet section. This allowed to measure through the entire outlet cross-section without any assembly, since the measurement could be automated in the computer program. Nevertheless, measuring with hot wire is not a simple task. A full workstation was built around the wind tunnel [Figure 18].

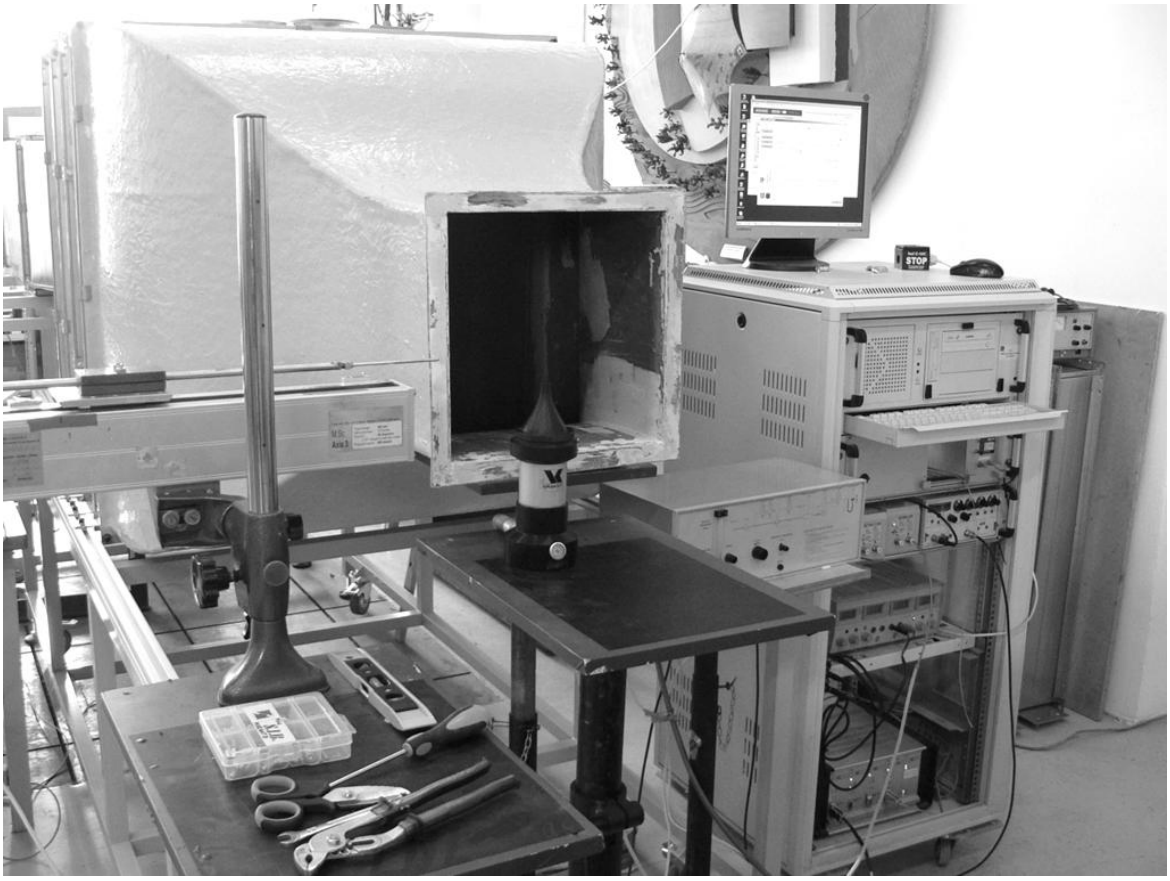

Figure 18 - Hot wire measurement

The probe was mounted into a moveable clamp which was fixed to a stand. The clamp was moved by the traverse, which was controlled through the computer. The electronic signal of the hot wire was received and processed by the computer. It is important to set the voltage control system of the hot wire to operate mode before measurement and reset to standby mode after finish. After calibrating the hot wire and setting up the proper position, the system was ready for measurement. However, there were a lot of thing to set and tune in the computer program. The so-called „Pressure&Force" signal processing, controlling and evaluating computer program was developed in *LabVIEW* by *Márton Balczó*.

5.2. Settings

The first task was to calibrate the wire before the measurement. The reference velocity was provided by a standard nozzle and the required pressure was generated by a compressor. The actual pressure difference was measured by a certificated pressure transmitter [Figure 19]. The signal of the pressure transmitter and the hot wire anemometer was processed and compared by the computer, thus the calibration curve was obtained [Diagram 8]. The probe was calibrated up to 28 m/s, which was expected to cover the entire measurement range.

Figure 19 - Hot wire calibration

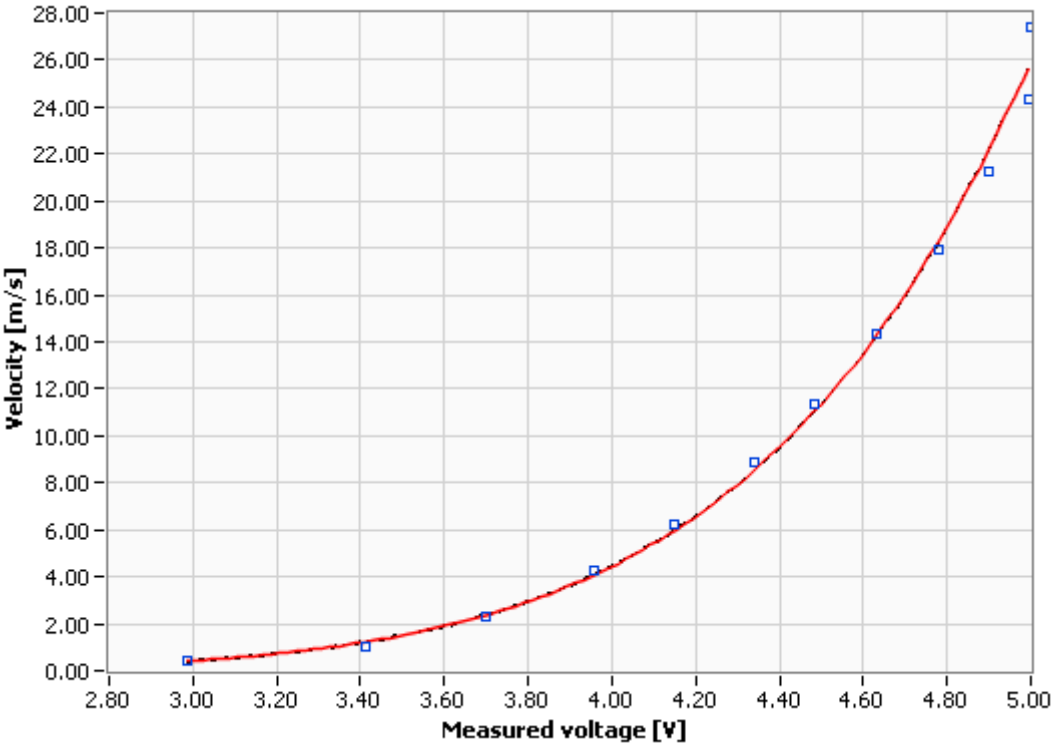

Diagram 8 - Calibration curve

5.3. Results

The measurement was performed at maximum volume flow rate. The measurement settings are listed below in Table 7.

Barometric pressure [Pa]	99500
Temperature [C]	20.8
Sampling rate [Hz]	5000
Sampling time [s]	5
Signal filtering	No
Time data format	Waveform spreadsheet

Table 7 - Program settings

The entire outlet cross-section was measured through with automatic measurement control. More than two hundred measurement points were recorded to get a great overview on the flow homogeneity. The measurement data was saved into *Notepad* file, then prepared in *Excel*, and finally evaluated in *Mathematica*. The presentation of three-dimensional velocity plot can be seen below [Figure 20].

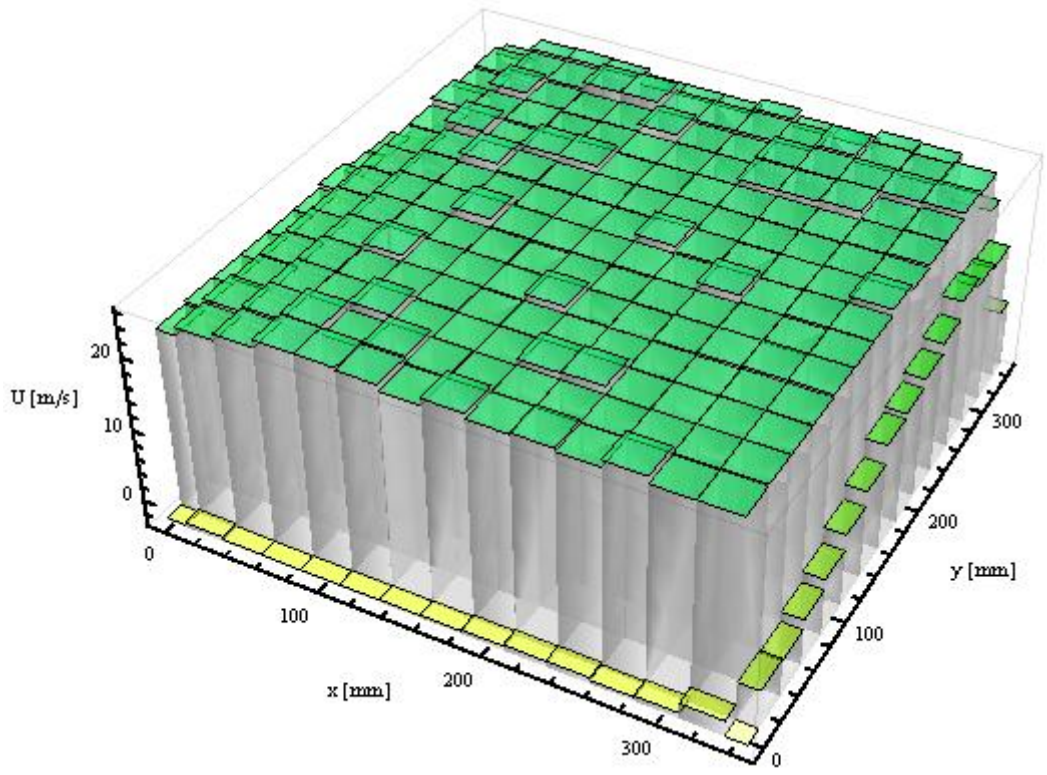

Figure 20 - 3D velocity point plot

The inhomogeneity at the edges is the result of a small zero-point error in the probe position, but this was expectable, since a free jet was measured instead of a closed test section. However, the middle velocity distribution is also not so uniform. Some sudden velocity jumps are observable, which is very strange and unreal. This phenomenon could mean unsteady flow conditions. The average turbulence intensity was about 2.5%, which is again unacceptable and implies high velocity fluctuations.

6. PROBLEM ANALYSIS

6.1. Measurement

To check, whether the flow is steady or not, a new measurement was carried out. Only one measurement point was recorded, the center of the outlet cross-section, where the flow was expected to be the most uniform. But instead of 5 seconds, now the measurement was run up to 30 seconds. The next figure shows the results [Diagram 9].

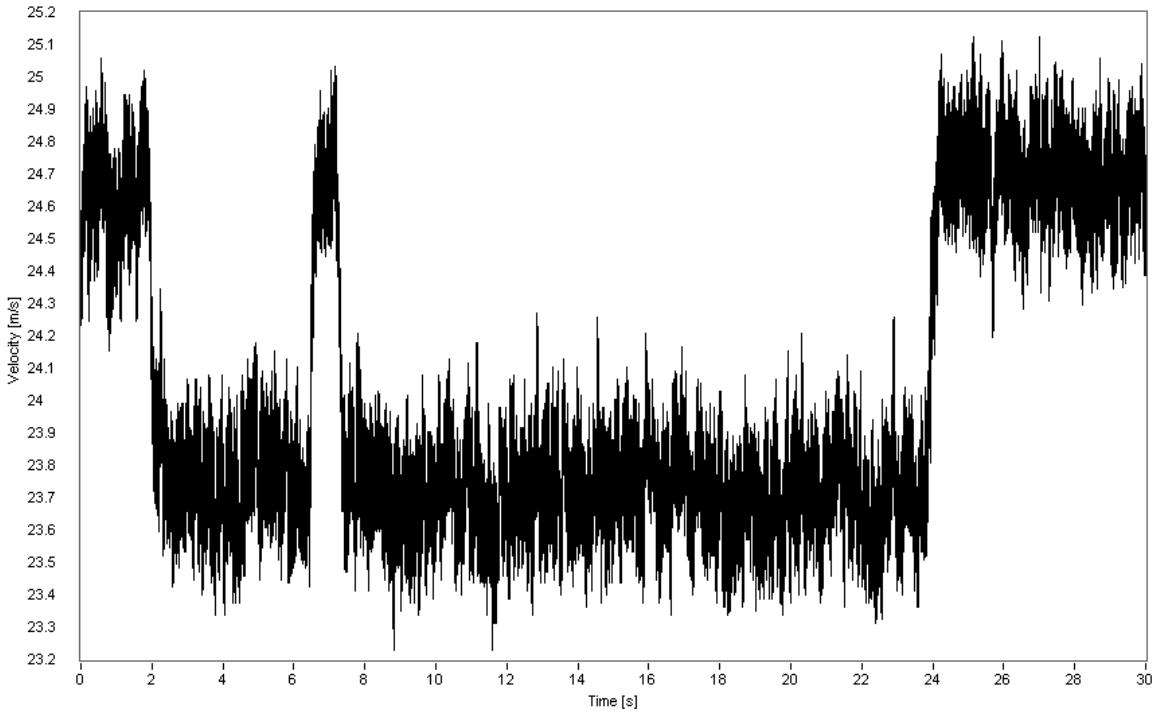

Diagram 9 - Velocity jump phenomenon

The velocity graph is quite surprising and abnormal. There is a slightly noisy velocity level at about 23.7 m/s, but sometimes it suddenly jumps up to 24.7 m/s for a while and then back. This phenomenon lasts only for a few seconds, but influences strongly the average velocity and the turbulence intensity as well.

6.2. Evaluation

After excluding measurement errors, the FFT of the hot wire signal was investigated. The measurement was run up to 30 seconds at 5000 Hz, which provided a very good overview on the disturbances. It was found, that at high frequencies the signal is quite smooth and constant. But at low frequencies the situation is totally different. High amplitude disturbances dominate the signal and two problematic frequency bands can be discerned: between 0-70 Hz and 160-180 Hz (denoted by lightblue streaks on Diagram 10).

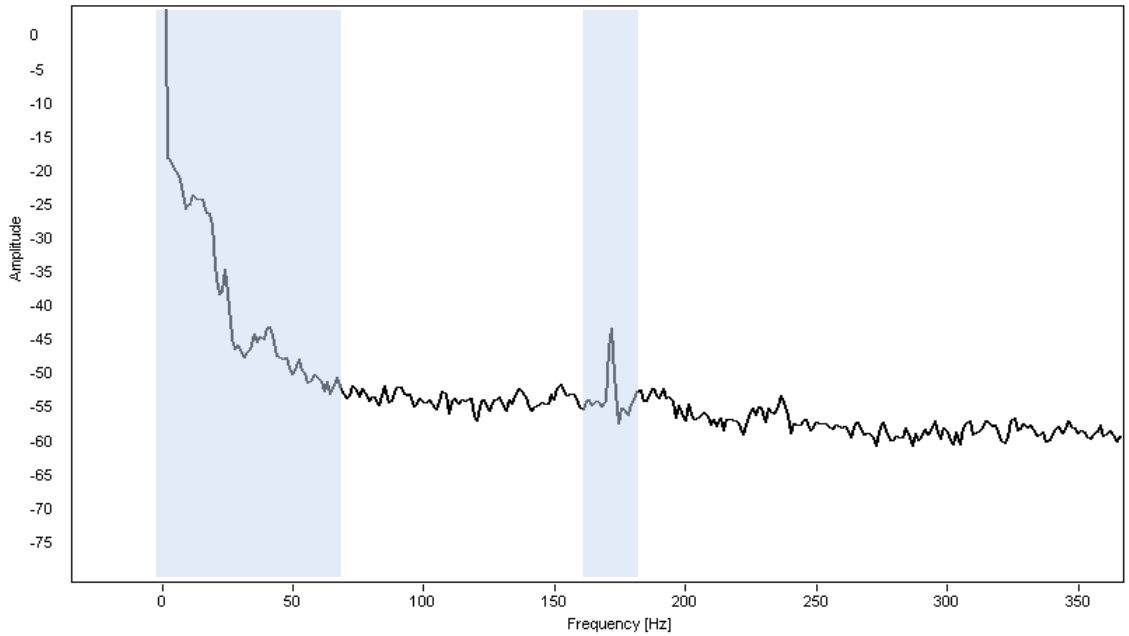

Diagram 10 - FFT of hot wire signal (low frequency domain)

The sudden velocity jump phenomenon lasts for seconds and the magnitude is quite significant. This means a very-very low frequency and high amplitude disturbance, which is covered by the first frequency band. The second frequency band is a local peak at around 170 Hz. At this point, the ventilator became suspicious. Now, the investigation of the fan follows. The fan is driven by a three-phase, four-pole electric motor, which runs at 1420 RPM on full throttle. The impeller consists of seven blades, thus the disturbance frequency can be calculated as follows.

$$n = 1420\frac{1}{\min} \cong 23.67\frac{1}{\sec} \tag{6.1}$$

$$f = n \cdot N \cong 23.67\frac{1}{\sec} \cdot 7 \cong 166\text{Hz} \tag{6.2}$$

Due to this short calculation it became clear, that the 170 Hz, high amplitude disturbances in the flow are synchronized with the impeller rotation. It is quite abnormal, that the rotational frequency can be detected so clearly at the confuser outlet. However, the main issue is the velocity jump phenomenon, so the source of the problem could not only be the ventilator, but any elements downstream. Therefore, further investigations were needed.

6.3. Investigations

Some important investigations and focused analyzes were carried out on the different sections of the wind tunnel in order to track down the source of the sudden velocity jump phenomenon. The following elements were under investigation.

6.3.1. Confuser

The problem was detected with hot wire anemometer right after the confuser at first. However, the confuser means a well-designed decreasing cross-section downstream, therefore rising velocity and reducing pressure in the flow. The confuser only accelerates and smoothens the flow. Its inside surface is very sleek and precisely manufactured. Consequently there is no danger of separation or any disturbance, so the velocity jump problem does not originates from this element.

6.3.2. Settling chamber

The settling chamber is a constant cross-section element, which consists of honeycomb and screens. It makes the velocity distribution smoother and smoother by design, similarly to the confuser. So the problem cannot originate from the settling chamber section.

6.3.3. Diffuser

Since the expansion angle of the diffuser is about 40 degrees, there is a possibility of separation, despite with the theoretical results. Therefore, some parts were disconnected from the wind tunnel and the airflow was investigated inside the diffuser. The flow was visualized by small pieces of yarns, which were fixed on a steel rod [Figure 21]. Due to the gap between the curved mesh and the sidewall, the whole section was accessible.

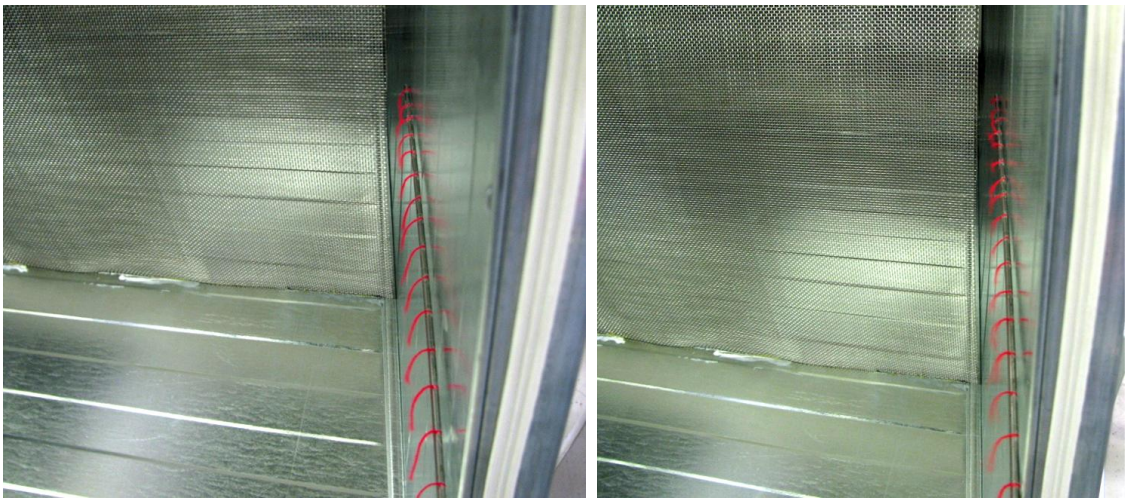

Figure 21 - Flow visualization in the diffuser at low speed (left) and high speed (right)

Thanks to this quick and simple technique, it became obvious that there is no separation in the diffuser at low speed and the flow is quite uniform near the wall. However, at high speed all yarns began to vibrating strongly and showed signs of separation before the middle mesh. After this short investigation, hot wire measurements were implemented at several points on the diffuser outlet surface. The measurement was run up to 30 seconds at 5000 Hz, in other words all settings were the same as previously. The objective was to get an exact overview on the time signal of the velocity. Diagram 11 represents a typical velocity graph (green curve).

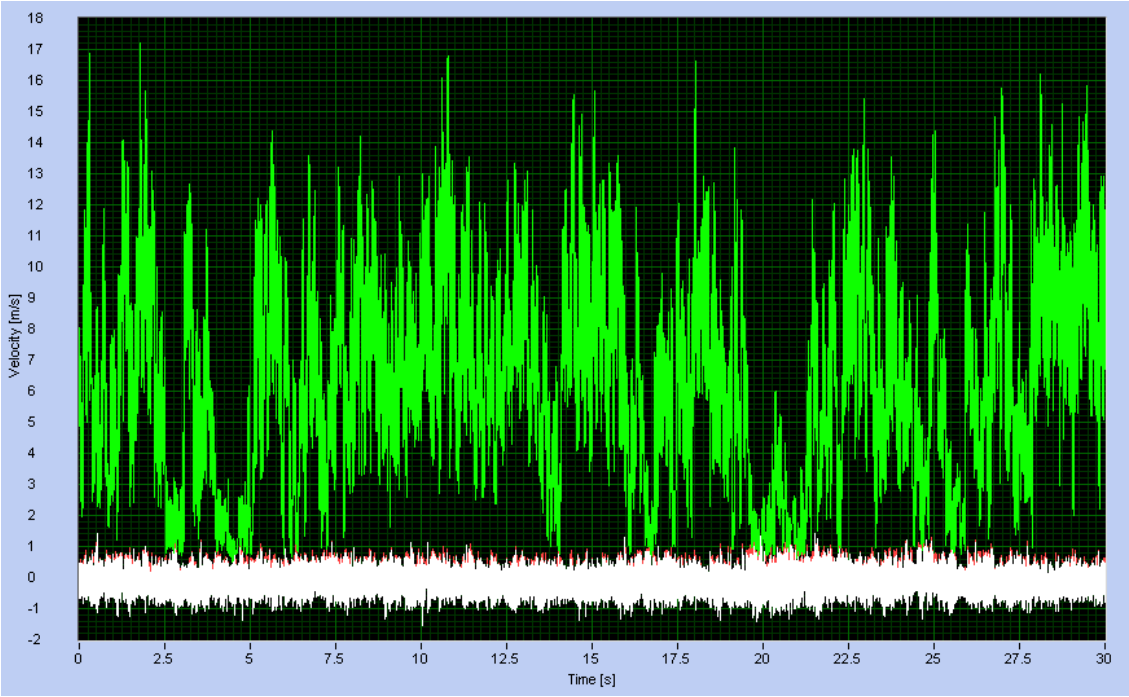

Diagram 11 - HWA measurement after the diffuser

Very strong fluctuation is observable, the velocity varies between 0 and 17 m/s, so it occurs that there is no flow for a while. The reason is that the diffuser angle is too high and the flow cannot follow the geometry, hence a flow jet develops, which does not fills out the cross-section fully. Moreover, this flow jet is unstable, causing transient velocity fluctuation in time and also in space. Two stable states were detected: initially the flow jet bended to the upper left corner, then suddenly pushed through the diagonal to the lower right corner and then back. The phenomenon was perceptible by hand, later it was indicated with a „yarn rod" and finally measured with thermal anemometer. The outlet cross-section was divided into 3x3 equal squares and the velocities were recorded at the centre points in both states [Figure 22]. The measurement points and the results can be seen below.

Figure 22 - Thermal anemometer measurement after the diffuser

As the next list shows, many errors were discovered inside the diffuser.

- Inhomogeneous velocity distribution
- Vibrating meshes and sidewalls
- Gap between curved meshes and sidewalls
- Separation at the inlet
- Velocity fluctuation
- Unstable flow

6.3.4. Guide vanes

The velocity jump problem could be affected also by the guide vanes, because of the separation danger after the leading edges of the curved vanes. The diffuser was removed and a hot wire measurement was implemented with unchanged settings at several points after the guide vanes. Unfortunately, the signal was so noisy and the fluctuations were so high, that no consequences could be drawn. This is because of the measurement area was too close to the impeller, thus the gust effect caused by the blades was very strong. Anyway, the guide vane series can strengthen or weaken the velocity jump phenomenon, but should not cause.

6.3.5. Ventilator

The main problem of the fan is the housing. More precisely, the design of the suction side is not favourable for the airflow. The reason is simple; this *Helios* ventilator was developed for HVAC applications, where the easy installation into building ventilation systems is crucial. Therefore, some fluid mechanics drawbacks were accepted by the manufacturer. As the next photos show, the ventilator sucks the air originally from the backside, and hence there is a strong break in the flow [Figure 23]. In case of radial fans, direct axial suction is more advantageous for the impeller [15]. Thus a new suction side was designed and implemented at the Department. The process will be demonstrated later.

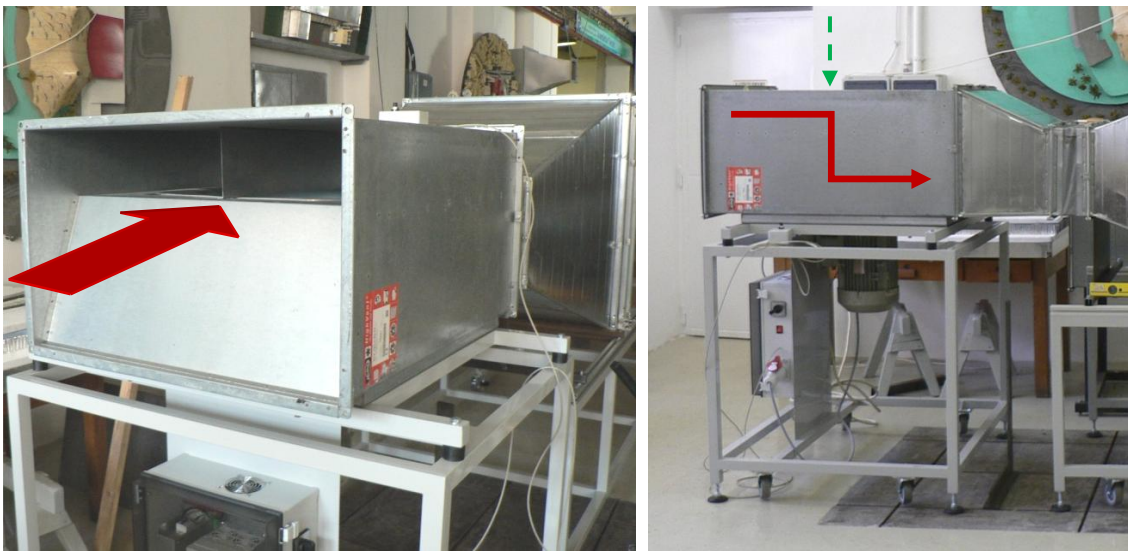

Figure 23 - Original suction design (red arrows) and optimal case (green arrow)

The *Helios* ventilator is bounded by a closed housing. No direct access is secured to the impeller; thereby it is hard to carry out precise measurements. However, one important investigation was implemented. The ventilator was set to maximal velocity and the impeller was flashed with a stroboscope from the intake opening. It was found, that the fan operates at constant RPM, thus the generated volume flow rate has to be constant too. Since the flow can be considered incompressible, the average velocity should be constant in each cross-section (except near the impeller, due to the pulsation of the blades). This suggests that the velocity jump problem has no close connection with the impeller rotation.

6.3.6. Conclusion

Table 8 below summarizes the investigated elements, the measurement methods and the results.

Section	Method	Conclusion
Confuser and settling chambers	Yarns HWA HWA	no separation improved flow homogeneity velocity jump
Diffuser	Yarns Visual TA TA HWA	strong separation Vibrating meshes and sidewalls Non-uniform velocity distribution Unstable flow conditions velocity jump
Ventilator	Stroboscope LDA Visual	Constant RPM Non-uniform velocity distribution Incorrect suction side and housing design

Table 8 - Problem analysis results

Taken all round, the wide-angle diffuser, the ventilator suction side and housing are suspicious to generate the experienced velocity jump problem. The diffuser has many errors, but the redesign of the diffuser is a serious and complex modification. The modification of the ventilator housing is again a special and more dangerous area. Thereby a new suction side was implemented and investigated at first.

7. SUCTION SIDE MODIFICATION

7.1. Options

Several possible solutions were investigated such as suction hole, flange, pipe, or cone [Figure 24]. A suction hole is very easy and cheap to manufacture, but it results accessible suction inlet and high disturbance sensitivity. A flange design is better, but still includes some fluid mechanics drawbacks due to significant separation zones around the inlet. A suction pipe means strong resistance against flow disturbances, but also higher losses, space requirements and so transportation problems. The suction cone design has only advantages from fluid mechanics point of view. It provides smooth intake flow, isolated suction inlet and minimal pressure losses. However, the cone can be manufactured only by external companies, so it is a quite expensive solution.

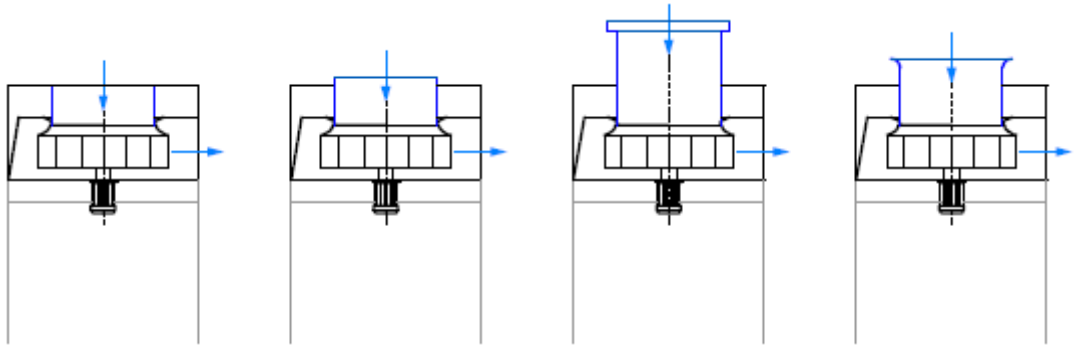

Figure 24 - Suction hole, flange, pipe, and cone sketches

7.2. Concept

Eventually, the highest possible flow quality, thus the suction cone solution was chosen. The ordered product and its properties are showed below [Figure 25].

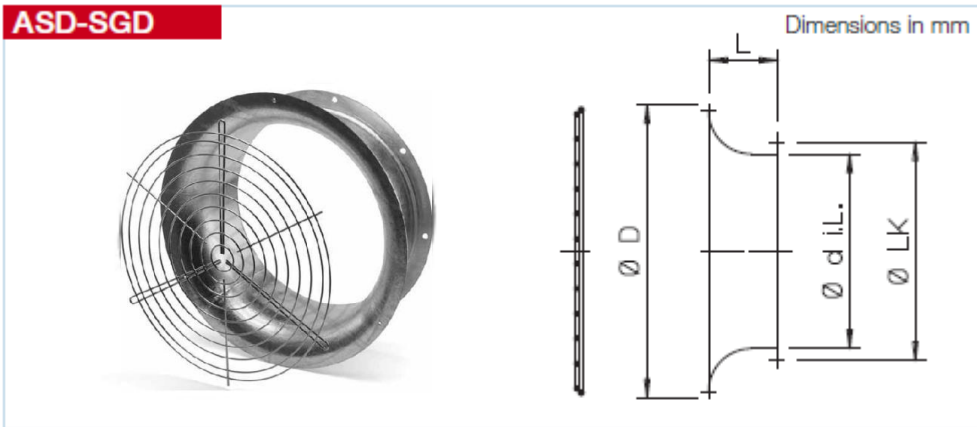

Type	Ref. No.	ø D	L	ø d i.L.	ø LK	Weight in kg
ASD-SGD 450	1419	595	140	450	487	5.7

Figure 25 - Helios bell mouth with wire guard

7.3. Realization

The ordered cone also contained a protection grid by design, which prevents the access to the rotating impeller. The installation was carried out as follows. First of all, a circular hole was cut out from the upper side of the housing, due to the cone diameter [Figure 26].

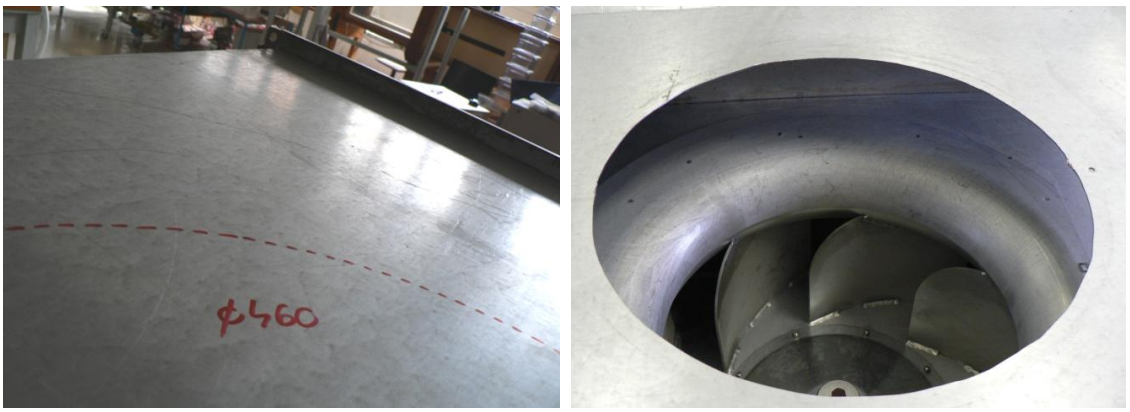

Figure 26 - Housing modification

Thereafter, a tube section was manufactured and attached to the cone, thus bridge the gap inside the ventilator box to the impeller [Figure 27].

Figure 27 - Suction cone with additional tube section

Before fixing the cone to the housing, a hermetic sealing was implemented between the outlet edge of the additional tube section and the lower sheet of the housing [Figure 28].

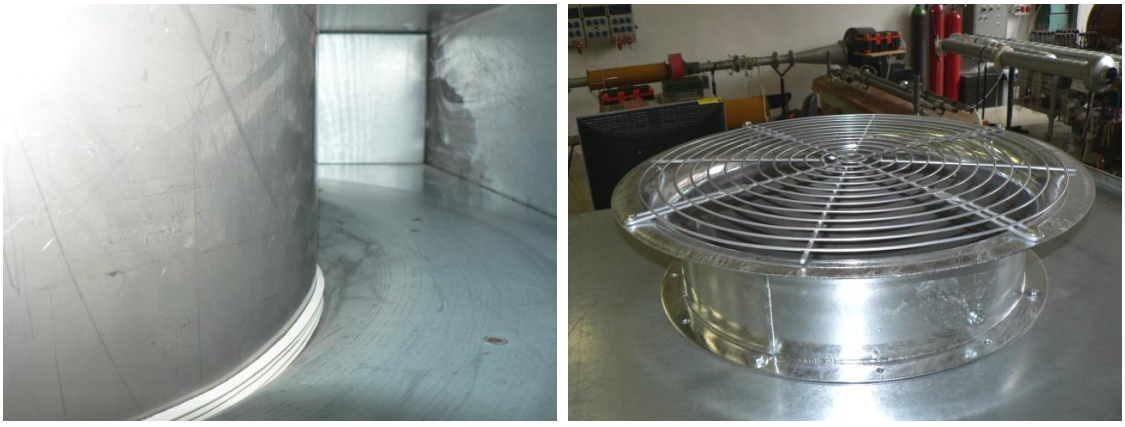

Figure 28 - Sealing and assembly results

Finally, the original suction side was closed down with its original cover sheet (as Figure 29 shows), thus the suction side modifications were finished and the wind tunnel was ready for new measurements.

Figure 29 - Closed backside

7.4. Measurement

After the suction side modification, a hot wire anemometer measurement was performed directly behind the confuser again at maximum volume flow rate. The measurement program settings are listed below in Table 9.

Barometric pressure [Pa]	99500
Temperature [C]	20.9
Sampling rate [Hz]	5000
Sampling time [s]	30
Signal filtering	No
Time data format	Waveform spreadsheet

Table 9 - Program settings

All settings were the same as before the suction side modification. A test measurement was performed at the center point of the cross-section to check the flow. The average velocity magnitude increased to 25 m/s thanks to the advantageous suction side modification. Unfortunately, the velocity jump phenomenon was still observable and the turbulence intensity did not changed at all. The new suction side design has many positive effects, but it did not solve the main problem. Thus the diffuser was decided to be redesigned. The next chapter represents the process.

8. DIFFUSER MODIFICATION

8.1. Options

The diffuser has many errors as investigated earlier and the main issue is the significant boundary layer separation. Separation is the consequence of wide-angle design, but the geometry is given, cannot be changed. Another possible solution could be a new mesh configuration.

Originally, the diffuser contains two meshes, one at the inlet and another at the half length by design. However, according to a recent series of experiments [10], the optimal mesh configuration inside a diffuser is usually different. The center mesh should be closer to the inlet or more meshes would be required to avoid separation. One problem is that more meshes cause higher losses in the flow. Another problem is that the fixing of a mesh into the diffuser is very complicated and expensive, and later the rearrangement is impossible. Finally, a new, empty diffuser was ordered and assembled to the wind tunnel without meshes. A hot wire measurement was implemented with the usual settings, but the sudden velocity jump problem did not disappeared. Hence, it became clear that the fluctuation phenomenon is independent from the mesh configuration.

This point was some kind of “dead end”, because neither the outer geometry was changeable, nor the mesh rearrangement was an option. Then I proposed a new idea based on a Formula One racecar. In 2009, the Brawn GP Team introduced a brand new solution on their cars: the so-called “double diffuser” [Figure 30]. This concept worked so perfectly, that the BGP001 cars dominated almost whole season and secured championship title before the last race [5].

Figure 30 - Brawn GP concept and results [5]

Originally, the diffuser angle has an upper limit, over which the flow separates and the diffuser efficiency drops down dramatically. The idea is to split the diffuser into two or more channels by guide vanes, thus forcing the airflow to follow the geometry [Figure 31].

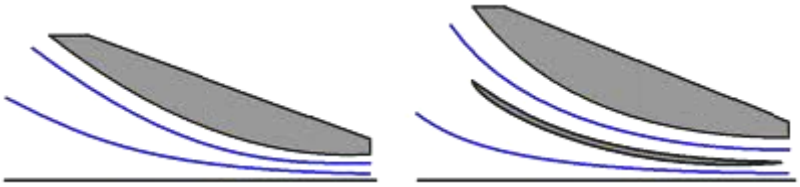

Figure 31 - Simple and double diffuser sketches

8.2. Concept

The split-level concept was chosen, not just because this was the only viable option, but it also has a lot of advantages. Splitting the volume of the diffuser is not so complicated and no internal meshes are needed. The splitters are rigid plates, thus there is no danger of vibration or fixing problems. This solution is quite compact and cheap. The split-level diffuser was designed and developed using CFD techniques.

8.3. Simulation

8.3.1. Velocity profile

First of all, the velocity distribution at the diffuser inlet was required, because this is a fundamental boundary condition in the simulation. Therefore, the velocity field was measured right behind the guide vane series with hot wire anemometry. Thanks to the traverse system the entire outlet cross-section was measured along without any assembly process. The measurement was controlled by „Pressure&Force" program. Table 10 lists the most important measurement settings and Figure 32 represents the measurement result.

Barometric pressure [Pa]	100700
Temperature [C]	28.3
Sampling rate [Hz]	256
Sampling time [s]	10
Signal filtering	No
Time data format	Waveform spreadsheet

Table 10 - HWA settings at diffuser inlet

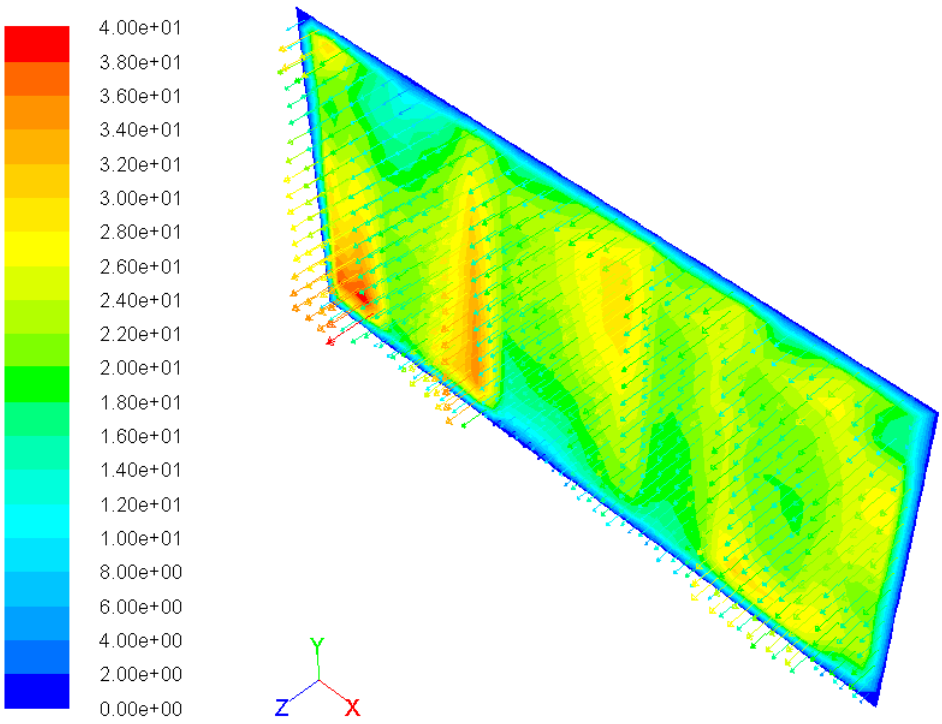

Figure 32 - Velocity profile after the guide vanes

Almost 400 measurement points were recorded. The velocity profile was prepared in *Excel*, and then imported into *ANSYS Workbench*. A very simple simulation was made in order to check the velocity inlet boundary condition. According to Figure 32, the velocity distribution is not uniform of course, because the measurement was implemented directly behind the vanes, which are otherwise not far from the rotating impeller. The contours of the trailing edges are slightly visible, since the velocity is different on the two sides of the vanes.

8.3.2. Validation

The validation of the simulation model is very important. Two diffusers were available at this time: the original diffuser with the central mesh inside, and the new one which was empty. As mentioned before, the meshed diffuser has many errors (vibration, gaps, unstable flow conditions…). But due to the split-level concept no meshes will be assembled. Therefore, the empty diffuser was chosen for the simulation and for the measurement.

Foremost, the theoretical static pressure curve was estimated. The average velocity was computed for the entire inlet cross-section from the velocity profile measurement. The size of the diffuser cross section changes linearly. Since the air density can be considered as a constant value, using the continuity equation [14], the average velocities, then the dynamic pressure distribution were calculated. Moreover, at the outlet the dynamic pressure is equal to the total pressure, because of the ambient static pressure. Since the total pressure is known, the ideal static pressure distribution can be calculated assuming constant total pressure along the diffuser. Finally, the real static pressure distribution was estimated based on the diffuser efficiency [14]. The theoretical results are listed below [Table 11].

z [m]	v [m/s]	p_{dyn} [Pa]	$p_{st,id}$ [Pa]	p_{st} [Pa]
0	21.24	270.7	-254.9	-99.4
0.1	19.45	227.0	-211.2	-82.4
0.2	17.66	187.1	-171.3	-66.8
0.3	15.87	151.1	-135.3	-52.8
0.4	14.08	118.9	-103.1	-40.2
0.5	12.29	90.6	-74.8	-29.2
0.6	10.50	66.1	-50.4	-19.6
0.7	8.71	45.5	-29.7	-11.6
0.8	6.92	28.7	-12.9	-5.0
0.9	5.13	15.8	0.0	0.0

Constant values	
ρ [kg/m^3]	1.2
p_{tot} [Pa]	15.8
η_{diff} [-]	0.39

Table 11 - Theoretical pressure distribution

Thereafter, pressure taps were soldered along the centrelines of the sidewalls and the static pressure distribution was measured at full speed with digital manometer around the diffuser. Figure 33 shows the notation of the sides in a specific cross section.

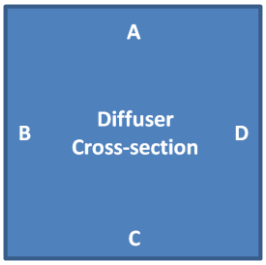

Figure 33 - Notation

The measurement results can be seen in Table 12. It has to be mentioned, that the pressure fluctuations were substantial, due to the strong flow separation. Hence, the listed measurement values are mean values. The static pressure average and the fluctuation amplitude were calculated in each cross-section to simplify further comparisons.

	z [m]	0.080	0.179	0.263	0.366	0.449	0.554	0.625	0.747	0.815
p_{st} [Pa]	side A	-82.5	-60	-42	-27	-19.5	-16.5	-16.5	-13.5	-13.5
	side B	-75	-	-72	-	-24	-	-18	-	-18
	side C	-156	-120	-60	-39	-28.5	-16.5	-15	4.5	30
	side D	-162	-	-48	-	-30	-	-27	-	12
Average [Pa]		*-118.9*	*-90.0*	*-55.5*	*-33.0*	*-25.5*	*-16.5*	*-19.1*	*-4.5*	*2.6*
Fluctuation [Pa]		±54.7	±47.5	±38.9	±33.3	±31.4	±29.1	±29.8	±26.1	±24.3

Table 12 - Static pressure distribution on diffuser sidewalls

Firstly, a recent article was investigated about simulation of a three-dimensional diffuser, which was very informative and helped to find proper settings [11]. The 3D geometric models were created in *Workbench Designer* [Figure 34]. The rubber element before the diffuser inlet, and the outlet section after the diffuser outlet were also modelled to improve simulation accuracy. However, the outer room was not modelled, because some simple preliminary simulations proved that it has no significant effect on the diffuser section, but highly increases computational time.

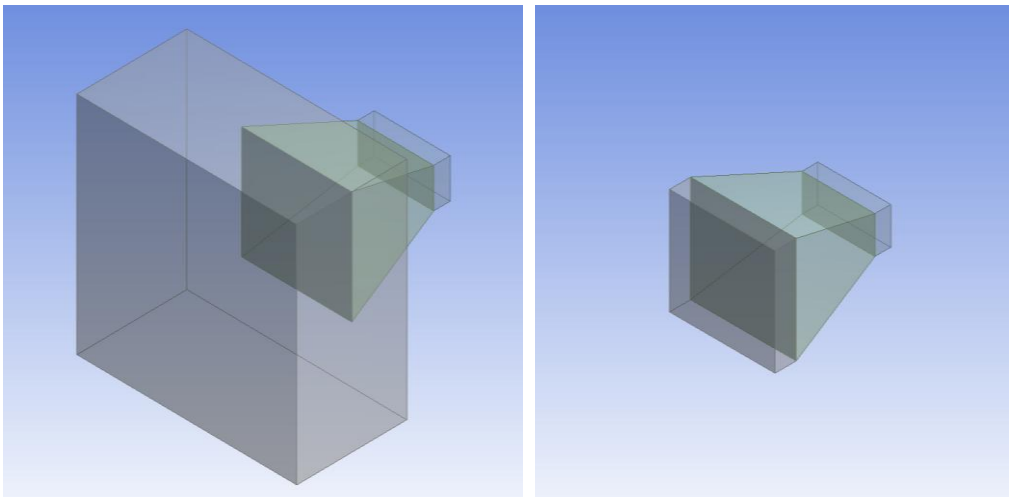

Figure 34 - Diffuser geometry model with and without outlet room

The mesh was generated in *Workbench Mesher* using the automatic algorithm with some prescribed refinements near the sidewalls [Figure 35]. The following parameters characterize the mesh quality:

- Quad elements
- 48.314 cells
- Maximum cell skewness = 5.14852e-001

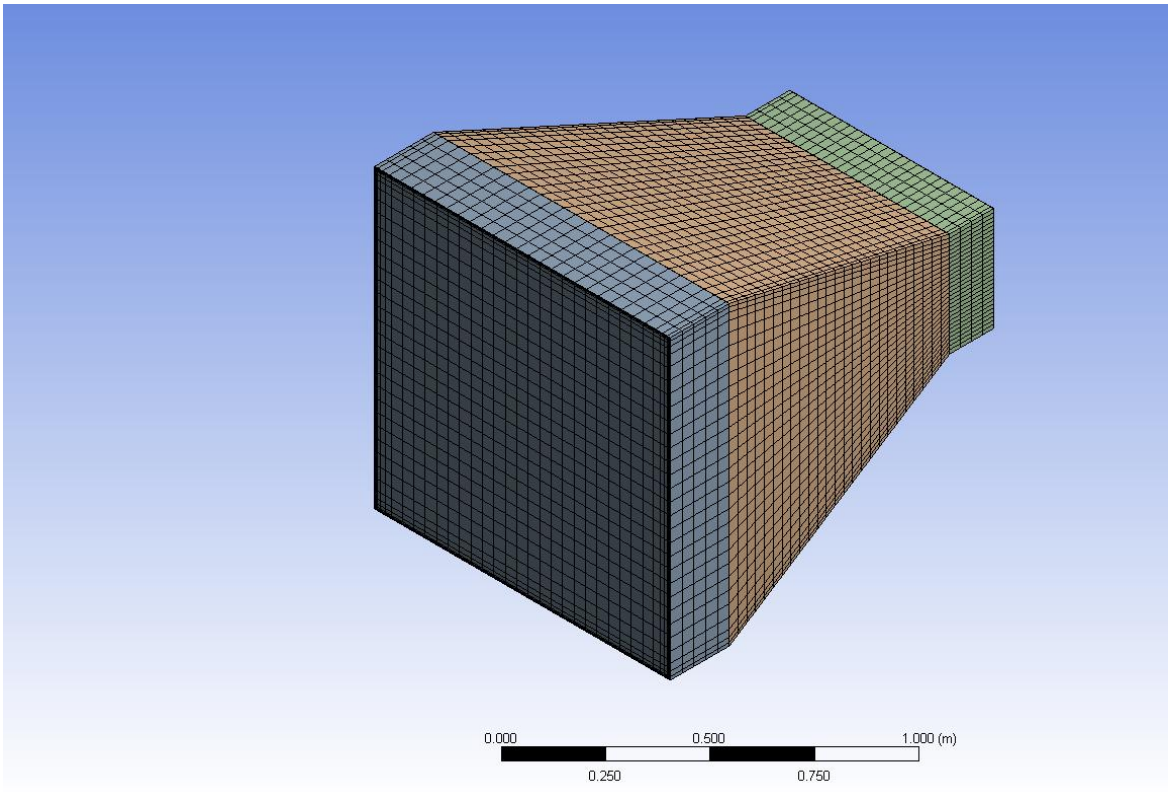

Figure 35 - Diffuser mesh

The mesh quality was acceptable for this quick and simple simulation. The CFD-model setup was defined to reach as simple and fast simulation as possible. The next settings were applied:

- Pressure-based, Steady, 3D space solver
- Viscous, Realizable k-Epsilon model with Enhanced Wall Treatment
- Constant air properties
- Simple scheme, Second Order Upwind
- Convergence criterion of Residuals up to 10^{-6}

After the simulation finished, the static pressure distributions were queried along the centerline of the four sidewalls [Diagram 12].

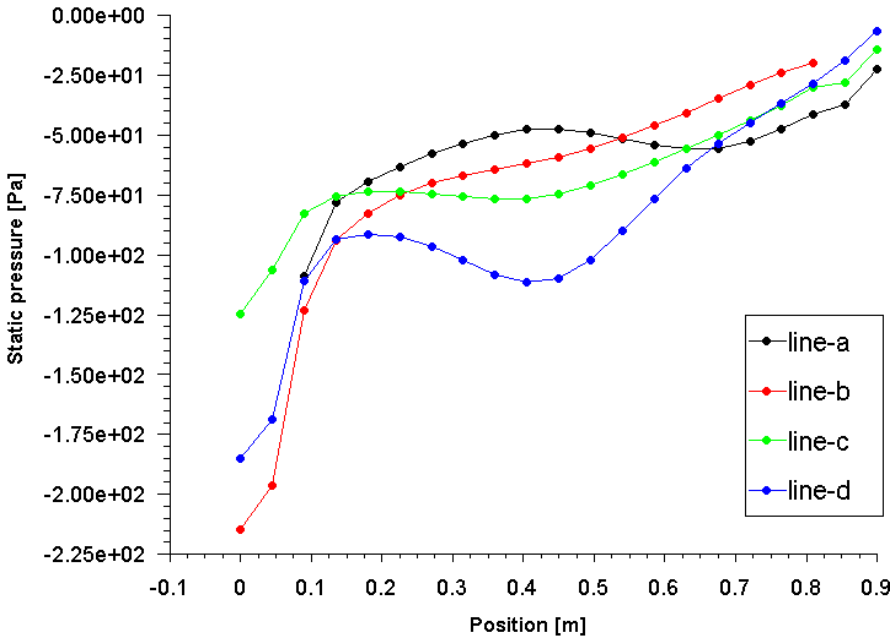

Diagram 12 - Static pressure distribution along diffuser sidewalls

The curves are very similar to each other, thus an average curve was calculated to simplify the diagram for further comparisons. The following diagram illustrates the theoretical, measured and simulation average static pressure curves [Diagram 13].

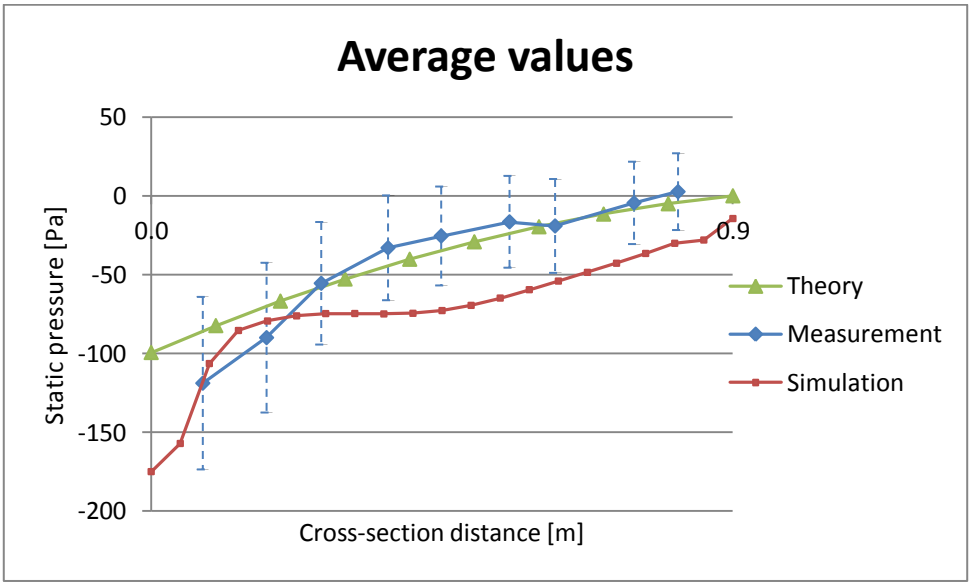

Diagram 13 - Average static pressure curves

This is just a rough comparison, but accurate enough to see that the curves are pretty close to each other. The theoretical and measured pressure curves match almost perfectly. The simulation pressure curve is not so identical. This is probably because of the strong separation phenomenon. However, the tendency is quite similar for all three curves and the simulation curve is close to the lower fluctuation limit of the measured distribution. Therefore, the simulation model and parameters were considered to be validated.

8.3.3. Simulation

After the empty diffuser simulation was validated, the split-level concept was investigated. The 3D geometry model was generated in *Workbench Designer* [Figure 36]. The inlet cross-section was splitted into nine equal channels and the plate angles were defined to be the half of the sidewall angles, thus providing lower risk of flow separation.

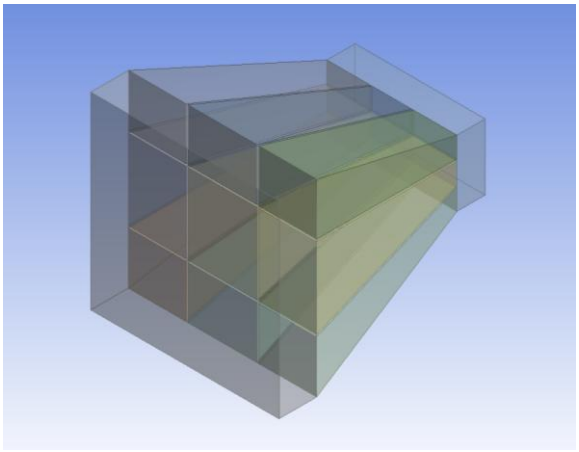

Figure 36 - Split-level diffuser model

The numerical mesh was produced in *Workbench Mesher* using the automatic algorithm with certain prescribed refinements near the walls [Figure 37]. The parameters below characterize roughly the mesh quality:

- Quad elements
- 166.000 cells
- Maximum cell skewness = 5.40747e-001

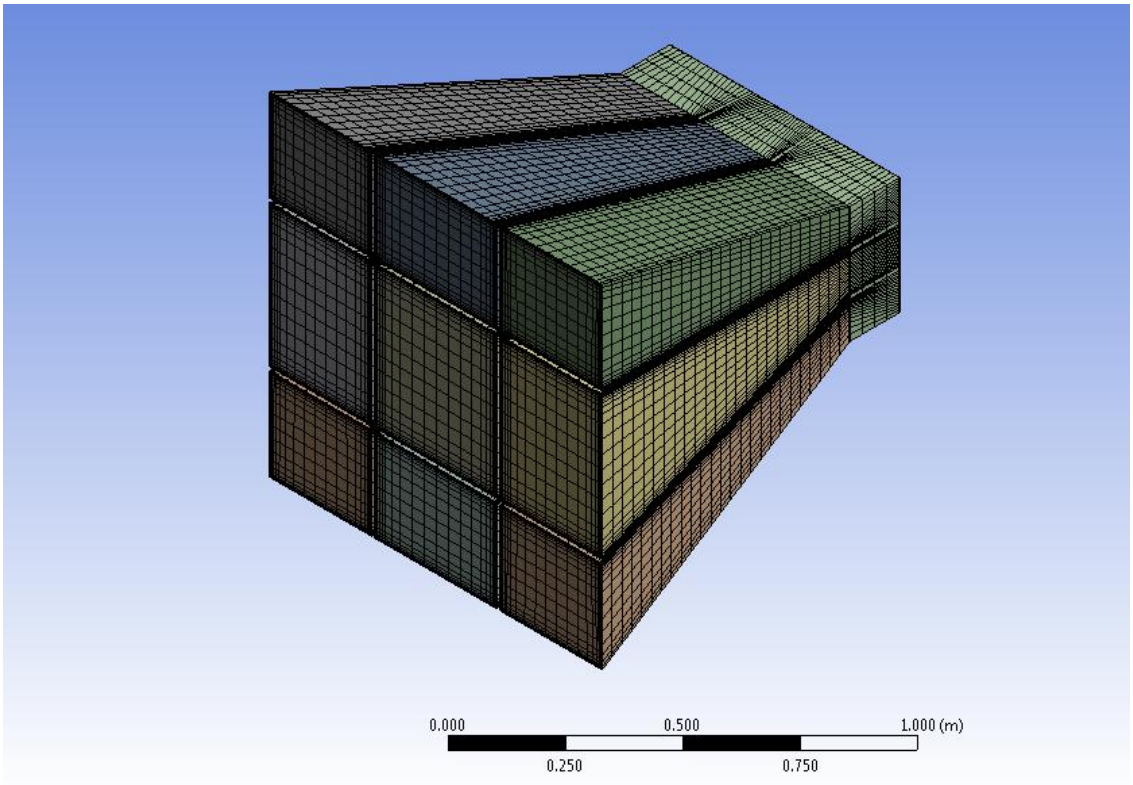

Figure 37 - Split-level diffuser mesh

The mesh quality was far sufficient for this quick and simple simulation. The same CFD-model setup was applied as in case of the empty diffuser previously. Firstly, the velocity distribution and the area-weighted velocity averages were queried at the inlet surface of the channels [Figure 38]. The average velocity values in the channels are very different. Due to the unfortunate distribution, there is no possible rearrangement of the horizontal and vertical plates to improve the flow homogenity. Therefore, this symmetric configuration was accepted, which otherwise also has advantages such as easy manufacture and assembling.

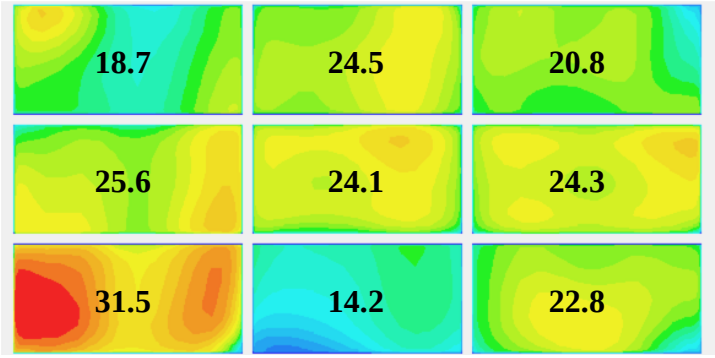

Figure 38 - Inlet velocity distribution [m/s]

During the investigation of the 3D streamlines, a separation was observed after the plate leading edges. Thus, a new simulation was implemented with curved plates to avoid inlet separation. Figure 39 compares the streamlines for the two different configurations. In case of curved plates, the inlet separation disappeared as expected. But at the outlet the situation became quite surprising; a strong separation appeared due to the curvature. Because of the outlet flow homogenity is more important; the flat plate design was kept.

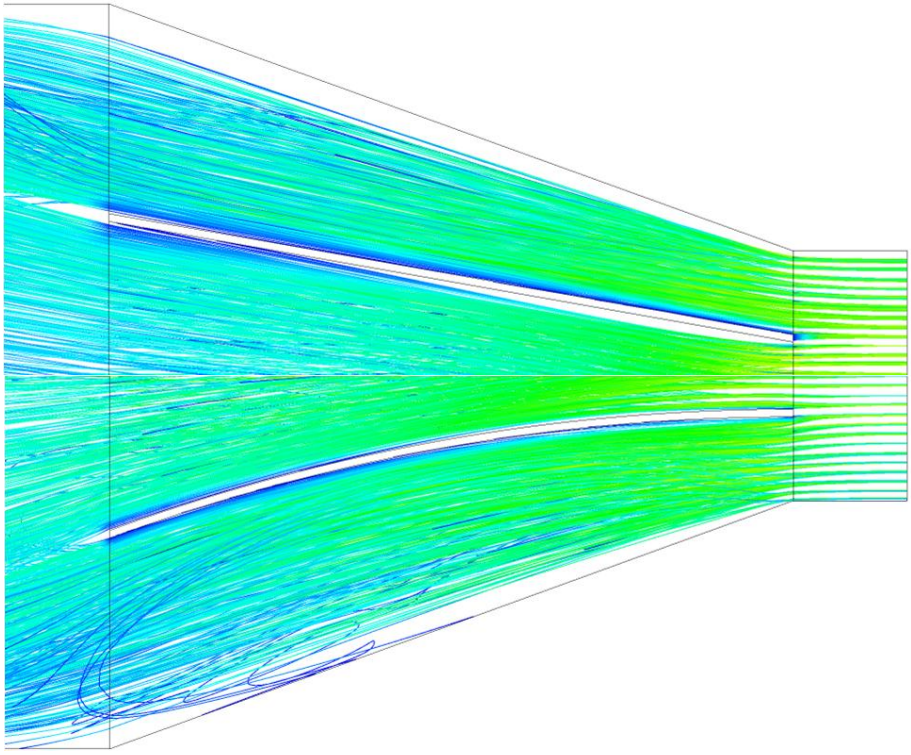

Figure 39 - Flat plates (upper) and curved plates (lower mirrored)

Finally, the velocity distributions were plotted at the diffuser outlet cross-section and then the area-weighted velocity averages were calculated for all flow channels. Figure 40 shows the results and the improvement compared to the empty diffuser.

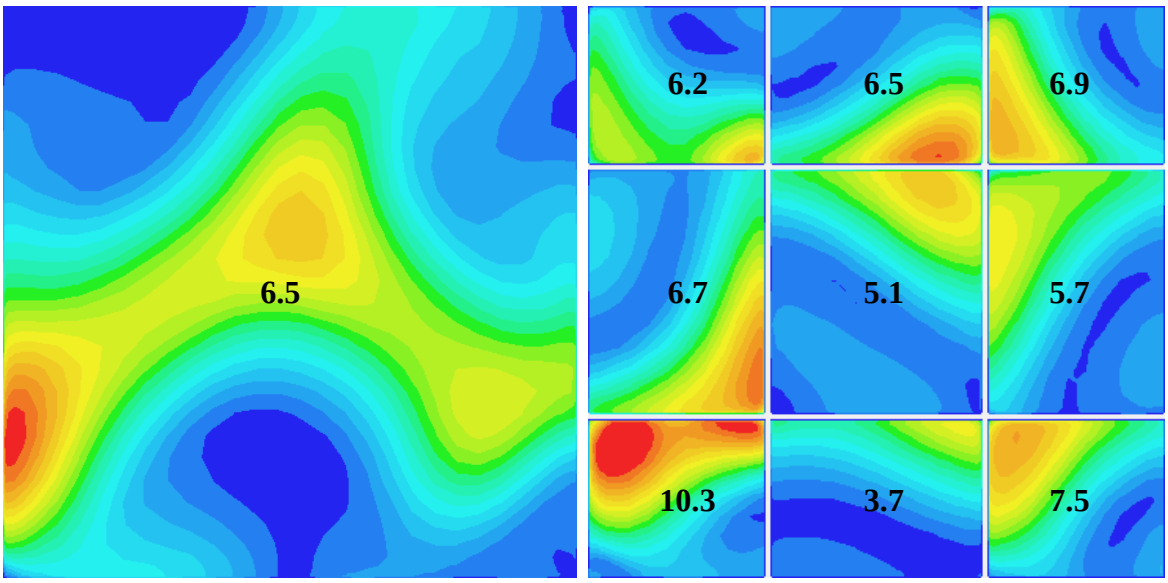

Figure 40 - Outlet velocity distributions for empty vs. splitted diffuser [m/s]

It is obvious that a significant flow homogenity improvement was reached, thus the simulation proved the efficiency of the split level diffuser construction. The velocity distribution is still not uniform, but the result is absolutely acceptable in the aware of the initial data.

8.4. Realization

As mentioned before, splitting the internal volume of the diffuser by wooden plates is very easy to implement. Flat pattern was created and the cut to size wooden plates were ordered from an external company. Than the plates were fixed together and assembled into the diffuser [Figure 41]. The sidewalls were screwed to the edges of the plates, thus providing a more rigid construction and smaller vibration.

Figure 41 - Split-level diffuser construction

8.5. Measurement

Using „yarn rod" quick investigations proved that the flow fills out all channels and there is no sign of any unstable phenomena. Then all remaining parts were attached, and the flow was measured at the center of the outlet cross section. The hot wire anemometer was not accessible at this time, so Prandtl-tube was used. Diagram 14 represents the measurement results below.

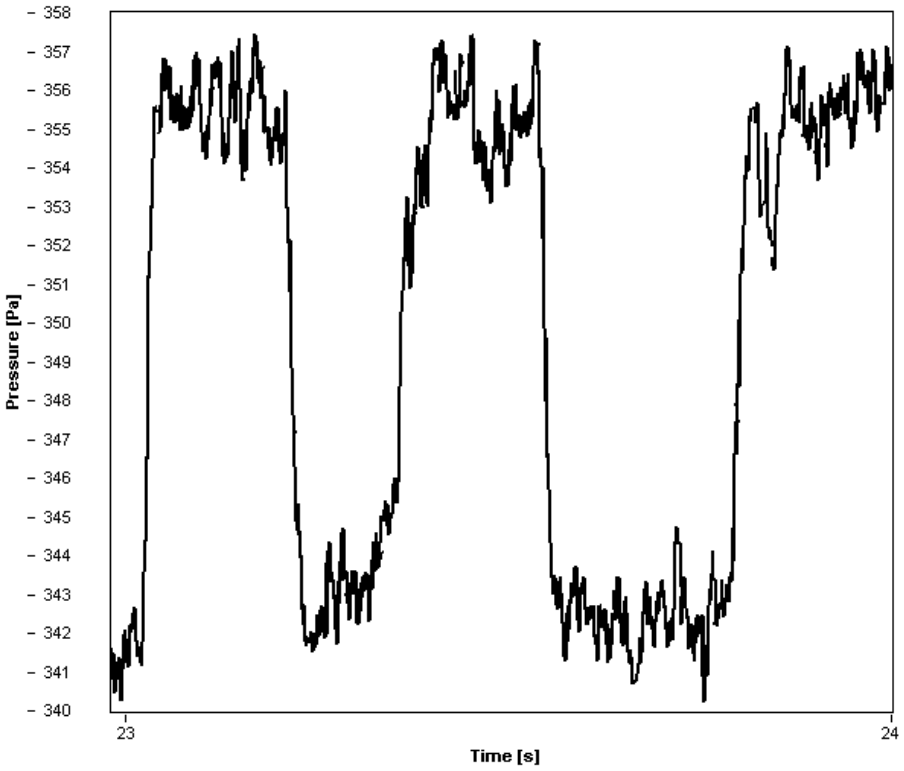

Diagram 14 - Dynamic pressure time signal

Unfortunately, the velocity jump effect is still observable in the flow. Even through the jump amplitude decreased, the turbulence intensity is about 3%, which is still totally unacceptable. However, the flow quality improved highly thanks to the split-level diffuser concept. Table 13 lists the main problems of the original diffuser and compares to the new one (colours: valid, moderate and solved problem).

Original diffuser	Problem	Split-level diffuser
	Inhomogeneous velocity distribution	
	Vibrating meshes and sidewalls	
	Gap at the curved meshes	
	Unstable flow conditions	
	Separation at the inlet	
	Velocity fluctuation	

Table 13 - Diffuser comparison

9. PRESSURE MEASUREMENTS

9.1. Introduction

After so many modifications, the sudden velocity jump phenomenon – which is the main problem of the wind tunnel – is still valid. Therefore, even more static pressure taps were soldered on the sidewalls of the wind tunnel. The idea was to measure the dynamic pressure at the outlet and the static pressure on the sidewalls of a specific element simultaneously. After that, considering the measured time signals, the time instant of the outlet velocity jump can be detected and compared to the static pressure curve of the given element. Thus, the source of the velocity jump problem can be found. The table below clarifies the location and number of the pressure taps [Table 14].

Element	**Number of pressure taps**	**Description**
Confuser	4	at the inlet
Settling chambers	8	4x2 on the vertical sidewalls
Diffuser	28	2x5 on the lower angle + 2x9 on the higher angle sidewall
Connection	2	at the middle of the vertical sidewalls
Ventilator	15	2x6 on the vertical sidewalls + 3 on the backside (cover removed)
SUM	57	

Table 14 - Static pressure taps

It has to be mentioned that quite long silicone tubes were used, because the pressure measurements covered the full length of the wind tunnel. The problem is that long silicone tubes can damp, or even amplify the fluctuations. Therefore, the RMS values cannot be considered as correct measurement results. However, very high amplitude (tens of Pascals) and very low frequency (seconds long) pressure jumps were expected to be measured, thus the disturbance of the long silicone tubes is not relevant. The mean pressure values and the signal tendency can be measured very accurately with this method.

9.2. Instruments

Silicone tubes were attached to the pressure taps, which were led to a 12-channel pressure transducer. The transducer voltage signals were sampled simultaneously by a dynamic data acquisition system, which was connected to the computer. The channel calibration was performed using a Betz-manometer. The calibration and measurement processes were implemented through "Pressure&Force" *LabVIEW* program. The measurement configuration is represented on Figure 42.

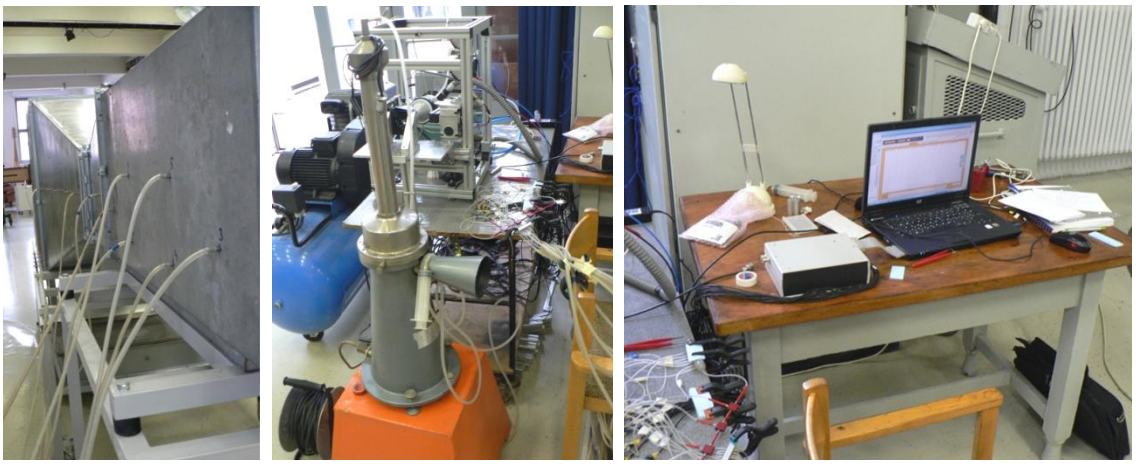

Figure 42 - Pressure measurement system

A Prandtl-tube was fixed at the center of the confuser outlet cross-section, which provided the reference pressure signal [Figure 43]. The digital manometer was needed only to check the outlet velocity magnitude quickly.

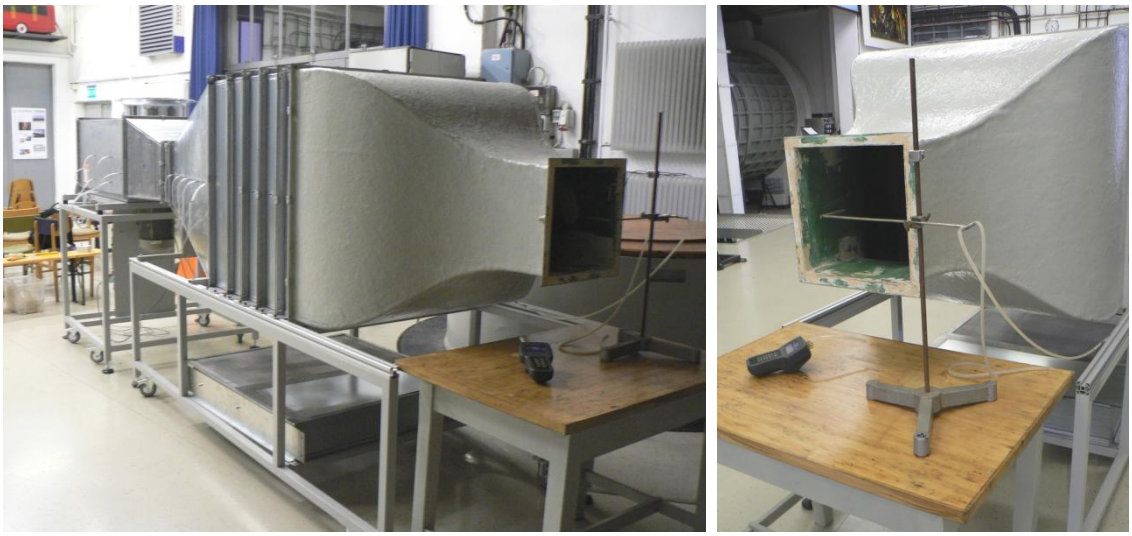

Figure 43 - Reference pressure

There was not enough channels to measure on all pressure taps at the same time of course, thus different configurations were figured out to get valuable and comparable measurement results.

9.3. Overall system investigation

Firstly, the ventilator housing, the connection element, the diffuser and the confuser (inlet and outlet) were measured. Then the guide vane series was removed and the measurement was repeated to investigate the effect of the vanes. The pressure channel configuration is illustrated on the schematic model below [Figure 44].

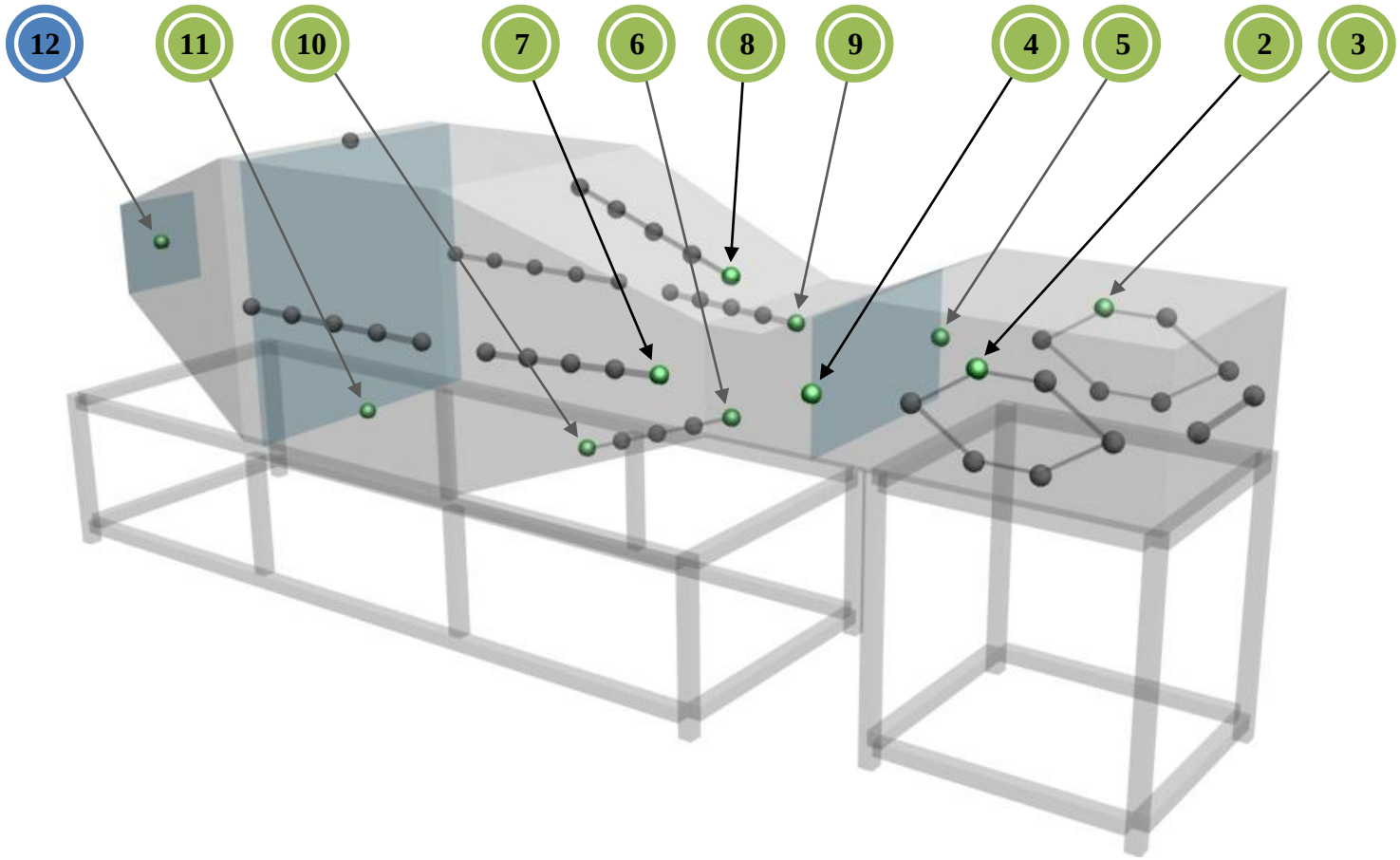

Figure 44 - Pressure channel configuration

The measurements were carried out on 50 Hz (maximal) fan speed for 300 seconds with 20 Hz sampling rate. The 20 Hz signals were recalculated to 2 Hz pressure curves and only the most characteristic 60 seconds were represented due to clarity. The measurement results with the guide vane series inside can be seen below. Diagram 15 shows the pressure curves and Table 15 demonstrates whether the specific channel signal follows the sudden dynamic pressure jump (detected on the reference channel) and also the type of the signal jump.

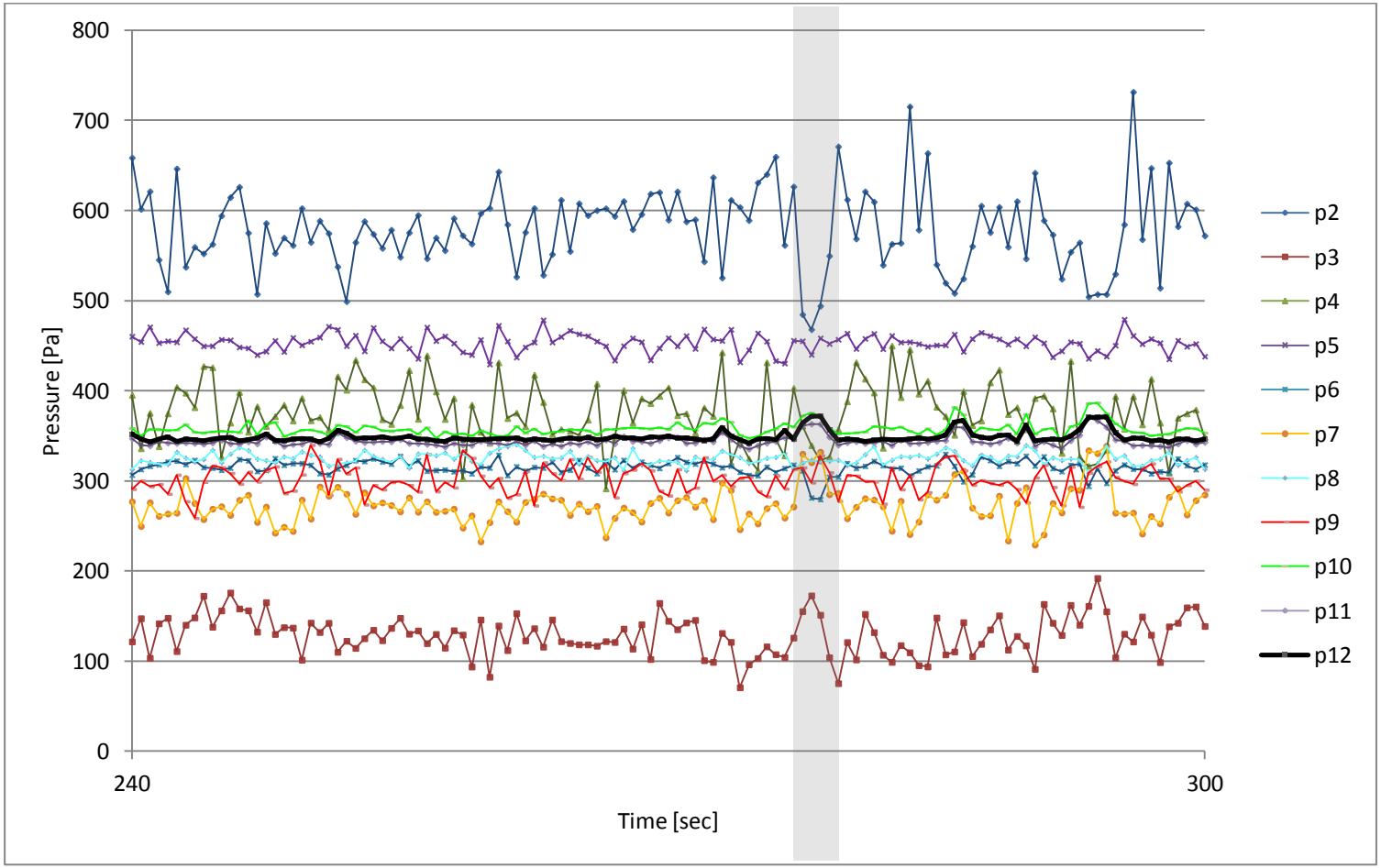

Diagram 15 - Pressure curves with guide vanes

Ch.	Follows?	Type
p2	yes	-
p3	slightly	+
p4	slightly	-
p5	chaotic	?
p6	yes	-
p7	yes	+
p8	chaotic	?
p9	slightly	+
p10	yes	+
p11	yes	+
p12	ref.	+

Table 15

The next measurement was implemented with the same settings, but without the guide vanes. Again, Diagram 16 shows the pressure curves and Table 16 demonstrates whether the specific channel signal follows the sudden dynamic pressure jump or not.

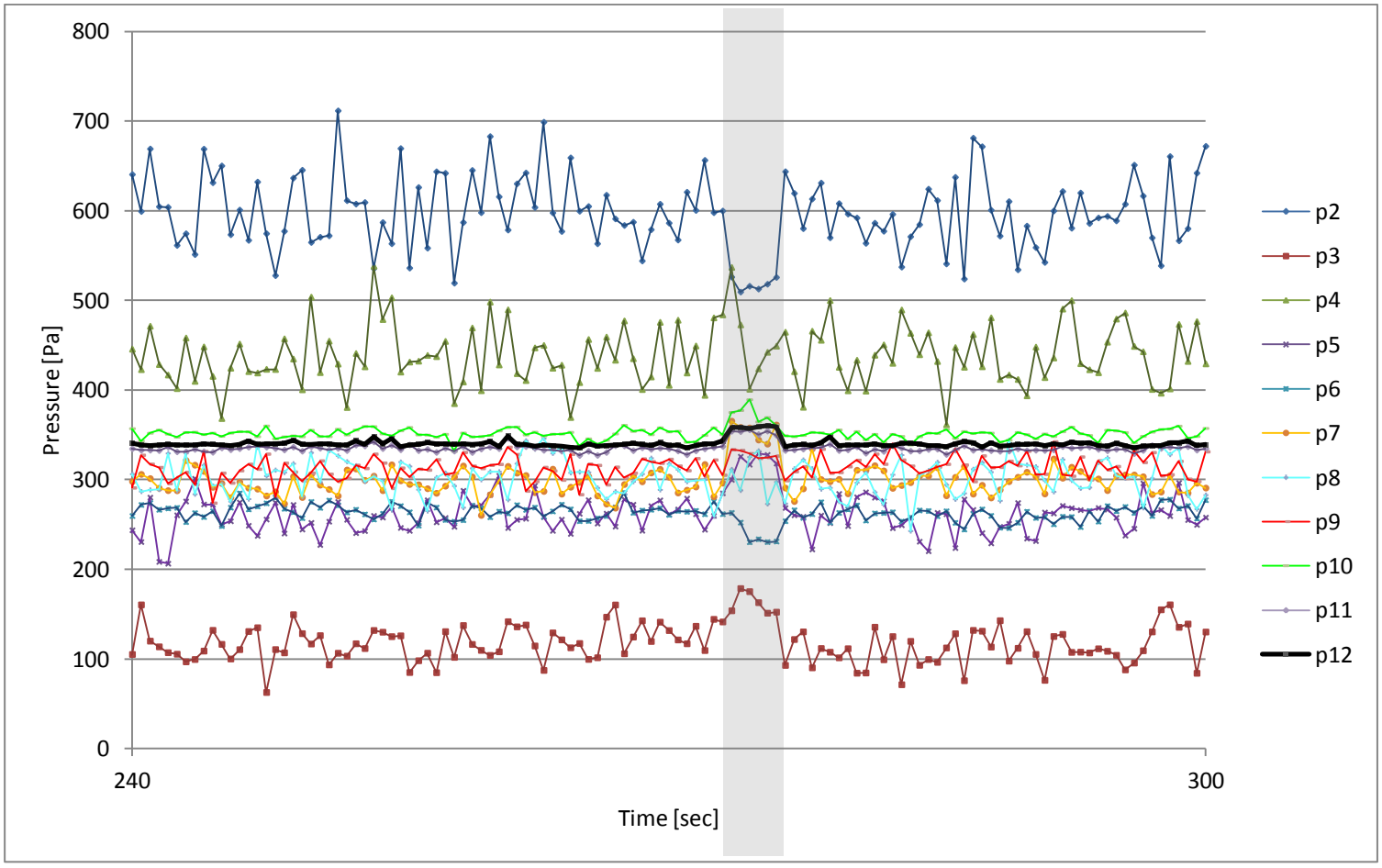

Diagram 16 - Pressure curves without guide vanes

Ch.	Follows?	Type
p2	yes	-
p3	slightly	+
p4	slightly	+
p5	yes	+
p6	yes	-
p7	yes	+
p8	chaotic	?
p9	yes	+
p10	yes	+
p11	yes	+
p12	ref.	+

Table 16

As Table 17 illustrates, the two measurements show good agreement. The only difference occurs in the connection element, but this was expectable because of the guide vane series was removed from it. The guide vane series does not influence the tendency of the overall system behaviour, but decreases signal jump amplitudes, so it makes the flow smoother and reduces unwanted fluctuations. Nevertheless it is not able to eliminate the sudden pressure jump, which is the main problem. This strange phenomenon can be observed in all sections of the wind tunnel, from the impeller to the confuser outlet. Therefore, the problem originates probably from the ventilator housing.

	Guide vanes In		*Guide vanes Out*		
Signal	**Follows?**	**Type**	**Follows?**	**Type**	**Section**
p2	yes	-	yes	-	*Ventilator housing*
p3	slightly	+	slightly	+	
p4	slightly	-	slightly	+	*Connection element*
p5	chaotic	?	yes	+	
p6	yes	-	yes	-	*Diffuser inlet*
p7	yes	+	yes	+	
p8	chaotic	?	chaotic	?	
p9	slightly	+	yes	+	
p10	yes	+	yes	+	*Diffuser outlet*
p11	yes	+	yes	+	*Confuser inlet*
p12	ref.	+	ref.	+	*Confuser outlet*

Table 17 - Result comparison

9.4. Ventilator housing investigation

A new measurement configuration was set as the next picture shows [Figure 45]. Silicone tubes were attached to pressure taps on the housing around the rotating impeller. The reference signal was provided again by the Prandtl-tube at the center of the confuser outlet cross-section.

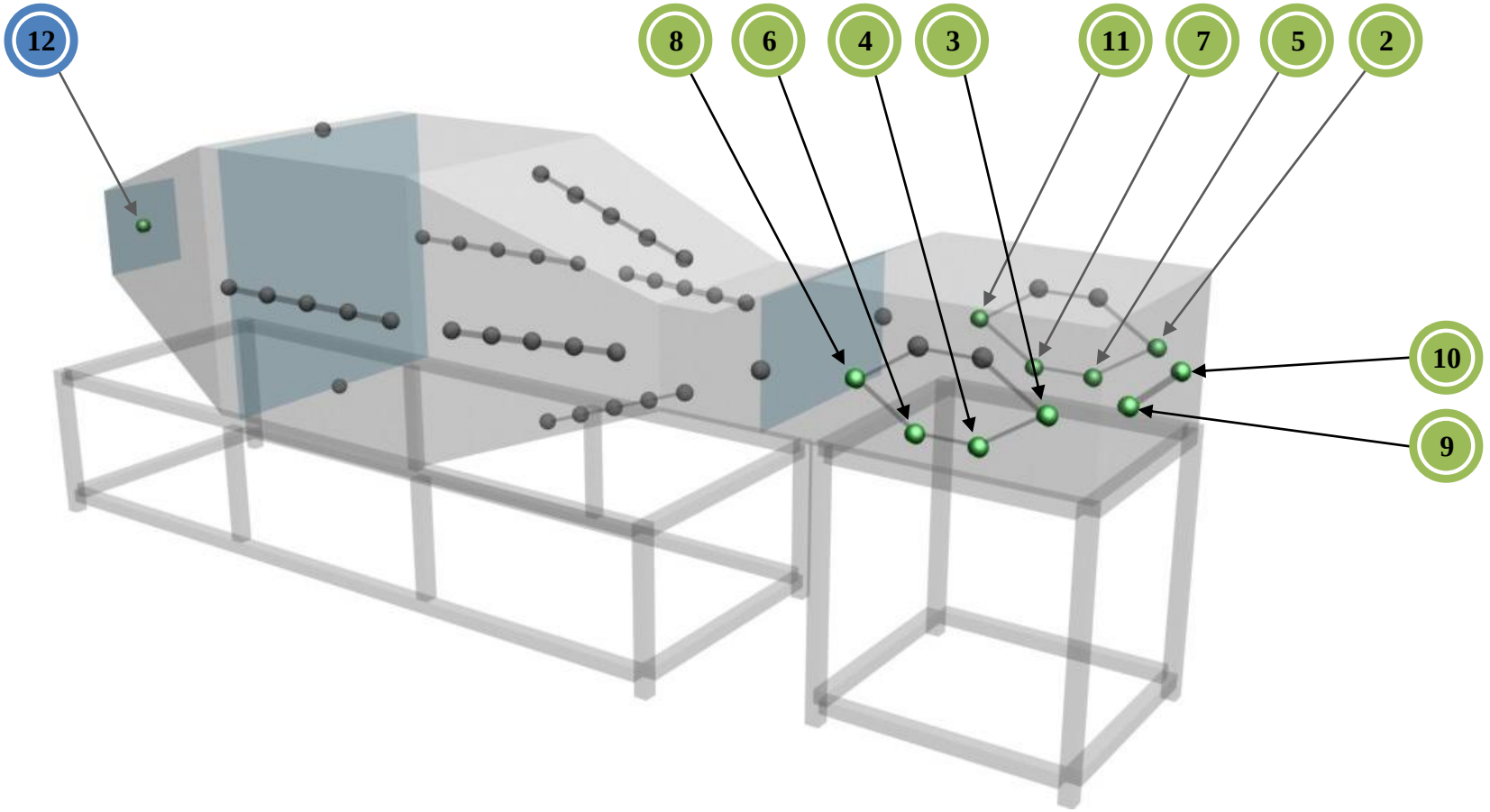

Figure 45 - Pressure channel configuration

Three measurements were carried out on three different fan speeds with the same settings to get a more detailed overview on the velocity jump phenomenon inside the housing. The measurement was run again for 300 seconds with 20 Hz sampling rate. Then the 20 Hz signals were recalculated to 2 Hz pressure curves and only the most characteristic 60 seconds were represented as well as previously. Diagram 17 shows the pressure curves and Table 18 represents the existence, the type and the amplitude of the signal jumps.

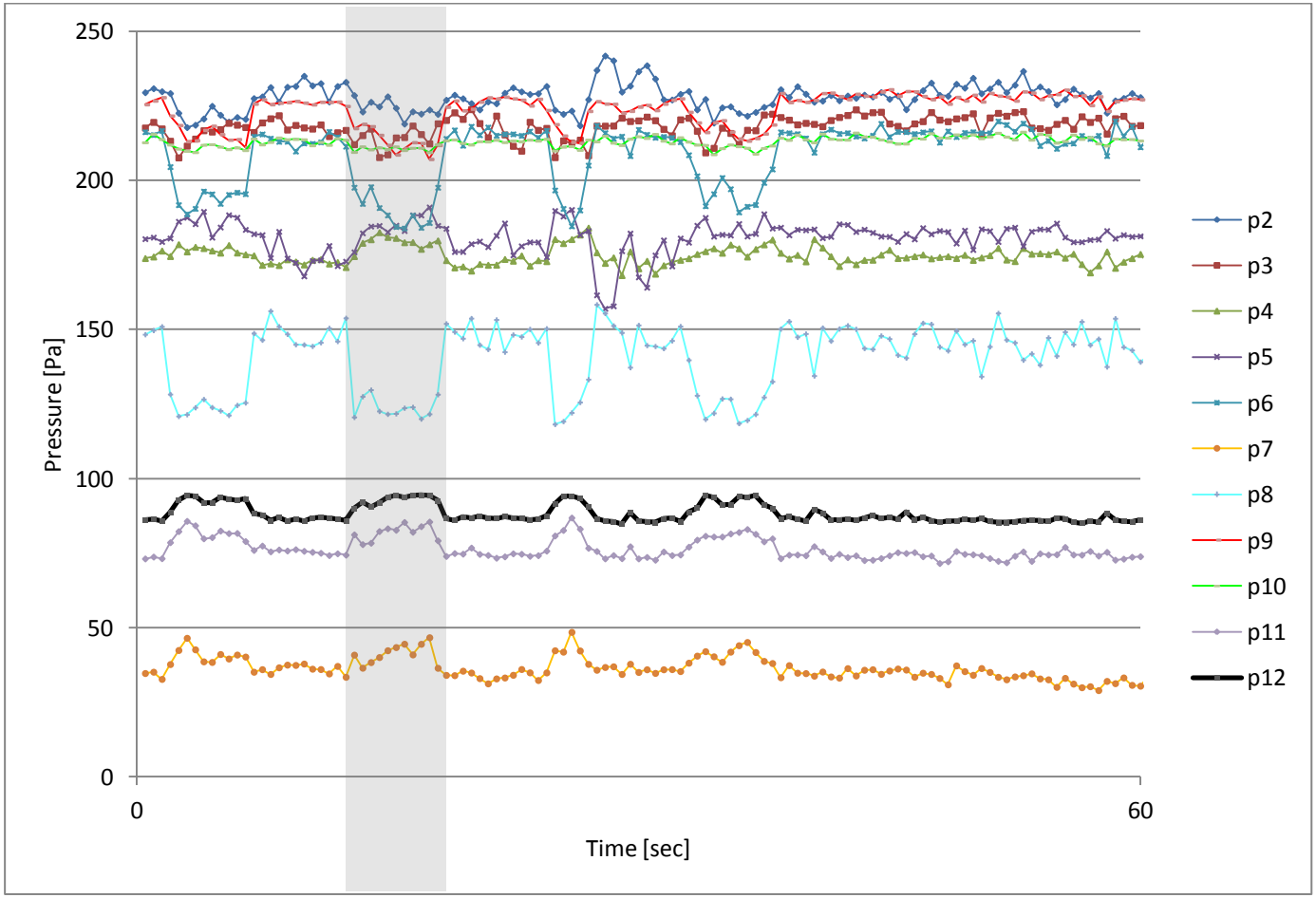

Diagram 17 - Pressure curves @25Hz

Ch.	Follows?	Type	Amplitude
p8	yes	-	high
p6	yes	-	high
p4	yes	+	normal
p3	yes	-	normal
p9	yes	-	normal
p10	yes	-	normal
p2	yes	-	normal
p5	yes	+	normal
p7	yes	+	normal
p11	yes	+	normal
p12	ref.	+	normal

Table 18

The next measurement was implemented with the same settings, but now on 40 Hz fan speed. Again, Diagram 18 shows the pressure curves and Table 19 demonstrates the existence, the type and the amplitude of the signal jumps.

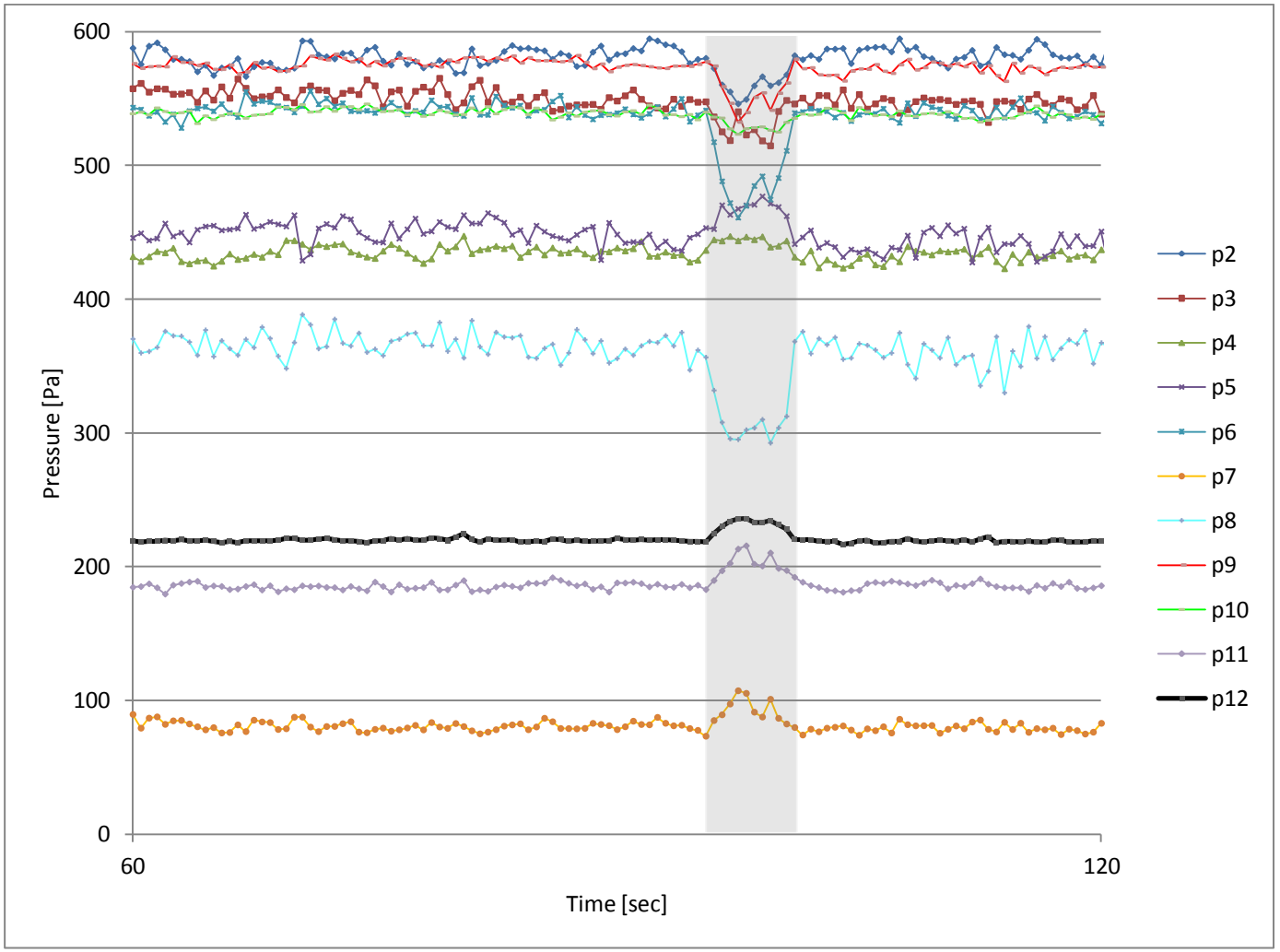

Diagram 18 - Pressure curves @40Hz

Ch.	Follows?	Type	Amplitude
p8	yes	-	high
p6	yes	-	high
p4	yes	+	normal
p3	yes	-	normal
p9	yes	-	normal
p10	yes	-	normal
p2	yes	-	normal
p5	yes	+	normal
p7	yes	+	normal
p11	yes	+	normal
p12	ref.	+	normal

Table 19

The last measurement was carried out on 50 Hz (maximal) fan speed. The pressure curves are illustrated on Diagram 19 and Table 20 represents the existence, the type and the amplitude of the signal jumps such as before.

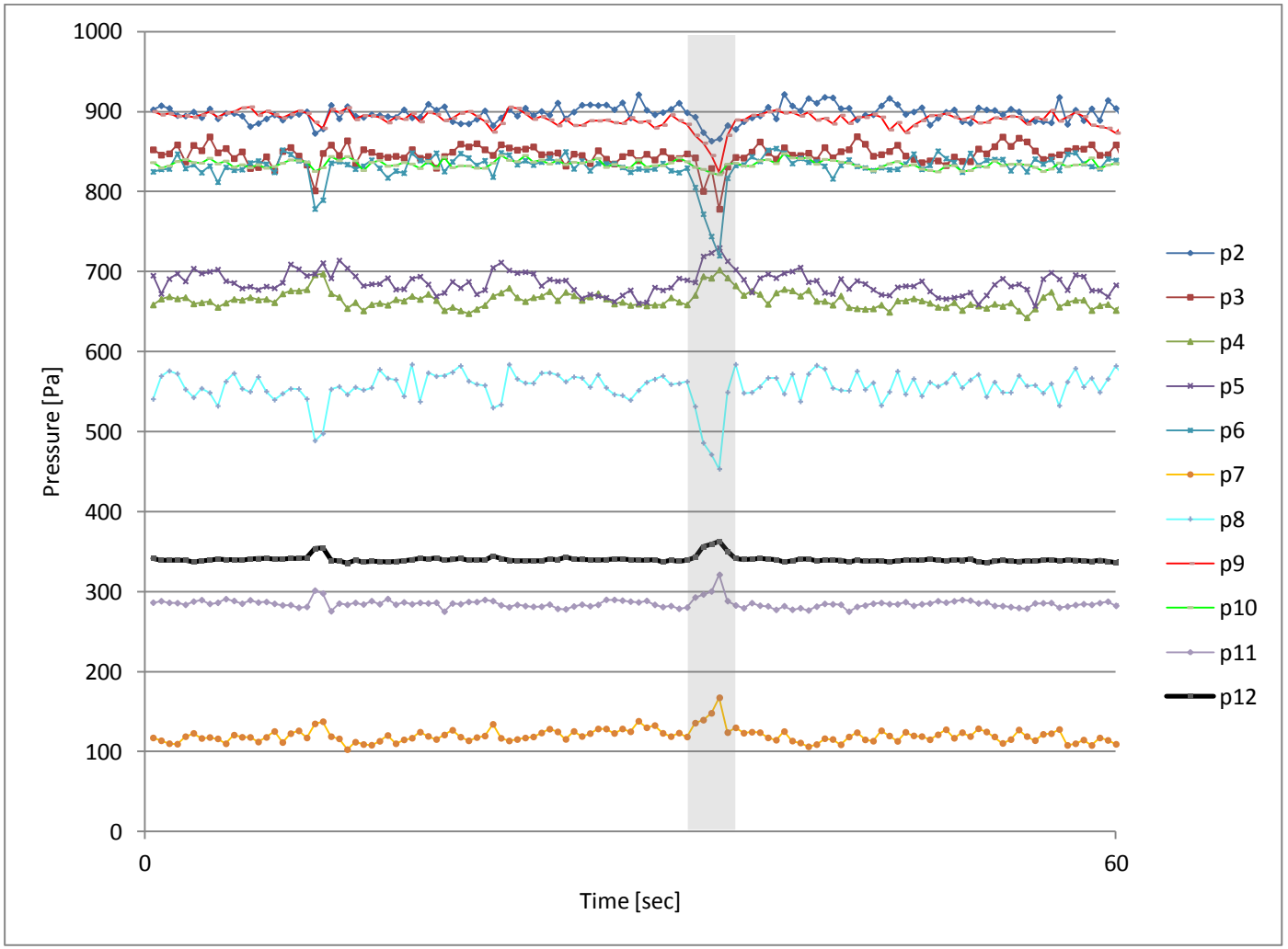

Diagram 19 - Pressure curves @50Hz

Ch.	Follow?	Type	Amplitude
p8	yes	-	high
p6	yes	-	high
p4	yes	+	normal
p3	yes	-	normal
p9	yes	-	normal
p10	yes	-	normal
p2	yes	-	normal
p5	yes	+	normal
p7	yes	+	normal
p11	yes	+	normal
p12	ref.	+	normal

Table 20

Due to the previous diagrams, it is obvious that the sudden pressure jump phenomenon originates from the ventilator. The qualitative pressure fluctuations measured on the taps were exactly the same for all three fan speeds. However, the density and the time length of the jumps decreased on higher velocities. The jump phenomenon was clearly detected on all pressure taps, so the entire housing is affected. The results can be found in the table below [Table 21].

Signal	Follows?	Type	Amplitude	Section
p8	yes	-	high	
p6	yes	-	high	*Housing*
p4	yes	+	normal	*left side*
p3	yes	-	normal	
p9	yes	-	normal	*Housing*
p10	yes	-	normal	*backside*
p2	yes	-	normal	
p5	yes	+	normal	*Housing*
p7	yes	+	normal	*right side*
p11	yes	+	normal	
p12	ref.	+	normal	*Confuser outlet*

Table 21 - Result comparison

First of all, it is important to clarify that the impeller rotates in right-back-left (dextrorotatory) direction. Now it is visible, that at sudden pressure jumps in the outflow (p12), pressure rise occurs at the right side, very strong pressure fall occurs at the left side and even at the back of the housing. This means that from the left and back regions a certain amount of air gets out suddenly, hits the right side and finally reaches the confuser outlet section. This phenomenon occurs probably because of the incorrect housing design.

9.5. Fan throttling Investigation

The idea was that the change of the fan operation point and the inlet flow may effects the sudden pressure jump phenomenon. Firstly, the diffuser inlet mesh was removed and a measurement was carried out without throttle. Then, the half surface of suction cone was covered with a plate from different directions. Therefore, the fan was investigated at new operating points with different inlet flow conditions.

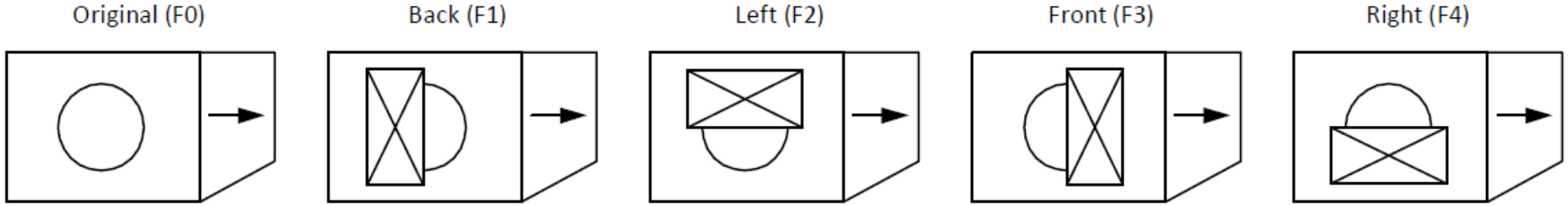

Figure 46 - Legend for measurement configurations

The static pressure on the ventilator housing (where the highest fluctuation amplitude was detected earlier) and the dynamic pressure at the confuser outlet was measured over time for each arrangement.

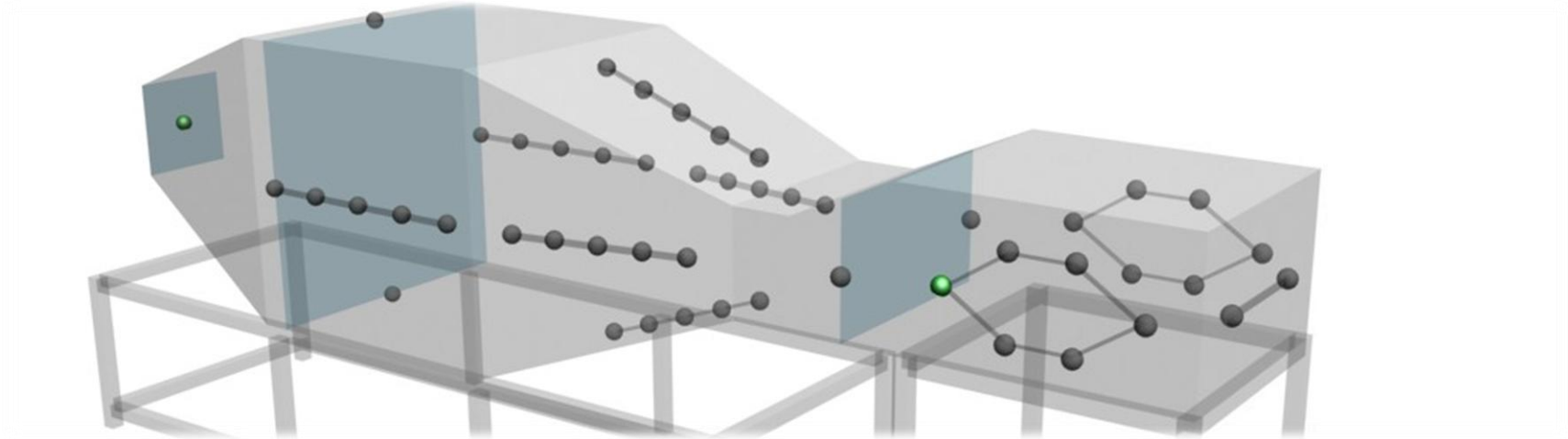

Figure 47 - Measurement points

The measurements were carried out on 50 Hz (maximal) fan speed for 300 seconds with 20 Hz sampling rate. Then the 20 Hz signals were recalculated to 2 Hz pressure curves and only the most characteristic 60 seconds were represented. The guide vane series was not assembled back, but as proved before it has no effect on the existence of the velocity jump problem.

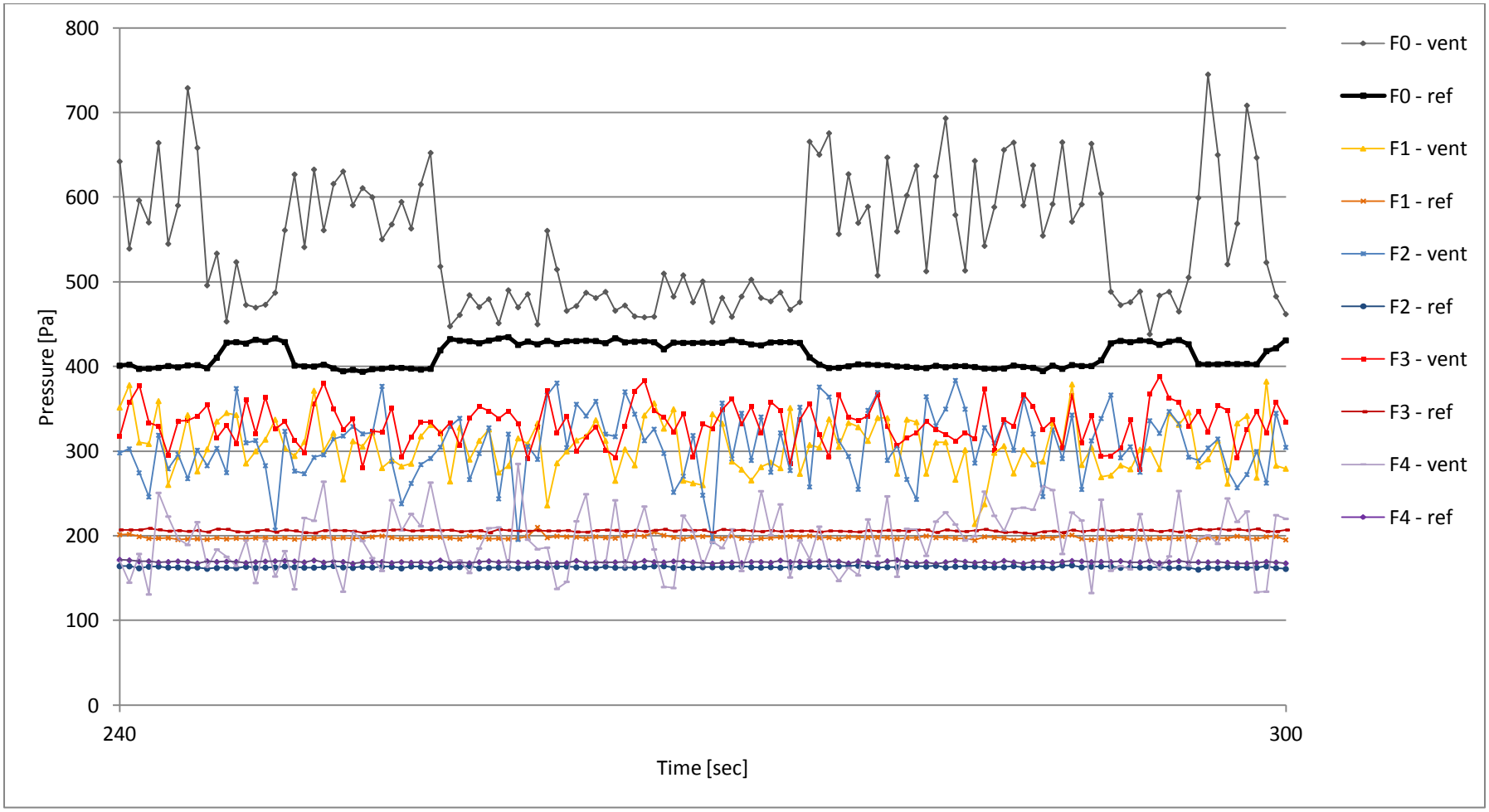

Diagram 20 - Pressure curves for throttling

According to the previous diagram, it is clearly shown that the throttling forced the ventilator to work at new operation points. Moreover, covering the suction cone from the left or right sides means a stronger throttling than the other two directions. Considering the pressure curves measured at the reference outlet, the fluctuation phenomenon seems to be disappeared with the throttling. The next table contains the mean and RMS values for both signal channels and for all measurement configurations [Table 22].

	Ventilator		*Reference*				
	Static pressure		*Dynamic pressure*				
	Mean [Pa]	RMS [Pa]	Mean [Pa]	[m/s]	RMS [Pa]	[m/s]	**[%]**
F0	583.7	150.8	404.3	26.0	12.1	0.39	**1.50**
F1	311.8	98.7	198.0	18.2	3.4	0.15	**0.85**
F2	312.1	110.8	162.4	16.5	2.5	0.13	**0.76**
F3	336.5	70.6	207.1	18.6	3.2	0.14	**0.76**
F4	197.4	120.1	169.3	16.8	2.8	0.14	**0.83**

Table 22 - Throttle results

At the confuser outlet the dynamic pressure mean and RMS values were recalculated to velocity. Thus, the turbulence intensity [%] could be estimated roughly for all cases. Due to the throttling the velocities decreased significantly and the turbulence intensity values became quite acceptable. The problem is that the fluctuation amplitudes changed only proportionally, and the available maximal flow velocity dropped far under the required value (which is 23 m/s by design). Moreover, former measurements indicated that the distortion of the longest silicone tube can be even 0.5% in the RMS value; therefore these turbulence intensity values are very optimistic.

The experiment proved that the unwanted pressure and velocity fluctuation phenomenon can be eliminated by throttling, so it depends on the ventilator operation point and on the inlet flow conditions. However, the turbulence intensity remains too high, while the designed flow speed cannot be reached. Hence throttling cannot be a good compromise. Based on this experiment, two new meshes were built in: a fine covering mesh over the suction cone and a rough mesh at the ventilator outlet. The diffuser inlet mesh was also replaced and repeated measurement confirmed that the turbulence intensity reduced to 1.1%, whereas the outlet velocity decreased 2 m/s. The turbulence intensity is still high, but the direction was right, so it was decided to keep the meshes.

10. HOUSING MODIFICATION

10.1. Options

Taken all round, after the pressure measurements it became obvious that the sudden velocity jump phenomenon…

- Originates from the ventilator housing
- Occurs on different characteristic curves of the fan (different speeds)
- Disappears on different operation points (at strong throttling), but the average fluctuations remain too high

Since the stroboscope investigation it is known that the impeller runs on constant speed. Therefore, the problem is a direct consequence of the incorrect housing design and there are no other influencing factors.

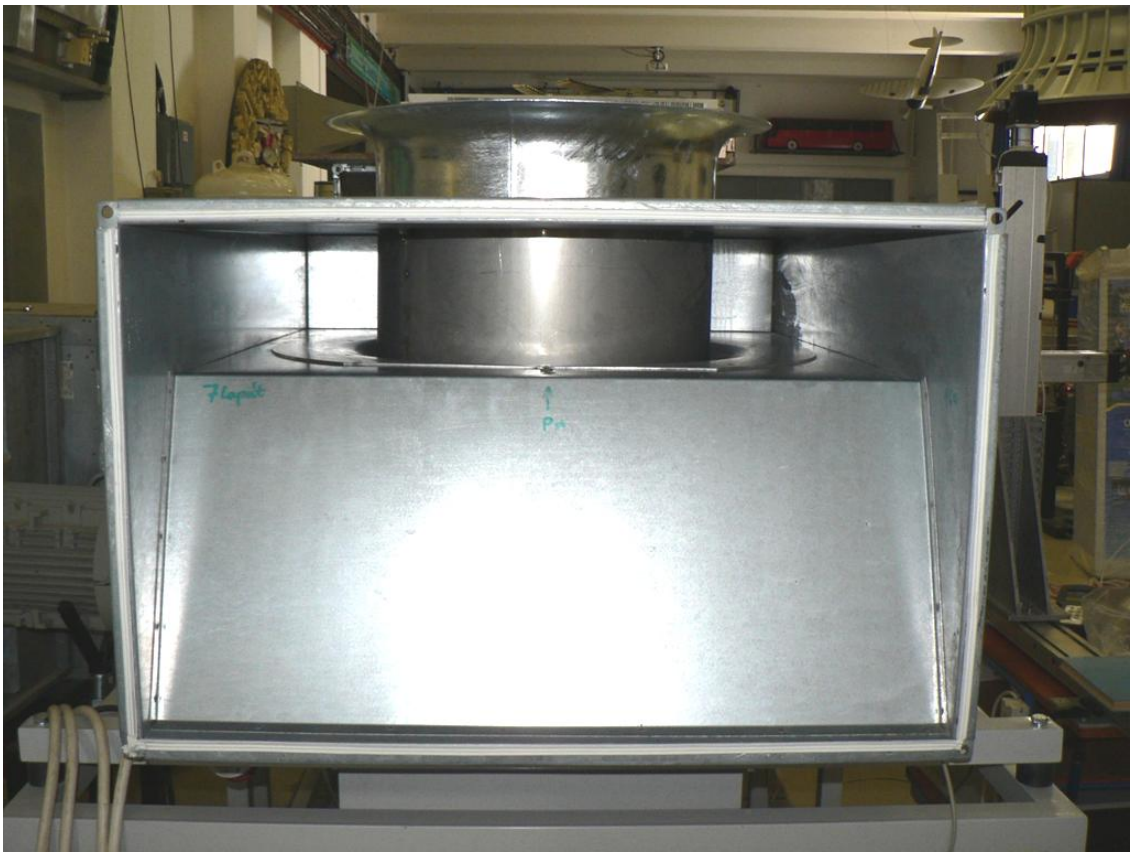

Figure 48 - Back view of the ventilator

As the previous picture shows [Figure 48], the inlet cannot be modified further, since the only possible modification; a new suction cone was already implemented. So the only way to kill the velocity jump phenomenon is to redesign the ventilator housing. This is a very unwanted solution, thanks to its complexity and dangerousness. In other words, modifying a standard fan is never expected to be simple and also could be dangerous, not just because of the risk of unpredictable flow conditions, but also the possibility of construction failures or accidents. Thus, very precise preliminary investigations, design and manufacturing processes are required.

Fortunately, there was another Helios BKD 560/4/80/50 ventilator at the department, which was free to move. Therefore, all preliminary investigations were carried out on this fan. As the next picture shows, the ventilator was turned to its side and the housing was opened to measure the inner dimensions [Figure 49]. Thus, the wind tunnel was not needed to be disassembled.

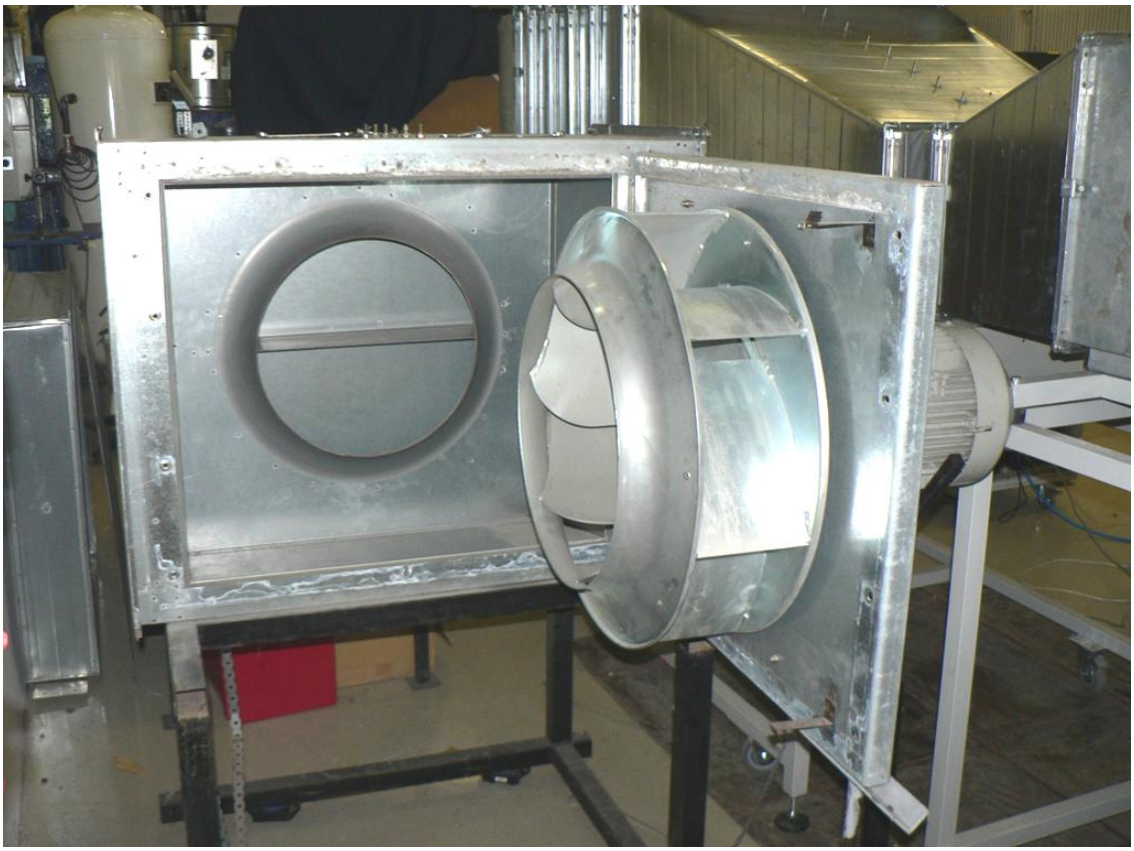

Figure 49 - Opened housing

As wrote earlier, this rectangular housing shape is very disadvantageous from fluid mechanich point of view. Because of the danger of separation zones and possibility of unstable flow conditions. The best concept for radial fans is the so-called scroll-shaped housing design [Figure 50].

Figure 50 - Scroll fan housing

10.2. Concept

In fact, there are no standards for scroll-shaped housing design; it is the result of long series of experiments and usually the secret of manufacturers. And due to the time constraints, it was not an option to design a brand new housing. Thus, the only way to improve the housing efficiency was to modify the original design. It is obvious, that the corners should be closed down in order to avoid separation. Therefore, bended sheets were designed around the impeller [Figure 51].

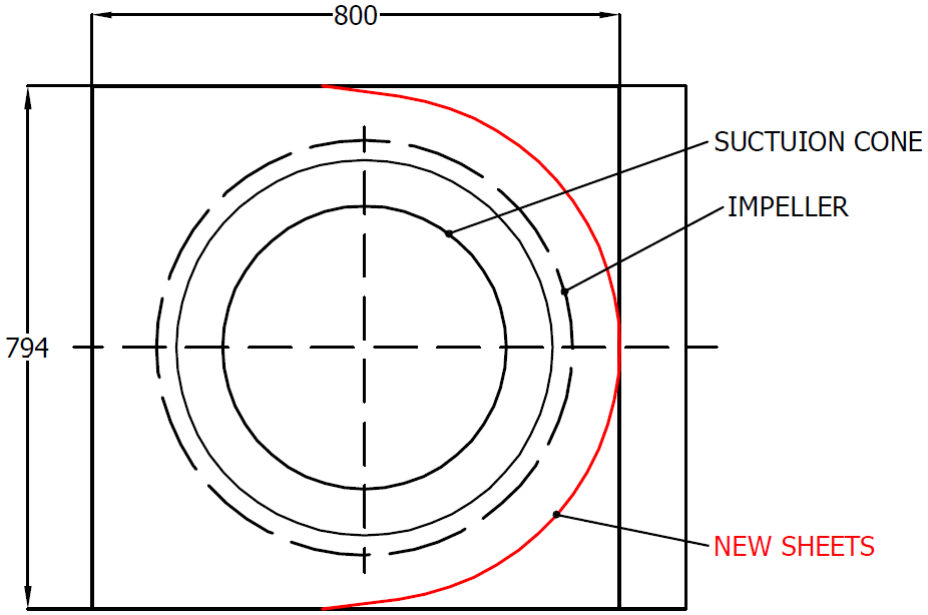

Figure 51 - Housing modification

10.3. Realization

Firstly, the ventilator was detached from the wind tunnel and the housing was opened up. After marking the proper position of the bended sheets in the housing, the flat pattern was calculated and then the manufacturing process was discussed and implemented. Finally, the bended sheets were fixed inside and the gaps were closed hermetically along the edges. The next photos illustrate the main steps [Figure 52].

Figure 52 - Bended sheets

10.4. Measurement

The modified ventilator was reattached to the wind tunnel and a new measurement was carried out using the hot wire anemometer. The measurement was run up to 300 seconds with 20 Hz sampling rate. The signal was recalculated to a 2 Hz velocity curve [Diagram 21].

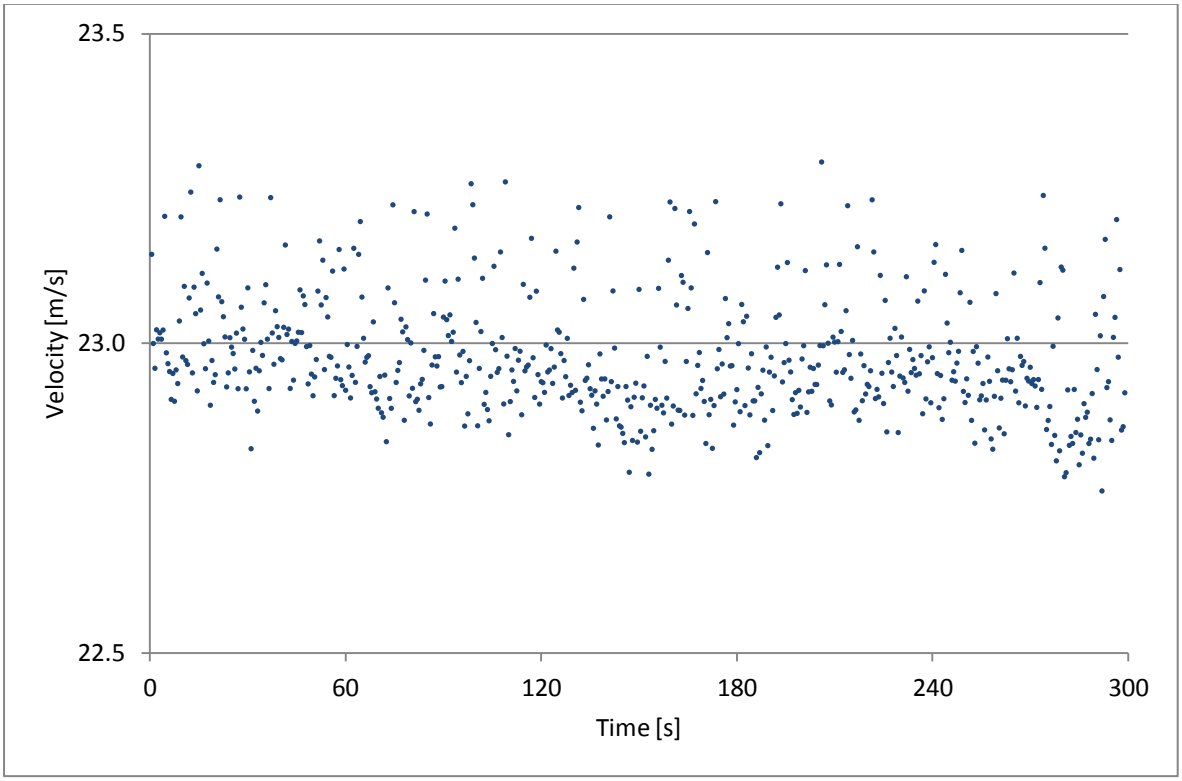

Diagram 21 - Velocity time signal

The velocity time signal is quite smooth; the sudden velocity jump phenomenon has disappeared! The next table contains the most important single quantities calculated from the velocity curve [Table 23].

Velocity signal	
AVG [m/s]	23.0
RMS [m/s]	0.18
T.I. [%]	0.78

Table 23

Due to the housing modification, not just the velocity jump problem was solved, but also the turbulence intensity dropped down to 0.78%, which is a pretty good value. The average velocity is acceptable, equals to the designing value. The operation was stable and reliable, so the modification was successful.

11. OPTIMAL CONFIGURATION

Finally, all problems of the wind tunnel have been solved. Table 24 lists the modifications and their effects on flow quality.

Element	Modification	Effects
Connection	Guide vane series	higher diffuser efficiency lower fluctuations smoother velocity distribution
Ventilator	Suction cone	better safety higher outlet velocity lower pressure loss
Diffuser	Split-level diffuser	no vibration and gaps reduced separation smoother velocity distribution **stable flow conditions** higher pressure loss
Ventilator	Curved sheets	closed internal dead space higher outlet velocity **no velocity jump phenomenon**
Ventilator	Inlet and outlet meshes	lower turbulence intensity higher pressure loss

Table 24 - Modification effects

However, so many modifications have been made, that the optimal mesh configuration is not obvious at all. Therefore, different arrangements were investigated measuring the flow velocity at the center of the confuser outlet cross-section with HWA. Table 25 represents the results.

Config.	Ventilator Inlet mesh	Ventilator Outlet mesh	Diffuser Inlet mesh	Diffuser Outlet mesh	Extra settling chamber	Mean Velocity	Turbulence Intensity
A	x	x				23.9	0.91
B	x	x	x			23.0	0.78
C	x	x		x	x	23.8	0.85
D	x	x	x	x	x	23.1	0.75
E	**x**	**x**	**x**	**x**		**23.1**	**0.74**
F		x	x	x		24.4	0.81

Table 25 - Different mesh configurations

Increasing the number of meshes, the maximal flow velocity and the turbulence intensity decreases as expected. With all meshes inside, the turbulence intensity is the best and the velocity is still over the designing value. The additional 200 mm long settling chamber section does not make the difference. Therefore, configuration E was accepted.

12. RASTER MEASUREMENT II.

12.1. Arrangement

The wind tunnel was assembled with the optimal mesh configuration and a complete measurement station [Figure 53] was built around the tunnel. A two-axis traverse system on special scaffolding was installed at the outlet section, which allowed to measure through the entire cross-section without any assembling process.

Figure 53 - Measurement system around the wind tunnel

12.2. Settings

After calibration, a hot wire measurement was performed directly behind the confuser with automatic measurement control. During the measurement 729 points were recorded on the surface to get a good overview on flow homogeneity. The data was saved into *Notepad*, then prepared in *Excel*, and finally evaluated in *Mathematica*. The measurement was performed at maximum volume flow rate; settings are represented below [Table 26].

Barometric pressure [Pa]	99800
Temperature [C]	21.0
Sampling rate [Hz]	2000
Sampling time [s]	5
Signal filtering	No
Time data format	Waveform spreadsheet

Table 26 - HWA settings

12.3. Results

The following figures illustrate the measurement results. Figure 54 represents a two-dimensional contour plot. The inhomogeneity at the edges is conspicuous, but this was expectable, because a free jet was measured instead of a closed test section. Anyway, without the edges the velocity distribution is very uniform through the entire cross-section.

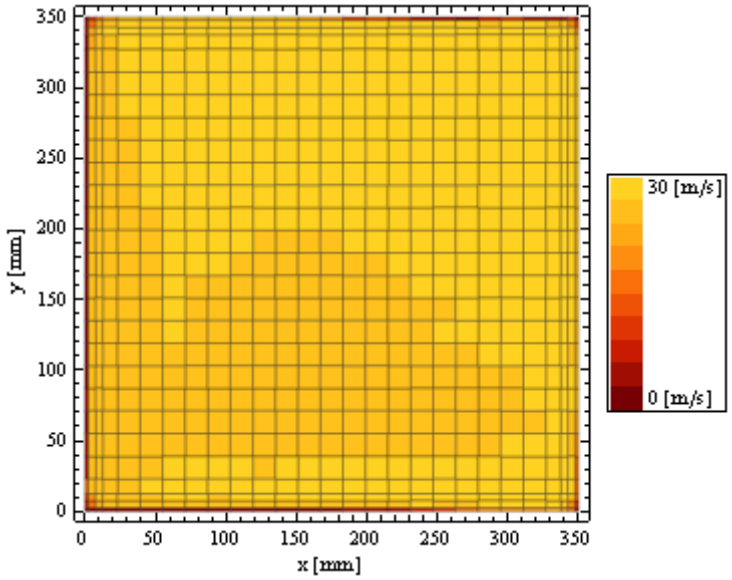

Figure 54 - Velocity contour plot

Figure 55 is a three-dimensional velocity plot, where all small differences are clearly visible. Due to this truly relevant picture, it is obvious that the velocity distribution is very nice and smooth indeed.

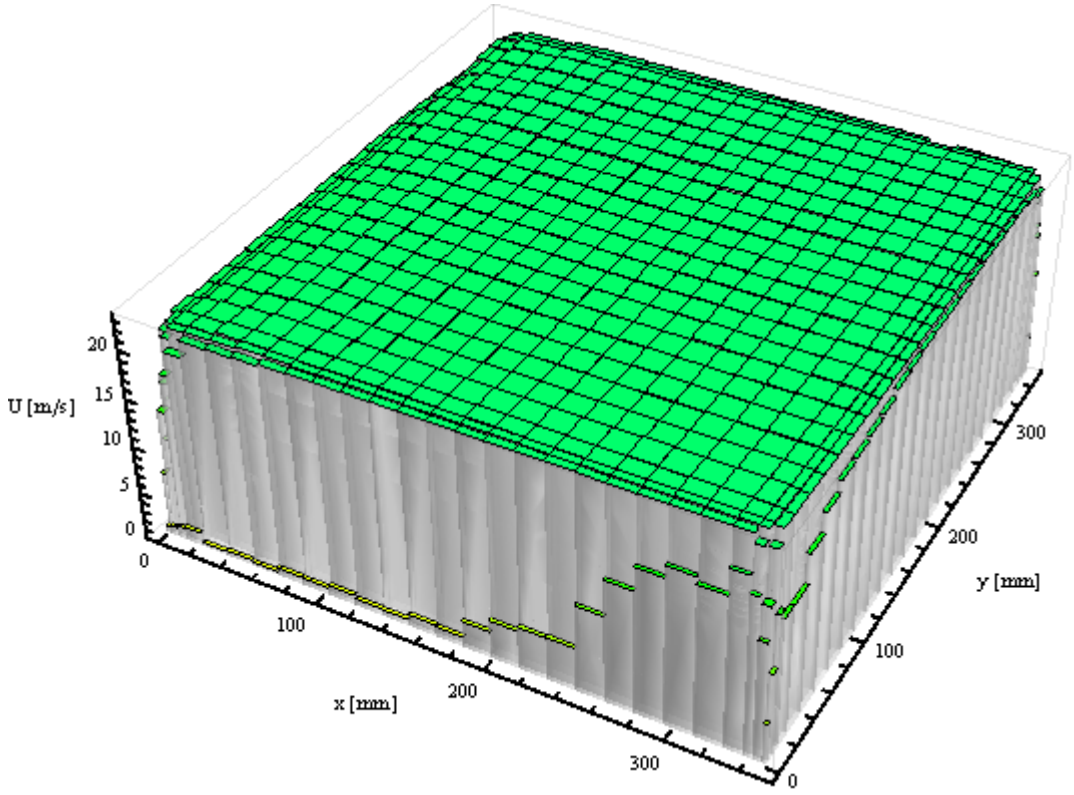

Figure 55 - 3D velocity plot

Finally, the outer 15 mm was removed from the measured surface to avoid the disturbance of the sidewalls and the free-jet effect. In other words, the velocity distribution was replotted on the middle 320×320 mm^2 area [Figure 56]. Automatic interpolation algorithm and relative colour scale were applied in order to gain a detailed insight on flow homogeneity. The distribution is more regular than expected, because velocity layers are observable. On the left side the velocities are lower, but this is still a probable consequence of the free-jet effect.

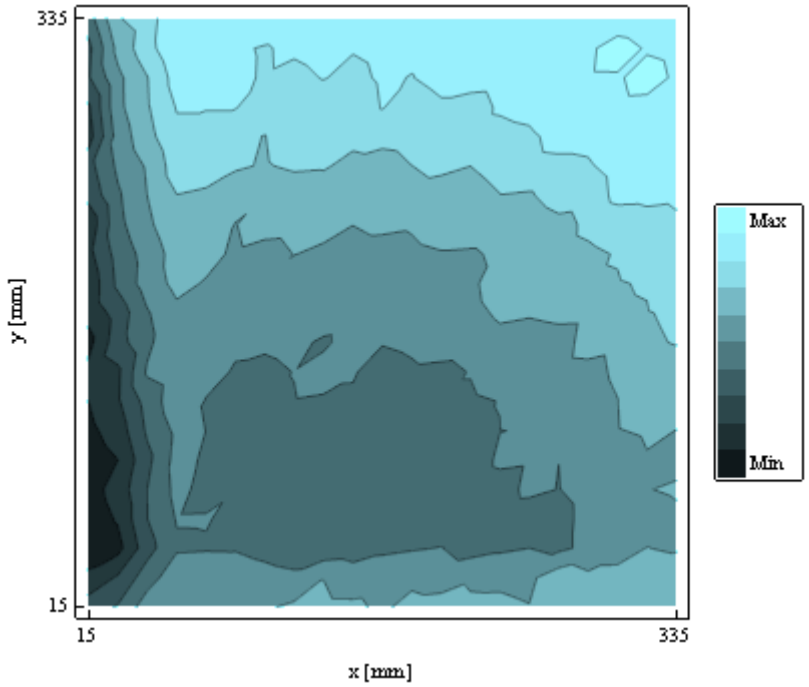

Figure 56 - Velocity contour plot

In addition the minimal, the maximal and the average flow velocity and turbulence intensity values were calculated. The final results are listed in Table 27 below.

	U [m/s]	T.I. [%]
Min	**21.66**	**0.53**
Max	**23.26**	**1.56**
AVG	**22.60**	**0.81**

Table 27 - Final result

Just for comparison, in the center of the cross-section the mean velocity was 23.1 m/s and the turbulence intensity 0.74%. Considering the whole outlet surface, the difference is quite small, so the results are pretty good. This means that the wind tunnel provides almost the same flow quality in each points of the outlet cross-section with small deviation.

13. APPLICATION EXAMPLES

13.1. Speed measuring system calibration

Shortly after the assembling and measurement processes, the wind tunnel got its first mission. The task was to calibrate the Pitot-tube on a radio-controlled airplane model, which also has an autopilot mode developed by scientist at MTA SZTAKI. The pressure difference between the Pitot-tube and the static pressure tap is detected by a sensor, so that the flying speed can be calculated and controlled by the on-board computer. The next photo illustrates the measurement arrangement [Figure 57].

Figure 57 - RC airplane velocity sensor calibration

The middle section of the wing was positioned close to the confuser outlet. Using the frequency-converter, different flow velocities was set up to 22 m/s, which was a wide enough range for the airplane. The measured pressure differences of the sensor and a standard Prandtl-tube were compared, thus the calibration curve was obtained.

13.2. Flow visualization around car models

The second application of the wind tunnel was performed on a Fluid Mechanics Division event. The task was to visualize the flow around old, East European car models. A special platform was attached to the outlet, which provided the ground for the models, and also the mounting for the laser planes. Oil mist was introduced in the flow using a mist generator. The next picture illustrates the visualization process [Figure 58].

Figure 58 - Flow visualization around car models

Several car models such as Lada, Wartburg, Zaporozhets, Moskvich and Barkas were investigated. The main goal was to indicate the separation zones and make approximate statements about the aerodynamic efficiency. It was found, that due to the square design, most of the cars has terrible aerodynamics as expected. But there was also a positive surprise: the Wartburg 313 Sport coupe. No separation bubbles could be detected as it has very smooth, well-designed bodywork.

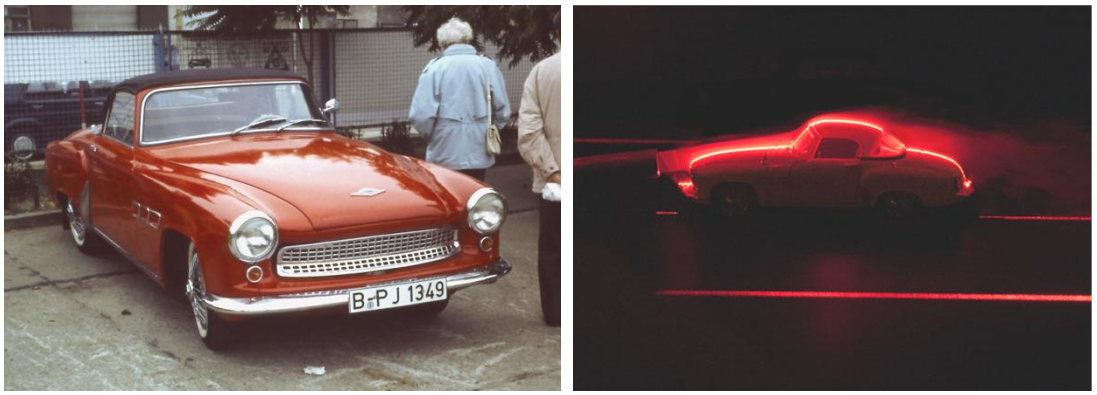

Figure 59 - Wartburg 313 Sport coupe in reality and in the wind tunnel

14. PROSPECTS

14.1. Overview

There are several further options to improve the efficiency and equipment level of the wind tunnel. The most important fields are listed below.

- Individual test section
  closed measurement space, plexiglass/black plate sides, pressure taps, oil mist intake, lightning
- Additional confusers and test sections
  large-scale, narrow-design
- Measurement control panel
  built-in computer, touch screen, measurement software
- Automatic measurement control
  flow speed setting, force measurement, data processing
- Noise reduction
  acoustic insulation of the ventilator
- Wind tunnel appearance design
  paint to colour, name and logo, technical paper, brochure

14.2. Test sections

Currently the wind tunnel is finished and the individual test section [Figure 60] is under construction (350×350×1000 mm^3). However, it is planned to design and manufacture new confusers and test sections [Table 28] to the wind tunnel in order to satisfy special measurement requirements too. The confusers will be interchangeable and rotatable as needed. Therefore, different test sections and a special scaffolding will be constructed. These additional elements will be designed by *András Gulyás*.

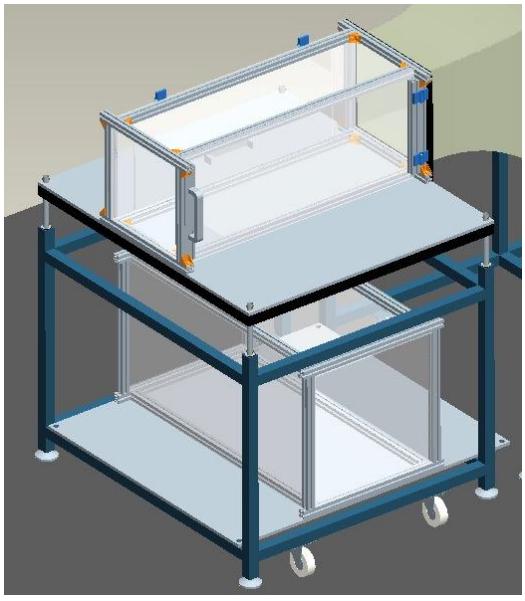

Figure 60 - Test sections and scaffolding

Test section configuration	Confuser outlet area	Meas. type	Max. velocity	*Application examples*
Default-size	350×350 mm^2	3D	23 m/s	*building / vehicle models, complex structures, special shapes*
Large-scale	400×500 mm^2	3D	14 m/s	
Narrow-design	150×1000 mm^2	2D	19 m/s	*wing profiles, flutter and Magnus effect*
No test section	various	various	various	*free-jet measurements*

Table 28 - Test section configurations

Both of the large-scale and narrow-design confusers (with the corresponding test section) can be attached in two ways thanks to the square inlet cross-section. Moreover, the large-scale test section is compatible with a new moving belt designed at the Department [13]. It allows high-precision vehicle aerodynamic measurements by simulating the relative motion between the ground and the body. Render pictures about the model can be seen on Figure 61 below.

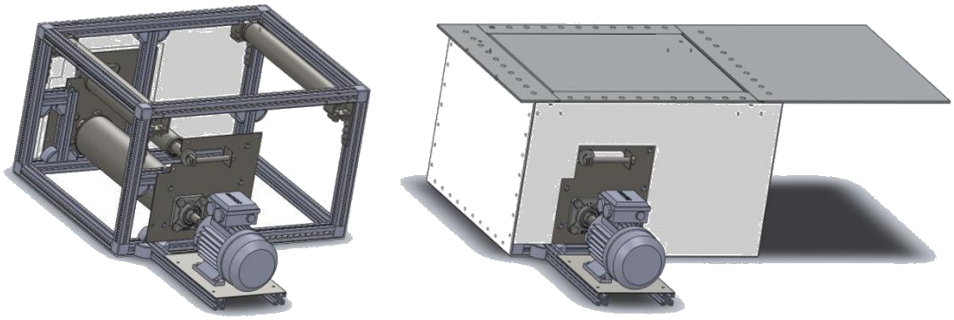

Figure 61 - Moving belt 3D model

14.3. Automatic measurement control

The final goal is to make the system capable for measuring the drag and lift coefficient – velocity curves automatically for a body. This task involves automatic data processing and flow speed control. The velocity can be controlled through the frequency converter and checked by the measured pressure signal at the confuser outlet for example. The forces acting on the body will be measured with a two-component load cell. The ambient air density will be calculated based on the built-in barometer and thermometer. The automatic control system and the measurement program will be accomplished during the next semester. The software will be optimized for touch screen interface, thus providing innovative and attractive operation.

SUMMARY

Within the confines of the Thesis, a small test-section wind tunnel was built, tested and optimized with great final results.

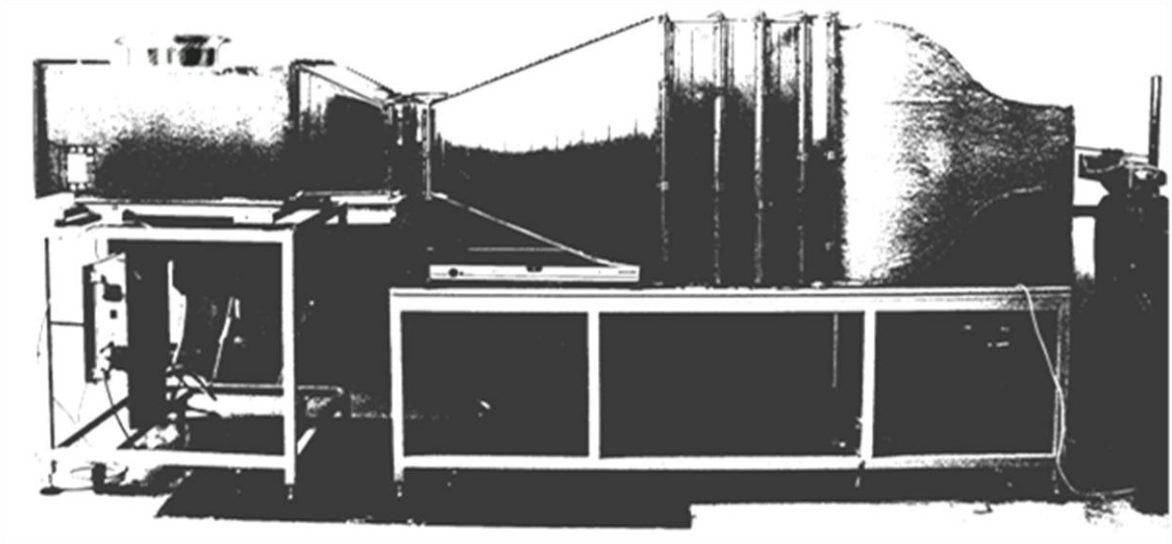

After the literature and design review, all of the wind tunnel components were introduced and investigated.

A measured velocity profile was given along the ventilator outlet surface, which was very inhomogeneous. Therefore, a changeable guide vane series was designed with CFD-techniques, then manufactured and installed. The checking measurements proved that it smoothes the flow effectively. The complete wind tunnel was assembled and velocity-profile measurements were carried out in certain cross-sections to show flow homogeneity development. The first results of the hot wire anemometry were not acceptable, the turbulence intensity was very high and a strong fluctuation phenomenon was observable at the outlet.

Different investigations were carried out affecting the whole wind tunnel and several errors were detected in different elements. Therefore, many modifications were implemented to overcome with the problems, such as a new suction side for the impeller, a new diffuser concept, a significant housing modification and an optimization of the settling chamber and mesh configuration. Thanks to these modifications, the fluctuation phenomenon was eliminated and the turbulence intensity dropped down under 1%, while the designing outlet velocity was kept. Finally, the entire confuser outlet cross-section was measured through with hot wire anemometer to get an exact overview on the outlet flow velocity distribution. The measurement results were great, thus no further modifications were needed.

In the last two chapters, the first applications of the wind tunnel and some further possible developments were presented.

ACKNOWLEDGEMENT

I would like to render thanks to my supervisor, Márton Balczó for his professional assistance and support throughout the two semesters. He defined the main tasks as well as the schedule and also ordered the required parts or raw materials from external companies.

Thanks to András Gulyás, who was my right-hand assistant in the laboratory, and actively involved in assembly and measurement processes. He designed the remaining measurement sections for the wind tunnel too.

Thanks to Árpád Varga, who assembled and configured the pressure transducer system, which allowed to measure pressure signal on twelve channels simultaneously. This device was indispensable to capture the sudden pressure jump phenomenon.

And last but not least, thanks to István Jezsó skilled worker, who manufactured the designed elements in the workshop of the Department and helped a lot in the assembling processes. His experience was essential during the construction of the wind tunnel.

All of them helped a lot also at consultations and brainstorming times to clarify the construction and implementation details.

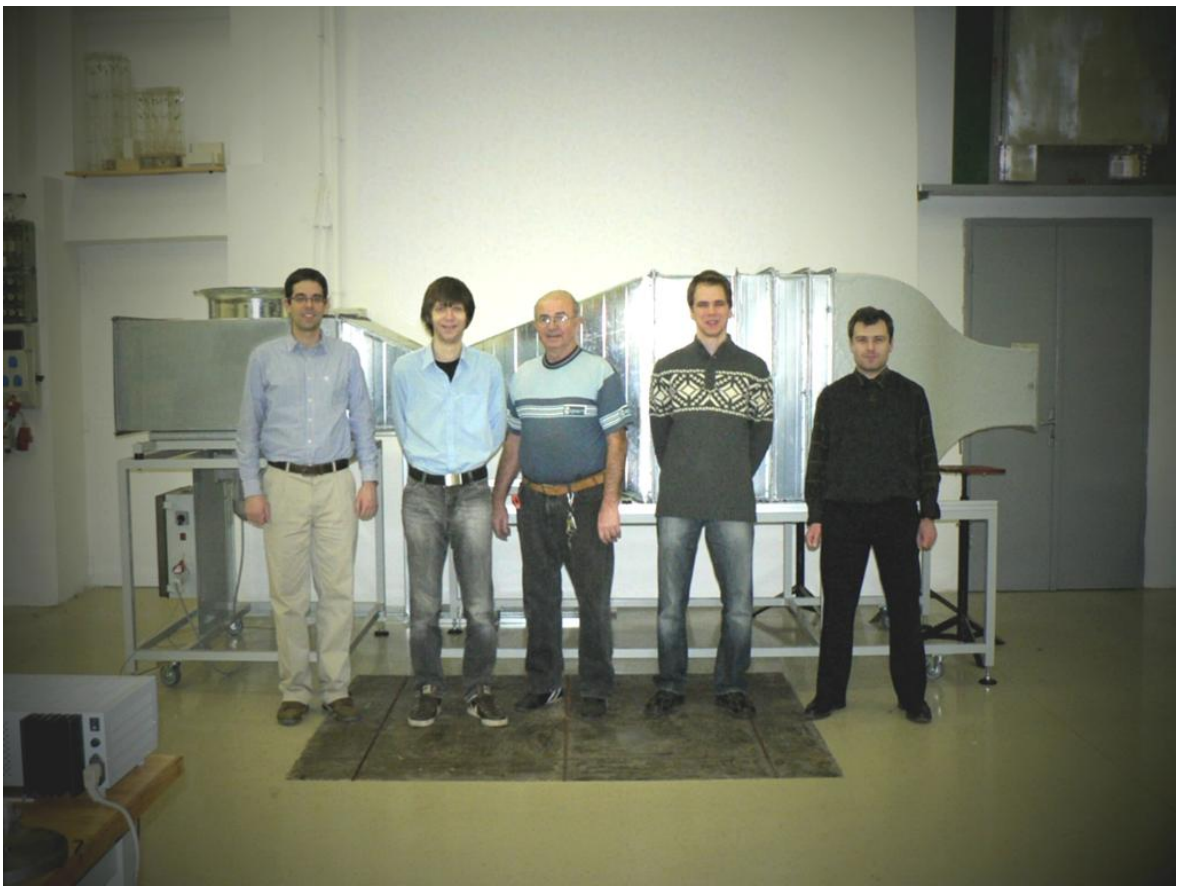

Márton Balczó, András Gulyás, István Jezsó, Péter Kurdi, Árpád Varga

REFERENCES

[1] AUDI official website, *www.audi.com*
[2] NRL (Naval Research Laboratory) official website, *www.nrl.navy.mil*
[3] NASA (National Aeronautics and Space Admin.) official website, *www.nasa.gov*
[4] HELIOS official website, *www.helios.de*
[5] FORMULA 1 official website, *www.formula1.com*

websites

[6] MEHTA, R.D. & BRADSHAW, P. (1979) "Design rules for small low speed wind tunnels" *The Aeronautical J. of the Royal Aeronautical Society*, pp.443-449.
[7] MEHTA, R.D. (1985) "Turbulent boundary layer perturbed by a screen" *J. AIAA* Vol.23 No.9, pp.1335-1342.
[8] WATMUFF, J.H. (1986) "Wind Tunnel Contraction Design" *9th Australasian Fluid Mechanics Conf.*, New Zealand, Auckland, pp.472-475.
[9] BELL, J.H. & MEHTA, R.D. (1988) "Contraction design for small low-speed wind tunnels" *NASA Contractor Report*, CR-182747.
[10] NOUI-MEHIDI, M.N.,WU, J. & SUTALO, I. (2004) "Velocity Distribution in an Asymmetric Diffuser with Perforated Plates" *15th Australasian Fluid Mechanics Conf.*, AUSTRALIA Sydney
[11] KARVINEN, A. & AHLSTEDT, H. (2009) "Simulation of Three-Dimensional Diffuser" *Pres. for Finnish OpenFOAM Users*, Finland, Tampere, pp.1-25.

articles

[12] ALPÁR, B. (2012) „Alacsony sebességű, kisméretű szélcsatorna tervezése" *MSc Thesis at Dept. of Fluid Mechanics, Budapest University of Technology and Economics*, HUNGARY Budapest
[13] SZABÓ, B. (2012) "Mounting & testing of moving ground simulation system designed for vehicle aerodynamic studies in the NPL type wind tunnel" *MSc Thesis at Dept. of Fluid Mechanics, Budapest University of Technology and Economics*, HUNGARY Budapest

dissertations

[14] Dr LAJOS, T. (2008) "Az áramlástan alapjai" rev.4, ISBN 9789630663823
[15] Dr GRUBER, J., et al. (1978) "Ventilátorok" rev.4, ISBN 19631022056

books